USE OF NMR RELAXOMETRY TO ASSESS PHYSICOCHEMICAL CHARACTERISTICS OF SEEDS AND GRAINS

A THESIS SUBMITTED TO
THE GRADUATE SCHOOL OF NATURAL AND APPLIED SCIENCES
OF
MIDDLE EAST TECHNICAL UNIVERSITY

BY

KÜBRA ÜNAL

IN PARTIAL FULFILLMENT OF THE REQUIREMENTS
FOR
THE DEGREE OF DOCTOR OF PHILOSOPHY
IN
FOOD ENGINEERING

AUGUST 2022

Approval of the thesis:

USE OF NMR RELAXOMETRY TO ASSESS PHYSICOCHEMICAL CHARACTERISTICS OF SEEDS AND GRAINS

submitted by **KÜBRA ÜNAL** in partial fulfillment of the requirements for the degree of **Doctor of Philosophy** i**n Food Engineering, Middle East Technical University** by,

Prof. Dr. Halil Kalıpçılar
Dean, Graduate School of **Natural and Applied Sciences** _____

Prof. Dr. Serpil Şahin
Head of the Department, **Food Engineering** _____

Assoc. Prof. Dr. H. Mecit Öztop
Supervisor, **Food Engineering, METU** _____

Prof. Dr. Hami Alpas
Co-Supervisor, **Food Engineering, METU** _____

Examining Committee Members:

Prof. Dr. Behiç Mert
Food Engineering, METU _____

Assoc. Prof. Dr. H. Mecit Öztop
Food Engineering, METU _____

Prof. Dr. Hakan Aktaş
Department of Horticulture,
Isparta University of Applied Science _____

Assoc. Prof. Dr. E. Burçin Özvural
Food Engineering, Çankırı Karatekin University. _____

Assoc. Prof. Dr. Bekir Gökçen Mazı
Food Engineering, Ordu University _____

Date: 09.08.2022

I hereby declare that all information in this document has been obtained and presented in accordance with academic rules and ethical conduct. I also declare that, as required by these rules and conduct, I have fully cited and referenced all material and results that are not original to this work.

Name Last name : Kübra Ünal

Signature :

ABSTRACT

USE OF NMR RELAXOMETRY TO ASSESS PHYSICOCHEMICAL CHARACTERISTICS OF SEEDS AND GRAINS

Ünal, Kübra
Doctor of Philosophy, Food Engineering
Supervisor : Assoc. Prof. Dr. Mecit Halil Öztop
Co-Supervisor: Prof. Dr. Hami Alpas

August 2022, 124 pages

Nuclear Magnetic Resonance (NMR) relaxometry is a widely used characterization method for the analysis of physiological and biochemical changes in a huge variety of samples. Time domain NMR (TD-NMR) relaxometry provides structural analysis at low magnetic fields. It is basically relies on the relaxation times of proton signals coming from the entire sample. Thus, it provides quantification of water absorption and analyzing its distribution within the biological systems. In this dissertation, plant tissues and starch-water interaction systems were investigated using TD-NMR relaxometry.

In the first part of the study, TD-NMR relaxometry was used to investigate the changes in the cell integrity of plant tissues. For plant tissues, tomato seed was selected and subjected to osmotic stress (OS) (10, 20, 30% NaCl solutions), ultrasonication (US) (5, 10 and 20 minutes) at 75% amplitude and high hydrostatic pressure (HHP) (300, 400 and 500 MPa for 15 min at 20°C). NMR relaxation spectra of tomato seed gave four peaks each corresponding to different water compartments due to multiexponential relaxation behavior of the plant cell. According to the

results, all the three treatments resulted in cell permeabilization and disruption of cellular compartmentalization. Among the treatments, HHP at 500 MPa for 15 min at 20°C resulted in the most detrimental effect in the cell structure and OS treatment with 10% NaCl solution caused the least changes in the cell structure. Seeds exposed to different treatments were also analyzed by Scanning Electron Microscope (SEM) to determine the extent of damage to the cell. These results have proved that NMR relaxometry is an effective method to analyze the cell membrane integrity of tomato seeds exposed to selected treatments.

Use of NMR relaxometry to assess physicochemical characteristics of starch-water interactions was the second part of the study. Quinoa starch was chosen to study starch-water interactions. Following starch isolation, NMR relaxometry was used to investigate the physiological changes in quinoa starch dispersions induced by HHP and US. HHP at 250, 350 and 500 MPa at 20°C and 40°C; ultrasonication (US) at 100% power with constant pulse for 15 min were applied as modification methods. Following the treatments, functional, rheological, particle size, morphological and structural analysis were carried out. Results showed that swelling power and water solubility index of quinoa starch was decreased significantly with both HHP and US treatments ($p<0.05$). Apparent viscosity of the starch samples decreased with increasing pressure and US treatment. The particle size distribution revealed a more apparent increase in the volume mean diameter (D [4,3]) with HHP treatment ($p<0.05$) compared to US. Time domain (TD) NMR relaxometry experiments confirmed that HHP treatment caused less granule swelling of starch. NMR relaxation spectra of quinoa seeds revealed mainly two distinct proton populations and HHP treatment at 500 MPa resulted in faster exchange of proton populations compared to the US treatment. DSC results are correlated with the results of NMR relaxometry. SEM images visualized the change in the morphology of the quinoa starches after treatments and structural changes were observed through FTIR and XRD experiments. These results have demonstrated that HHP treatment had a strong modification effect on quinoa starch compared to US and provide modified quinoa

starch with better quality. Moreover, the investigation of the quinoa starch and water interactions under these conditions was demonstrated to be effective with the use of NMR relaxometry.

To conclude, this dissertation has proved that TD-NMR relaxometry is an effective method for characterization of cell integrity of tomato seeds and physiological changes in quinoa starch dispersions. This study may provide information for further research in food applications.

Keywords: TD-NMR Relaxometry, High Hydrostatic Pressure (HHP), Ultrasonication (US), Plant seed, Quinoa starch

ÖZ

TOHUM VE TAHILLARIN FİZİKOKİMYASAL ÖZELLİKLERİNİ DEĞERLENDİRMEK İÇİN NMR RELAKSOMETRENİN KULLANIMI

Ünal, Kübra
Doktora, Gıda Mühendisliği
Tez Yöneticisi: Doç. Dr. Mecit Halil Öztop
Ortak Tez Yöneticisi: Prof. Dr. Hami Alpas

Ağustos 2022, 124 sayfa

Nükleer Manyetik Rezonans (NMR) relaksometri çok çeşitli numunelerdeki fizyolojik ve biyokimyasal değişikliklerin analizi için yaygın olarak kullanılan bir karakterizasyon yöntemidir. Zamansal alanlı NMR (TD-NMR) relaksometre ölçümü, düşük manyetik alanlarda yapısal analiz sağlar. Temel olarak tüm numuneden gelen proton sinyallerinin gevşeme sürelerine dayanır. Böylece su absorpsiyonunun nicelleştirilmesini ve biyolojik sistemler içindeki dağılımının analiz edilmesini sağlar. Bu çalışmada, bitki dokuları ve nişasta-su etkileşim sistemleri TD-NMR relaksometre kullanılarak araştırılmıştır.

Çalışmanın ilk bölümünde, bitki dokularının hücre bütünlüğündeki değişikliklerini araştırmak için TD-NMR relaksometre kullanılmıştır. Bitki dokusu olarak domates tohumu seçilmiş ve ozmotik strese (OS) (10, 20, %30 NaCl çözeltileri), %75 güçte ultrasonikasyona (US) (5, 10 ve 20 dakika) ve yüksek hidrostatik basınca (HHP) (20°C'de 15 dakika boyunca 300, 400 ve 500 MPa) tabi tutulmuştur. Domates tohumunun NMR relaksometre spektrumu, bitki hücresinin çok üslü gevşeme davranışından dolayı her biri farklı su bölmelerine karşılık gelen dört tepe elde edilmiştir. Her üç uygulama da hücre geçirgenliğinin ve hücresel bölümlendirmenin

bozulmasına neden olmuştur. İşlemler arasında, 20°C'de 15 dakika boyunca 500 MPa'da uygulanan HHP, hücre yapısında en zararlı etkiye neden olurken, %10 NaCl çözeltisi ile uygulanan OS, hücre yapısında en az değişikliğe neden olmuştur. Farklı işlemlere maruz kalan tohumlar, hücreye verilen hasarın derecesini belirlemek için Taramalı Elektron Mikroskobu (SEM) ile de analiz edilmiştir. Bu sonuçlar, NMR relaksometrenin, çalışmada belirtilen uygulamalara maruz bırakılan domates tohumlarının hücre zarı bütünlüğünü analiz etmek için etkili bir yöntem olduğunu kanıtlamıştır.

Nişasta-su etkileşimlerinin fizikokimyasal özelliklerini değerlendirmek için NMR relaksometrenin kullanılması çalışmanın ikinci kısmını oluşturmaktadır. Nişasta-su etkileşimlerini çalışmak için kinoa nişastası seçilmiştir. Nişasta elde edilmesinden sonra HHP ve US uygulamalarına maruz kalan kinoa nişasta dispersiyonlarındaki fizyolojik değişiklikleri araştırmak için NMR relaksometre kullanılmıştır. Modifikasyon yöntemi olarak 250, 350 ve 500 MPa basınçta, 20 ve 40°C sıcaklıkta yüksek hidrostatik basınç (HHP) ve 15 dk sabit darbe ile %100 güçte ultrasonikasyon (US) uygulanmıştır. İşlemlerin ardından fonksiyonel, reolojik, partikül boyutu, morfolojik ve yapısal analizler yapılmıştır. Sonuçlar, kinoa nişastasının şişme gücü ve suda çözünürlük indeksinin hem HHP hem de US uygulamaları ile önemli ölçüde azaldığını göstermiştir ($p<0.05$). Nişasta örneklerinin görünen viskozitesi artan basınç ve US muamelesi ile azalmıştır. Parçacık boyutu dağılımında, US işlemi ile kıyaslandığında HHP işlemine maruz kalan nişastanın ($p<0.05$) hacim ortalama çapında (D [4,3]) daha belirgin bir artış ortaya koyduğu gözlemlenmiştir. Zamansal alanlı (TD) NMR sonuçları, HHP uygulamasının nişastanın daha az granül şişmesine neden olduğunu doğrulamıştır. Kinoa tohumlarına ait NMR relaksometre spektrumları, esas olarak iki farklı proton popülasyonu ortaya çıkarmış ve 500 MPa basınç seviyesinde HHP uygulaması, US uygulamasına kıyasla daha hızlı proton popülasyonu değişimine neden olmuştur. DSC sonuçları, NMR relaksometre sonuçlarını doğrulamaktadır. SEM görüntüleri modifikasyon işlemlerinden sonra

kinoa nişastalarının morfolojisindeki değişim görselleştirilmiş ve FTIR ve XRD deneyleri ile yapısal değişiklikler gözlemlenmiştir.

Bu sonuçlar, HHP uygulamasının US uygulamasına kıyasla kinoa nişastası üzerinde güçlü bir modifikasyon etkisine sahip olduğunu ve daha iyi kalitede modifiye kinoa nişastası sağladığını göstermiş ve NMR relaksometre ölçümünün, farklı işlemlere tabi tutulan kinoa nişastası ve su etkileşimlerini araştırmak için etkili bir araç olduğu kanıtlanmıştır.

Sonuç olarak, bu tez, TD-NMR relaksometrenin, domates tohumlarının hücre bütünlüğünün ve kinoa nişasta dispersiyonlarındaki fizyolojik değişikliklerin karakterizasyonu için etkili bir yöntem olduğunu kanıtlamıştır. Bu çalışma, gıda uygulamalarında daha ileri araştırmalar için bilgi sağlama niteliğindedir.

Anahtar Kelimeler: TD-NMR Relaksometre, Yüksek Hidrostatik Basınç (HHP), Ultrasonikasyon (US), Tohum, Kinoa nişastası

To my family

ACKNOWLEDGMENTS

First and foremost, I would like to express my deepest gratitude and respect to my supervisor Assoc. Prof. Dr. H. Mecit Oztop for her encouragement, guidance, valuable suggestions and kindly attitude throughout this study. I would also thank to my co-supervisor, Prof. Dr. Hami Alpas for her assistive suggestions throughout my thesis. I am grateful for their knowledgeable guidance, continuous support and patience. The thesis would not have been written successfully without their continuous supervision.

I would like to thank my committee members, Prof. Dr. Behiç Mert, Prof. Dr. Hakan Aktaş, Assoc. Prof. Dr. E. Burçin Özvural, Assoc. Prof. Dr. Bekir Gökçen Mazı for serving as my committee members.

I also would like to thank all my dear laboratory mates in both 'Öztop Lab' and 'Basınç Lab' for enlightening me with their practical and scientific knowledge whenever I faced with a problem during my study. I especially thank my dear friends, Esma İlhan, Zikrullah Bölükkaya, Ülkü Ertuğrul, Elif Gökçen Ateş, Şirvan Uğuz, İlhami Okur, Pürlen Okur for their valuable accompany during the analyses throughout my thesis.

My special thanks go to Selen Güner for her valuable friendship and endless support. I would like to express my special gratitude to my friends and colleagues Barış Özel, Ayça Aydoğdu, Emrah Kırtıl, Sevil Çıkrıkcı, Bade Tonyalı, Cansu Kabakçı, Eda Yıldız, Derya Ucbaş, Pelin Poçan, Kübra Ertan, Özge Güven, Serap Şahin and my other colleagues who were with me throughout my PhD education for their friendship and valuable suggestions.

I would like to thank the executives of my workplace TÜRKPATENT for encouraging me and my colleagues for their support.

Last and certainly not least, I want to express my deepest gratitude to my lovely family for their unconditional love and tireless devotion throughout my life. This accomplishment would not have been possible without their valuable support.

This work is partially funded by Republic of Turkey Ministry of Agriculture and Forestry General Directorate of Agricultural Research and Policies (TAGEM) Research and Development Grants (Grant no: TAGEM Ar-Ge 13/41). I would like to thank TAGEM for giving the opportunity to complete the study.

I would also like to acknowledge Science Fellowships and Grant Program (TÜBİTAK-BIDEB) for granting under TUBITAK 2211-A General Domestic PhD Scholarship Program during my research study.

TABLE OF CONTENTS

LIST OF TABLES

TABLES

LIST OF FIGURES

FIGURES

CHAPTER 1

INTRODUCTION

From a botanical point of view, although seeds and grains are related, they are different. They differ significantly in terms of nutrition and digestion. A germinated seed differs from a sprouted seed through physical and chemical alterations that occurred during or after the germination process, similar to the rise of caterpillar from its shell as a butterfly (Carna4, 2015).

A seed is an embryonic plant that is enclosed in a seed coat and produced from the mature ovule of plants upon fertilization. The seed includes all of the nutrients necessary for the growth of a new plant. Until the seed is germinated or sprouted, the nutrients are dormant and upon waking up they become highly digestible, as well as a good source of nutrition for the livings who consume it (Carna4, 2015). Seeds from a variety of species include pepper, tomato, strawberry, grape, fig, carrot, cabbage, basil, kiwifruit, beet, sunflower, rice, flaxseed, pomegranate, corn, wheat, peanut, and legumes (Maity, 2021).

A grain is the small edible part of the specific grassy plants conventionally described as cereals and legumes. A grain includes an embryo, an endosperm, a testa, and a pericarp. The term cereal refers to the grassy plant and the term grain refers to the edible seed part of that grassy plant. These terms are being used alternatively or used by combining two of them. Grains constitute a big nutrient source for humans and livestock due to having high starch content of their endosperm. Cereal grains include wheat, rice, oats, barley, rye, barley, millet, corn, triticale, and sorghum which are all rich in carbohydrate content. In addition to cereal grains, there are grains cultivated from pseudo-cereals like chia, quinoa, and buckwheat grains. Grains obtained from legumes are chickpeas, mung beans, soybeans, common beans, lentils,

and lima beans which have a high protein content than cereal grains (Evers & Millar, 2002).

In this dissertation, the focus will be tomato seed, quinoa and assessing their physicochemical characteristics.

1.1 Seed

1.1.1 Seed and Seed Quality

Seeds have a vital role in agriculture since they provide the majority of the world's food requirements (Bewley, 1997). The size of the global seed market in 2021 is estimated to be US $ 63 billion and is expected to reach US $ 86.8 billion in 2026. Cereals and grains are expected to have the biggest seed market share due to their widespread use as a staple meal and in the food and feed processing sectors (*Seeds Market by Type, Trait, Crop Type And Region - Global Forecast to 2026*, 2021). Seeds are responsible of propagating new crops and determining their genetic potential. Seed quality determines the ability for germination of living and resistant seedlings (Bewley, 1997). They are abundant in protein, carbohydrate, and oil reserves, which aid in the early phases of plant growth and development. Many cereals and legumes are key food sources for a substantial proportion of the world's population because of these reserves (Taiz & Zeiger, 2006).

Seed quality is crucial in agricultural production since it restricts the possible yield and affects the farmer's labor productivity. In this aspect, it is important to deliver good quality seeds to farmers in order to ensure efficient agriculture and food security. The parameters of the seed quality attributes include healthy seed (lack of disease causing organisms, such as bacteria and viruses), minimum of damaged seed, adapted to the local conditions and high yielding ability (FAO Seed and Plant Genetic Resources Service, n.d.).

In this study, the focus will be tomato seed and explained in more detail.

1.1.2 Tomato Seed and Structure

Tomato is a member of Solanaceae family and belongs to the *Lycopersicon* genus. It has been consumed since sixteenth century and today it is one of the world's most important horticultural crops (Hilhorst, Groot, & Bino, 1998).

Tomato seeds are members of Solanoideae subgroup of Solanacae, like pepper seeds. Fig.1.1 shows the structure of mature tomato seed (Finch-Savage & Leubner-Metzger, 2006). In mature tomato seeds, the embryo is surrounded by a thin testa (seed coat) and a rather hard and brittle endosperm. The endosperm provides nutrition to the embryo for germination. The embryos are in a curved and flattened shape. The seeds are discoid shaped and the radicle tip is covered with a micropylar cap-like structure made up of endosperm and testa (Finch-Savage & Leubner-Metzger, 2006).

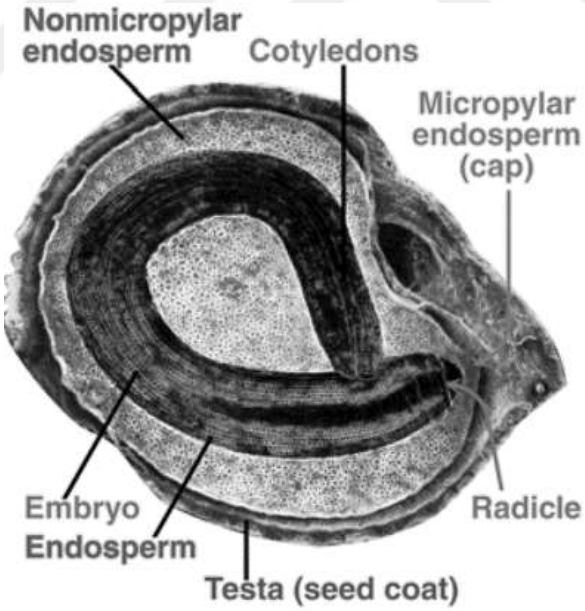

Figure 1.1. Structure of mature tomato seed (Finch-Savage & Leubner-Metzger, 2006)

Tomato seed is a plant seed and plant seed tissue cells contain a basic eukaryotic cell structure, which includes a nucleus, cytoplasm, and subcellular organelles, all of which are bounded by the cell membrane and cell wall. Fig.1.2 shows diagrammatic representation of a plant cell. A cell's cytoplasm is protected by the cell membrane, which is a thin semi-permeable membrane. A massive central water-filled vacuole, capable of covering 80–90% of the cell's total volume, is enclosed by the tonoplast, a vacuolar membrane, in mature viable plant cells. The biochemical reactions that are required for life take place in membrane-bounded compartments or organelles in plant cells (Taiz & Zeiger, 2006).

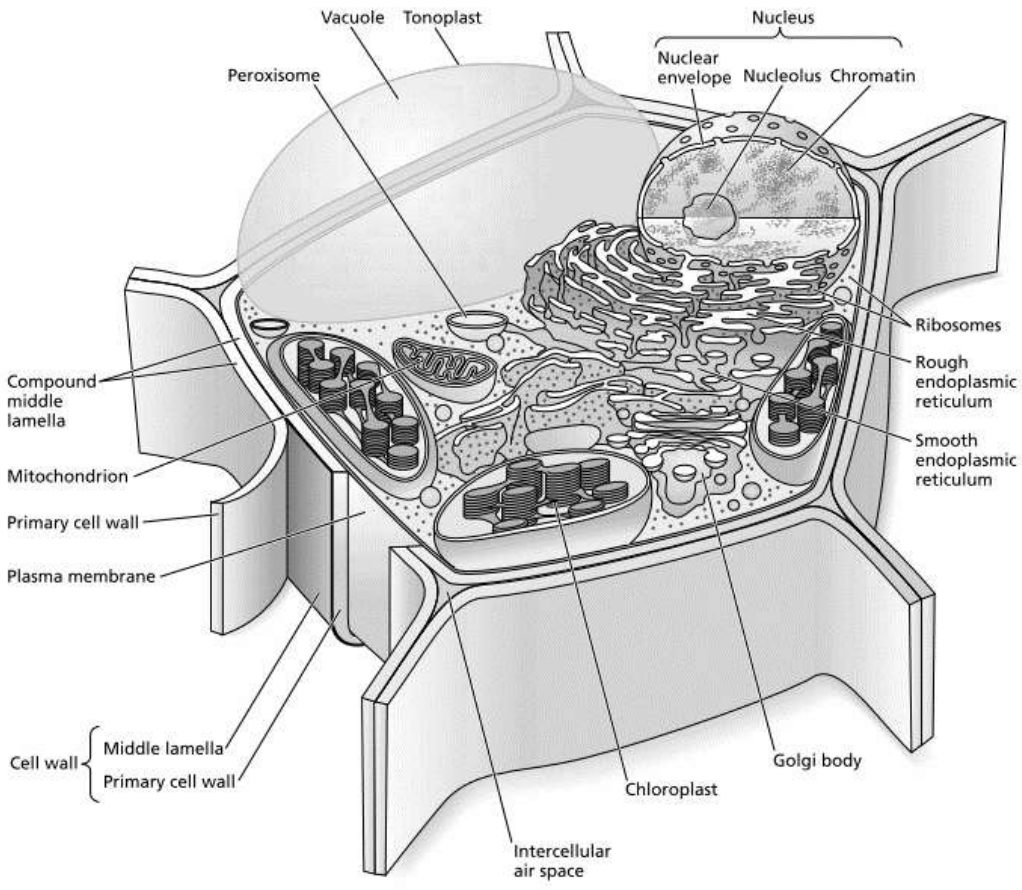

Figure 1.2. Diagrammatic representation of a plant cell (Taiz & Zeiger, 2006)

Environmental stresses, whether natural or artificial, have an impact on the quality of seeds and, ultimately, agricultural production. Cell membranes are one of the primary targets of stress in plants, and alterations in membrane structure can lead to a loss of semipermeability. The cell membrane works as a permeability barrier for proton exchange, and if the membrane's semipermeability is destroyed, the cell's integrity is also lost, resulting in a change in cellular compartmentalization (Taiz & Zeiger, 2006; Vasquez-tello, Zuily-fodil, Thi, & Da Silva, 1990).

1.2 Quinoa

Another focus of the study is to investigate quinoa and its characteristic features.

Quinoa (*Chenopodium quinoa* Willd.) a seed that is characterized as a pseudocereal, which is broadleaf plant and used like cereals. Quinoa, a native of the Andes, has a history of more than 5000 years and dates to the Incan, Aztec, Quechua and Aymara. Quinoa is a member of the Dicotyledoneae class, *Chenopodiaceae* family, Chenopodium genus, and *quinoa* species. *Chenopodium quinoa* Willd. is the botanical name for this plant (Abugoch James, 2009).

Quinoa is an annual plant of Andean region in South America, that grows between sea level and the Bolivian Altiplano, which is roughly 4000 meters above sea level. Although the majority of the quinoa is grown still in South America, it is also harvested in more than 70 countries including China, Europe, Canada, Peru, Bolivia, and India, as well as the United States (Colorado and California) (Abugoch James, 2009). In the years between 2015-2019, the global quinoa production volume amounted to about 163 thousand metric tons in average (FAO, 2021).

Quinoa is a fascinating food because of its wide range of nutritional benefits. Because it is a starchy dicotyledonous seed, it is referred to as a pseudocereal rather than a cereal. Because of the high quality and nutritional content of its proteins, this seed has received a lot of attention. It is a nutritionally balanced food that contains high amounts of protein, the essential amino acid lysine, carbohydrate, essential fatty

acids, bioactive compounds, and minerals. Moreover, quinoa does not contain gluten, so it can be a gluten-free alternative for celiac patients. Table 1.1 compares the nutritional values of quinoa to rice and wheat, which are two of the most important foods in both human and animal nutrition around the world (Abugoch James, 2009; Nowak, Du, & Charrondière, 2016; Vilcacundo & Hernández-Ledesma, 2017).

Table 1.1. Comparison of the nutritional values of quinoa, wheat and rice (Vilcacundo & Hernández-Ledesma, 2017)

Nutrient	Quinoa, raw	Wheat	Rice
Energy (kcal)	357–368	340	354
Total protein[a]	13.1–16.7	11.3	6.8
Total fat[a]	5.5–7.4	1.7	0.7
Carbohydrates[a]	59.9–74.7	63.7	79.7
Fiber[a]	7.0–11.7	12.2	0.6
Ash[a]	2.7–3.8	1.5	0.5
Minerals[b]			
Ca	27.5–148.7	35.0	22.0
Fe	1.4–16.7	5.0	1.4
Mg	26.0–502.0	103.0	NA
P	140.0–530.0	393.0	119.0
K	696.7–1475.0	478.0	80.0
Na	11.0–31.0	2.0	31.0
Zn	2.8–4.8	3.7	0.6
Cu	1.0–9.5	0.4	0.1
Vitamins[b]			
Ascorbic acid (C)	4.0–16.4	ND	ND
α-Tocopherol (E)	2.6–5.4	1.4	0.7
Thiamin (B_1)	0.3–0.4	0.5	0.2
Riboflavin (B_2)	0.3–0.4	0.1	0.1
Niacin (B_3)	1.1–1.5	5.1	4.4
Pyridoxine (B_6)	0.5	0.3	0.3
Folate	0.2	0.1	0.1
Essential amino acids[c]			
His	1.4–5.4	2.4	2.4
Ile	0.8–7.4	4.3	4.3
Leu	2.3–9.4	8.3	8.3
Lys	2.4–7.8	3.6	3.6
Met	0.3–9.1	2.4	2.4
Cys	0.1–2.7	2.1	2.0
Phe + Tyr	2.7–10.3	8.7	8.7
Thr	2.1–8.9	3.6	3.6
Trp	0.6–1.9	1.2	1.2
Val	0.8–6.1	6.1	6.1

[a] g/100 g edible material.
[b] mg/100 g dry matter.
[c] g/100 g protein.
NA: not available; ND: not detected.

Starch grains are found in the perisperm cells, while lipid and protein occupy the endosperm and embryo tissue storage components. The embryo also contains ash, fiber and saponins. Quinoa seeds contain carbohydrate in the range of 48-69%, protein in the range of 14-18% and lipid in the range of 4.4-8.8%. Quinoa seed is demonstrated in Fig.1.3 (Abugoch James, 2009).

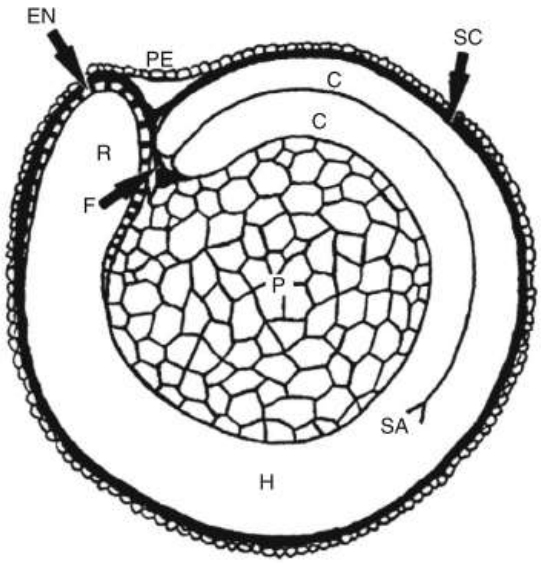

Figure 1.3. Medial longitudinal section of quinoa seed. It represents pericarp (PE), seed coat (SC), hypocotyl-radical axis (H), cotelydons (C), endosperm (EN) (in the micropylar region only), radicle (R), funicle (F), shoot appendix (SA) and perisperm (P).(Abugoch James, 2009)

Starch is the major component of quinoa carbohydrate, which comprises more than 50% of the dry weight. Quinoa starch includes two polysaccharides: amylose and amylopectin. Quinoa starch has a low amylose content, which is close to the amylose content of rice and higher than amylose content of barley. Quinoa starch contains in the ranges from 3% to 20% amylose and the amylopectin content higher than 70%, leading to highly branched structure. In quinoa starch, the amylopectin content is higher than amylose content. Quinoa amylopectin owns a unique chain length distribution, a large number of short chains and a small number of longer chains

compared to other cereal starches. Thus, it is attributed as amylopectin type short chain branched glucan. Quinoa starch has a very small granule size, and it is determined to be in 0.4 - 2μm. The quinoa seeds are small, polygonal shaped and flat seeds which are usually in pale yellow but can range from white to black or pink to red color (Abugoch James, 2009; Lindeboom, Chang, Falk, & Tyler, 2005).

The amount and characteristic molecular structure and small granule size of quinoa starch gives quinoa starch different physiochemical properties such as swelling, solubility, pasting, gelatinization, and retrogradation (S. Wang & Zhu, 2016).

There are many quinoa related products including bread, sourdough bread, Chinese steamed bread, pasta, snacks and cookies quinoa starch-based film, quinoa protein-based film and quinoa starch-based stabilizer for pickering emulsions (S. Wang & Zhu, 2016). The moisture content of quinoa is ranging from 4.6 to 25.8% on dry basis (Vilche, Gely, & Santalla, 2003).

1.2.1 Starch

Starch is one of the major carbohydrate reserves in the world. It is a principal food storage media in green plants for photosynthesized sugars (Kim, Kim, & Baik, 2012). Starch is a widely available polysaccharide molecule that is found in nature and is biodegradable, inexpensive, and renewable. The plentiful sources of starch include cereal (corn, oat, rice, wheat, millet, barley, rye and sorghum), pseudocereal (quinoa, buckwheat, amaranth), legume (lentil bean, navy bean, green pea, grass pea, soybean, and other various beans), root and tuber (cassava, potato, sweet potato, yam, and cocoyam) and unripe fruits (mango, banana, plantain, and pawpaw) and etc. (Ashogbon & Akintayo, 2014). Seeds, roots, tubers, as well as stems, leaves, fruits, and even pollen, contain starch granules. In food and non-food industry, it has been used for thickening, stabilization, gel-formation, retention of water, and coating or glazing (Ashogbon & Akintayo, 2014; Kim et al., 2012).

1.2.2 Starch Structure and Properties

Starch is a polysaccharide of glucose and occurs in the form of granule, comprising amylose and amylopectin. The content ratio of amylose and amylopectin is 15-30% and 70-85%, respectively. This ratio of amylose and amylopectin is dependent on the origin of the plant. Corn starch is generally categorized depending on the amylose content such as waxy for lack of amylose, normal for 20–35% amylose or high-amylose for higher than 40% amylose content. This categorization also depends on the origin of the plant. Amylose is a linear chain which contains α-(1,4) linked D-glucose units. Whereas amylopectin is a highly branched polymer which contains α-(1,4) and α-(1,6) links and is arranged in double helix configuration, which brings out crystallinity. Fig.1.4 shows the amylose and amylopectin chemical structure (Kim et al., 2012). In starch-water interactions, amylose has a strong tendency to retrograde and leads to stiff gel, while amylopectin is more stable against retrogradation and leads to soft gels (Ashogbon & Akintayo, 2014).

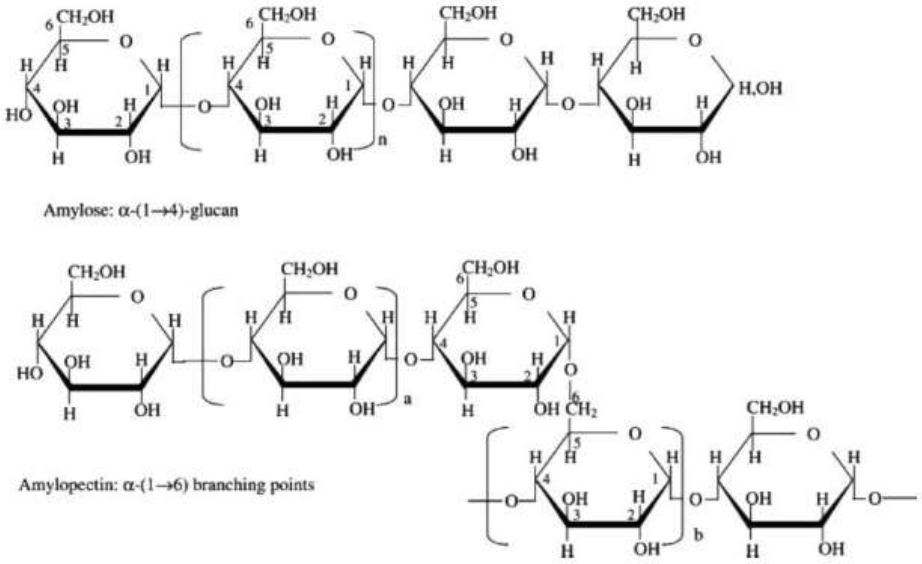

Figure 1.4. Chemical structures of amylose and amylopectin (Kim et al., 2012)

As shown in Fig.1.5, amylopectin molecules contain three types of chains: A, B and C chains. A chain has a relatively low degree of polymerization and attached itself to other B or C chain and do not allow new branches to grow over itself. B chain allows new branches to rise and has a relatively higher degree of polymerization. C chain is the backbone and is the only one containing a reducing end with an average polymerization degree (Kim et al., 2012).

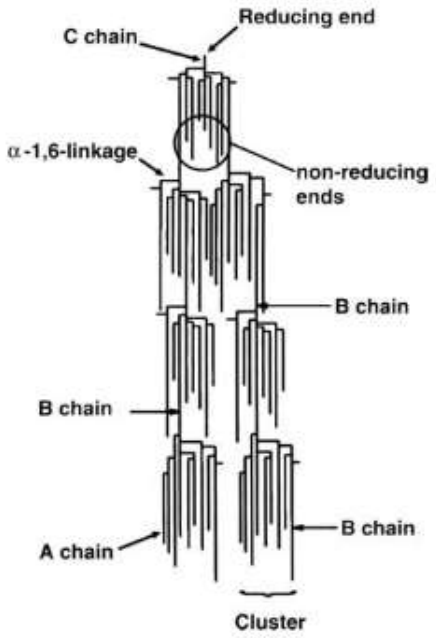

Figure 1.5. The cluster model of amylopectin (Kim et al., 2012)

Starch granules contain semi-crystalline and amorphous growth rings. Thickness of semi-crystalline growth ring increases as the amylose content increases. Amorphous lamellae are accounted for the branch point regions of amylopectin molecules, while crystalline lamellae correspond to the amylopectin chain clusters. These clusters are occurred through double-helical interactions of branch chains and accounted for the semi-crystalline nature of starch granules (Kim et al., 2012). Figure 1.6 shows the schematic representation of crystalline and amorphous lamellae in the starch granule (Patindol, Siebenmorgen, & Wang, 2015).

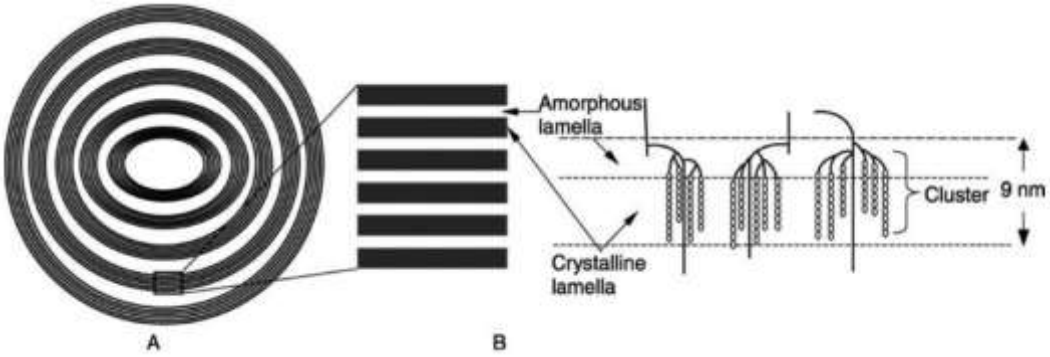

Figure 1.6. Schematic representation of a starch granule: (A) concentric semi-crystalline and amorphous growth rings of a starch granule, (B) the crystalline lamella comprising amylopectin branch points and crystalline lamella comprising double-helix chains (Patindol et al., 2015)

According to the packing configuration of amylopectin double helices, A-type, B-type, or C-type starches are formed. Packing configuration of amylopectin double helices of A-type crystalline structure is denser than the one of B-type as starch enclosing a helical column of well-ordered water molecules (Buléon, Colonna, Planchot, & Ball, 1998). C-type starch contains both A-type and B-type crystalline structures. The ratio of A-type starch to B-type starches affects some functional properties of starch such as the gelatinization behavior, pasting property, crystallinity or swelling (Kim et al., 2012).

Physical properties of starch are mostly determined by the structure of amorphous and crystalline regions within the starch. Significant properties of starch contain granule swelling, gelatinization, pasting and retrogradation. Swelling occurs through water absorption and subsequent granule disintegration. When starch granules are heated in excess water, the semi-crystalline structure is destroyed, and water molecules bind to the amylose and amylopectin molecules via H-bonds. Thus, water absorption of starch molecule leads to destruction of crystallinity and following amylose leaching. As a result of swelling, granule size of starch increases and the degree of swelling is influenced by amylose-amylopectin ratio, chain length and molecular configuration. Swelling is a reversible process until reaching a 30%

increase in the volume. It is a first step in other pasting properties of starch (Alcázar-Alay & Meireles, 2015).

When native starch granules are heated to high temperatures in excess water, a phase transition occur known as gelatinization. Gelatinization can be described as the breakdown of molecular order of starch granule by interruption of H-bonds resulting in complementary and irreversible effects including swelling, melting of crystallites, loss of birefringence, solubilization of starch, and viscosity development (Biliaderis, 2009).

1.3 Physical Treatments Applied on Seeds and Grains

Plant seeds are usually affected negatively by salt, drought, high or low temperature, disease causing organisms such as viruses or other adverse stresses. In this study, tomato seeds are exposed to some physical treatments which are high hydrostatic pressure (HHP), ultrasonication (US) and osmotic stress (OS). These treatments will be covered in more detailed.

High hydrostatic pressure (HHP), ultrasonication (US) and heat treatment are applied on quinoa starch. These treatments resulted in modifications on the starch structure.

Native starch are unstable molecules under different temperature, pH, and shear conditions. This property of native starch causes limited use in the food industry. In order to enhance its functional properties and to make it more stable, different modification methods are commonly applied (Chiu & Solarek, 2009; Pei-Ling, Xiao-Song, & Qun, 2010). Modification is significant for improving positive features and depressing negative features of the starch. Starch modification provides higher stability, increase in resistant starch content, desired viscosity, and gelatinization time of starch, improved paste or gel texture, enhanced film formation, improved adhesion, improved emulsion stabilization and freeze-thaw stability. Furthermore, starch modification can inhibit the retrogradation and syneresis tendency of unmodified starch (Chiu & Solarek, 2009; Kaur, Ariffin, Bhat, & Karim, 2012).

Modified starch derivatives have a very huge market in the food industry such as thickening and gelling agent, stabilizer, emulsifier, encapsulating agent, adhesives and in the paper industry, in cosmetic industry and in plastics (Chiu & Solarek, 2009). In food industry, modified starches can be used in various products such as bakery products, infant foods, ready to eat foods, ice creams, confectionary products, high resistant starch-low glycemic index containing foods, soups, fat replacers and soft drinks (Biliaderis, 2009; Chiu & Solarek, 2009). In industry, modification of starch has evolved new processing technologies and new market trends. Modified starches are adopted to enhance product aesthetic, decrease the production costs, increase product consistency, increase product shelf life and giving market advantage in a new product (Kaur et al., 2012). In the last decades, various ways have been used for modification of starch to create desired functions for various applications. Modification of starch can be performed through physical, chemical, enzymatic, biotechnological methods or with their combinations (Chiu & Solarek, 2009; Kaur et al., 2012).

Physical Modification is the most widely used modification method in response to the growing demand for the functional modified starches in the industry. Starch modification via physical methods gained much interest especially because of its safety for human health. It is simple and inexpensive. It is also regarded as environmentally friendly since it does not demand any chemical or biological agent (Ashogbon & Akintayo, 2014).

Mainly, there are three types of physical methods used for starch modification: pre-gelatinization, hydrothermal and non-thermal processes. In physical modification, molecular structure of starch is destroyed or sustained (Ashogbon & Akintayo, 2014).

Pre-gelatinization is defined as cooking starches that have been completely gelatinized and dried. It leads to breakdown of granular structure and thus disintegration of the molecule. Pre-gelatinized starch provides increase in water solubility and absorption in cold water dispersions which makes possible instant starch slurries without heating. The methods used for pre-gelatinization include drum drying, spray drying, and extrusion

cooking. The source of starch, cooking and drying conditions affect the functional properties of pre-gelatinized starch (Ashogbon & Akintayo, 2014).

Hydrothermal methods include ANN (Annealing) and HMT (Heat-moisture treatment) which preserve the molecular structure of the starch. Both methods performed at temperatures higher than glass transition temperature but lower than the gelatinization temperature. ANN is used when starch is in excess water (40-55% or <65% (w/w)) whereas HMT is used when moisture level is low (Ashogbon & Akintayo, 2014).

Physical and chemical modification of starches are commonly applied in order to eliminate the lack of stability of native starch under process conditions, to increase the resistant starch content and to decrease viscosity and gelatinization time (Pei-Ling et al., 2010).

Non-thermal modification methods are gaining attraction since they keep the nutritional value and organoleptic properties of the products in addition to the extension of the shelf life of the products unlike traditional methods. Traditional methods used to inactivation of microorganisms result in loss of nutritional value besides asthetics corruption. Non-thermal methods include high pressure, ultrasound, microwave and electric pulses. In high hydrostatic pressure (HHP) technology, it is studied that pressure levels between 400-600 MPa increased the starch functinality. The HHP treatment reduces the swelling power of starch granules, resulting in a lower viscosity than heat processed starches (Ashogbon & Akintayo, 2014). Effect of HHP on starch is further discussed in part 1.3.1.3. Ultrasound can destroy the crystalline region of starch granule according to the previous studies (Jambrak et al., 2010). Effect of ultrasound on stach is further discussed in part 1.3.2. Electric pulses cause irreversible disruption of cell mebranes depending on the treatment conditions (Ashogbon & Akintayo, 2014).

Chemical modification mainly relies on introducing functional groups to the starch granule to alter the physicochemical properties. Methods used for chemical modification include derivatization which are acetylation, cationization, oxidation, acid hydrolysis, and cross-linking. However, the use of these methods are restricted

in terms of human health concerns. A new approach termed dual modification is gaining atraction, and it combines the use of both physical and chemical agents, such as microwave-assisted acetylation or HHP-assisted phosphorylation (Ashogbon & Akintayo, 2014).

Enzymatic modification mainly uses hydrolyzing enzymes to alter starch functions. There are many enzymes discovered for enzymatic modification. One of them is amylomaltase which breaks an α-(1,4) bond between two glucose units and make a new α-(1,4) bond. It is used to form thermoreversible gels. Syrup whether glucose or high fructose corn syrup is one of the product obtained by enzymatic modification. Enzmatic modification method is used in food industry, cosmetic and pharmaceutical industry, and detergants.

1.3.1 High Hydrostatic Pressure (HHP)

The high-pressure process (HPP) is a nonthermal method that was first utilized for food processing in 1882, with effective starch to glucose conversion. Hite was the first to use this method for inactivation of microorganisms and extension of shelf life, in 1899. The researcher employed 680 MPa pressure to milk using a hydraulic press and ensured at least 1 day of preservation compared to raw milk. Between Hite's findings and the introduction of HHP as a commercial food stabilizing method, a significant time has elapsed. The principal reason for this was the necessity to create materials that could work at larger pressures (up to 1000 MPa) for longer periods of time and, eventually, at higher temperatures (Augusto, Tribst, & Cristianini, 2018).

After first studies of Hite, the first commercial HHP-processed food items, fruit jams, were sold in Japan in the 1990s. In 1914, Prof. P.W. Bridgman introduced the alteration of egg white protein. Later in 1973, Macfarlane remarked on the possibilities of HHP process for meat tenderization. In 1991, Japanese fruit juice producers implemented semicontinuous high-pressure equipment for citrus juice

bulk processing, as well as yogurts, fruit jellies, salad dressings, and fruit sauces (Rahman, 2007; Yamamoto, 2017).

For microbial inactivation, traditional thermal processes applied affect adversely the color, flavor, and nutrition of the food. When heat treatment is applied, chemical processes occur resulting in the production of new color and flavor components as well as the loss of beneficial components. HHP, on the other hand, does not speed up chemical reactions and it causes physical changes in molecules on a microscale and/or macroscale. Active heating does not used in the HHP treatment, although passive heating and cooling via adiabatic compression and decompression are unavoidable. The HHP process, on the other hand, reduces the damage and inactivates microorganisms to generate quality, safe foods (Yamamoto, 2017).

When it comes to energy usage, thermal process requires relatively high energy, since it necessitate continuous heat input and output. In contrast to thermal process, HHP is environmentally friendly since it does not require any additional energy to maintain the pressure without leakage after it was raised once (Yamamoto, 2017).

Due to its benefits of retaining the quality and organoleptic features of foods, high hydrostatic pressure (HHP), which is regarded one of the most important advances in food processing in the last 50 years, has become a reality in the food industry and has spread worldwide. HHP is today the most important nonthermal technology for food processing, with annual market sales of US$2.5 billion and around 125 pieces of industrial HHP equipment for food processing were in production by the middle of 2008, with nearly 85 percent of them installed after 2000 (Augusto et al., 2018; Buzrul, 2014)

1.3.1.1 Working Principle

The HHP process is an isostatic pressure process, based on Le Chatelier principle. The isostatic principle is demonstrated in Figure 1.7. It assumes that pressure is exerted uniformly in all directions, therefore pressure is distributed uniformly and

instantly, regardless of the composition, size, or shape of the food and when the pressure is released, the food product returns to its original shape. This approach ensures that there are no pressure gradients in the process and that nonporous foods retain their shape following HHP (Rahman, 2007; Yamamoto, 2017).

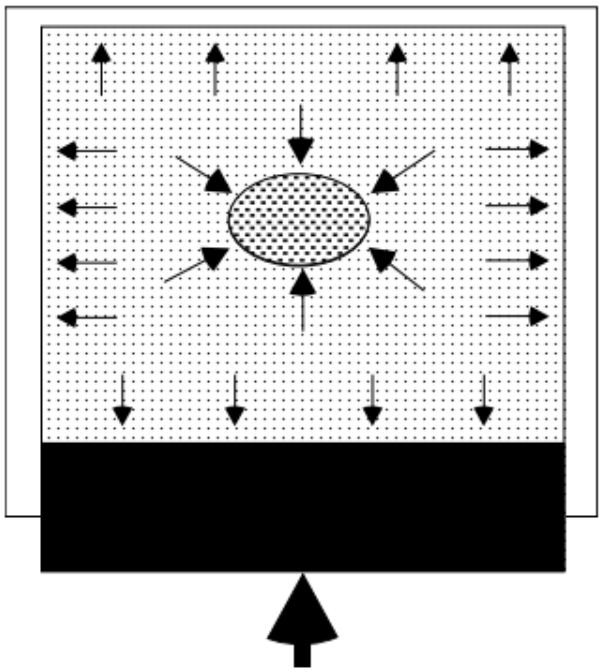

Figure 1.7. Isostatic processing principle (Rahman, 2007)

A high-pressure system includes a high-pressure vessel and its closure, as well as a pressure producing system, a temperature control device, and a material handling system. Once the pre-packed sealed food is placed into the chamber and closed, pressure transmitting medium (water or oil) fills the chamber. For packing procedure, ethylene-vinyl alcohol copolymer (EVOH), polyvinyl alcohol (PVOH) films and much rarely from multilayer plastics and aluminum packages are chosen and designed to fill the chamber volume. Uniform distribution of pressure prevents any deformation in the package. Air is removed from the vessel and high hydrostatic pressure is generated. Pressurization occurs either directly (through a piston) or indirectly (by transmission of pressurized fluid inside the chamber until the

necessary pressure is reached). Direct compression system has some limitations in the piston's high-pressure dynamic seal with the internal surface of the chamber, thus in industrial isostatic pressing systems, indirect compression is used mostly. High pressure generation system by direct and indirect compression is presented in Fig.1.8 (Rahman, 2007).

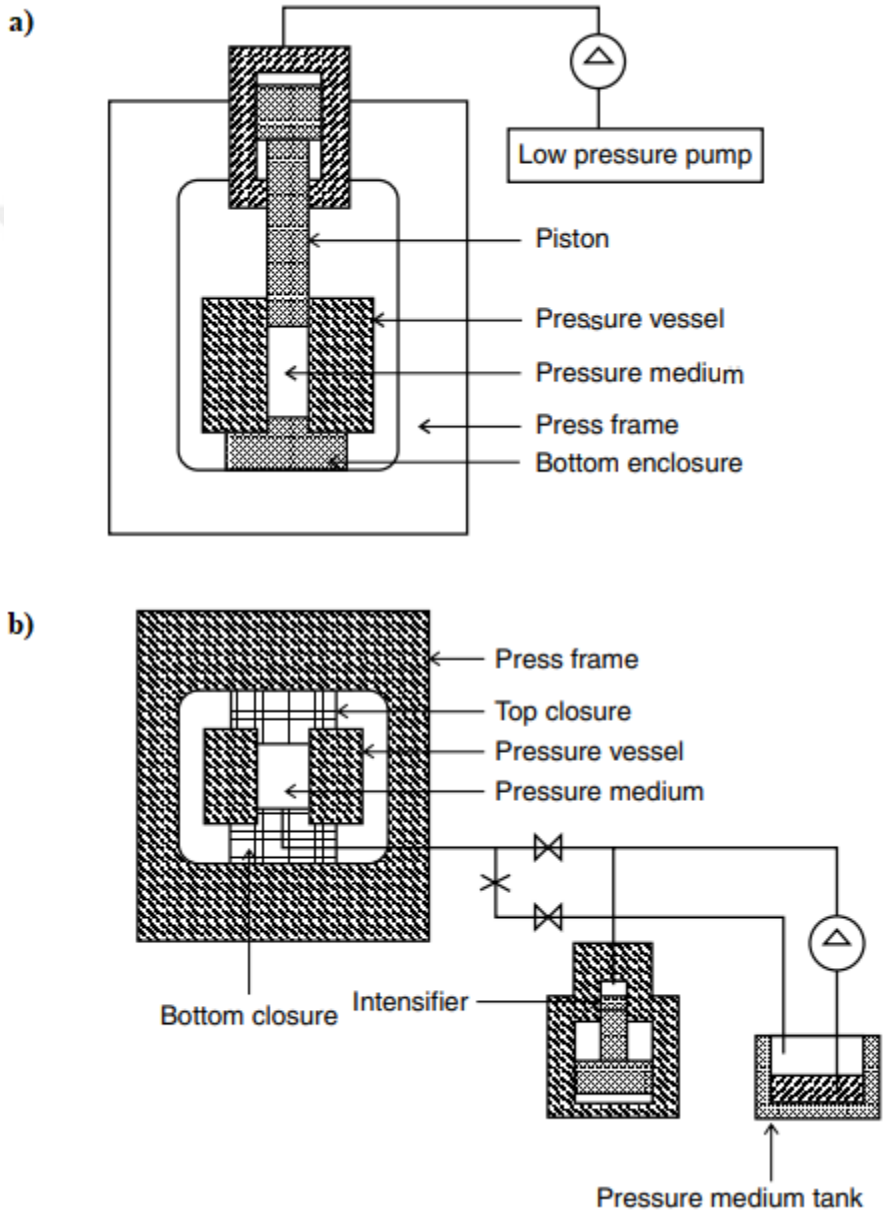

Figure 1.8. Schematic diagram of high pressure generation by direct (a) and indirect (b) compression of the pressure transmitting medium (Rahman, 2007)

The HHP treatment has been investigated from the perspectives of microbiological safety, physiological changes and biochemical changes in the food component (Yamamoto, 2017).

The two main effect of HHP, effect on microorganisms and starch gelatinization, will be detailed in the following chapter.

1.3.1.2 Effect of HHP Treatment on Microorganisms

Food preservation is largely concerned with the inactivation, growth retardation, or prevention of spoilage and pathogenic bacteria. Heat treatment has been used as a conventional treatment for inactivation of microorganisms. High hydrostatic pressure is used as a food preservation technology for microbial inactivation with minimal degradation of food components. In the HHP induced microbial inactivation, the change in the permeabilization of the cellular membrane is responsible for microbial death. It disrupts the cell's physicochemical balance. Furthermore, the volume reduction followed by HHP causes restriction in protein and enzyme synthesis, changes in cellular structures, and abnormalities in reproductive and survival system. HHP treatment can be used a secondary pasteurization method for microbial inactivation and extension of shelf life without the use of food additives (Augusto et al., 2018).

In terms of resistance to HHP, bacterial spores are resistant to HHP due to their thick bacterial spore coats and create a challenge for HHP technology. Combination of other treatments with pressure can be used for inactivation of bacterial spores. The resistance of eukaryotic species (such as fungus and protozoa) is lower than that of prokaryotic organisms (bacteria). Gram-positive bacteria are usually more resistant than gram-negative bacteria because their cell wall is more rigid than gram negative ones (Rahman, 2007).

1.3.1.3 Effect of HHP Treatment on Starch

In addition to its sterilization applications, it is commonly used to change the physicochemical structure of food macromolecules, such as starch gelatinization, protein denaturation, and lipid phase transition. The effect of HHP on the change of physicochemical properties of various starches has been researched for decades for various starches of including wheat, barley, corn, potato, oat, lotus root and rice (Pei-Ling et al., 2010; Yamamoto, 2017).

Starch is an essential nutritional food component that serves as an energy source as well as a gel-forming texture modifier. The detailed explanations about structure of starch can be found in titles 1.2.1 and 1.2.2.

HHP has the ability to damage the structure of starches. Reversible hydration of the amorphous phase is followed by irreversible deformation of the crystalline region of the starch granules, in which secondary and tertiary structures are destroyed but covalent bonds remain unchanged, resulting in granular structural disintegration (Pei-Ling et al., 2010).

When the starch is heated enough in the presence of water, heat gelatinization can occur. Gelatinization is usually thought to be a multi-step procedure. Firstly, the amorphous regions of the starch granule are hydrated, inducing swelling of the granule. Following the swelling of the granule, the granule's growth ring structure begins to disintegrate, and the crystalline domains melt with increasing hydration, leading to the destruction of the granule structure. Then, the crystalline region becomes more accessible for water. Increase in particle size and reunion of solubilized amylose led to increase in viscosity and stable gel formation. Besides from heat-induced gelatinization, HHP can also gelatinize starch granules in the starch-water solution, regardless of temperature. Although modest changes in the degradation (or disintegration) of starch granules are observed, the mechanism of pressure induced gelatinization is comparable to that of heat induced gelatinization. In Figure.1.9, starch gelatinization scheme induced by temperature and pressure is

demonstrated. As can be seen in the Fig.1.9, in the presence of excess water, amorphous region becomes hydrated and amorphous lamellae is formed in the crystalline domain, resulting in granule swelling. When the gelatinization temperature is exceeded, the smectic crystalline structure is loosened due to dissociation of helix–helix and formation of helix-coil structure. The disintegration of the macromolecule under pressure is assumed as be incomplete because van der Waals and hydrogen bonds preserved which promotes the helix configuration (Knorr, Heinz, & Buckow, 2006).

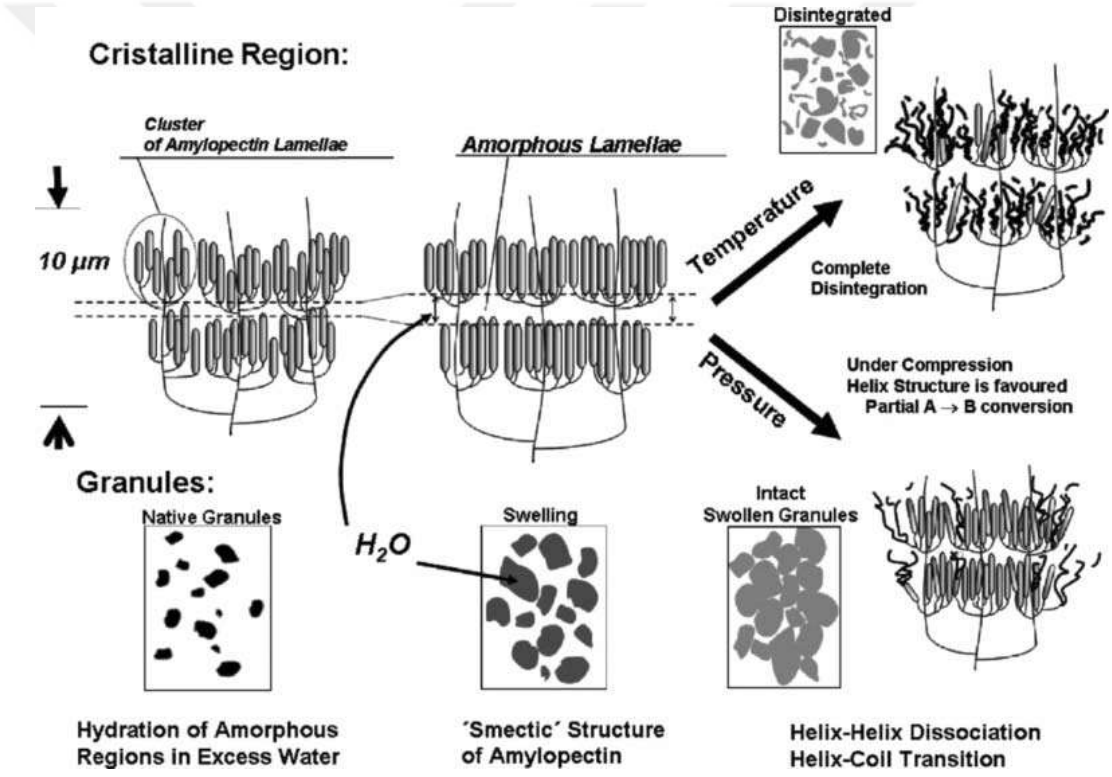

Figure 1.9. Schematic diagrams of starch granule gelatinization induced by either heat or pressure (Knorr et al., 2006)

Unlike heat gelatinization, pressure treated starch granules remain intact or only partially dissolved and amylose has a rather low solubilization rate. It has been considered that the melting of crystalline region is prevented since the amylopectin

in the granule is maintained by the amylose that is still present in the granule. Since limited swelling and decreased amylose leaching reinforce granular structure, the starch granule structure is better preserved after pressure treatment (Choi, Kim, Park, Kim, & Baik, 2009; Douzals, Marechal, Coquille, & Gervais, 1996; Kim et al., 2012; Knorr et al., 2006; Pei-Ling et al., 2010).

According to Douzals et al. (1996), increasing pressure levels resulted in a decrease in the bulk volume of the starch-water suspension, indicating that excessive hydration and permanent swelling of starch granules occurred under HHP (Douzals et al., 1996). Further increase in pressure promotes hydration and swelling of amorphous lamellae in crystalline regions of starch granules. This leads in smectic configurations of amylopectin double-helices in crystal lamellae (Knorr et al., 2006).

In literature, there are many studies related to pressure induced starch gelatinization. Some studies are summarized in Table 1.2.

Table 1.2. Studies in the literature about HHP processing of starch from different plant origins

Starch type	HHP treatment conditions	Starch concentration (w/w)	References
Potato	0-2500 atm	0.40%	(Thevelein, Van Assche, Heremans, & Gerlsma, 1981)
25 starch kind including corn, waxy corn, rice	0–600 MPa; 20℃;15 min	5-58%	(Stute, Klingler, Boguslawski, Eshtiaghi, & Knorr, 1996)
Potato, wheat, tapioca	0–700 MPa	5%	(Bauer & Knorr, 2005)
Potato	600, 800, 1000 MPa	10–70%	(Kawai, Fukami, & Yamamoto, 2007)
Sorghum starch	200-600 MPa; 10 min	60-95℃	(Vallons & Arendt, 2009)
Pea starch	300, 400, 500 and 600 MPa;15 min; 25℃	4%	(Leite, de Jesus, Schmiele, Tribst, & Cristianini, 2017)
Quinoa	300-600 MPa; 25-70℃; 15 min	1:1; 1:2; 1:1; 1:4	(Ahmed, Thomas, Arfat, & Joseph, 2018)
Quinoa and Maize	100-600 MPa; 55-95℃; 5 min	10%	(Li & Zhu, 2018)
Corn starch	400 and 500 MPa;20, 30, and 40℃; 5, 15, and 30 min	10%	(Okur, Ozel, Oztop, & Alpas, 2019)

1.3.1.3.1 Critical Factors of HHP induced Starch Gelatinization

In pressure induced gelatinization, the degree of gelatinization is affected by some critical factors. It can be controlled by adjusting the condition parameters of HHP process such as pressure/temperature, pressure holding time and starch concentration (Kim et al., 2012).

Pressure and temperature are important parameters that affect the rate and degree of the starch gelatinization. With increased treatment pressure, the degree of gelatinization increases. In the presence of excess water, barley and sorghum gelatinizes between 300-600 MPa, wheat starch gelatinized between 300-450 MPa and corn gelatinized between 450-600 MPa pressure ranges. The majority of the experiments are conducted at treatment pressures of up to 600 MPa or 800 MPa. (Pei-Ling et al., 2010). At a given temperature, increasing the pressure level of a starch-water suspension increases the degree of gelatinization. Although HHP treatment of starch granules are performed generally at temperatures between 20 and 30°C, a rise in temperature within a given pressure level also increases gelatinization of starch granules in the starch-water suspension. However, if the pressure is high enough, HHP can gelatinize any kind of starch even at cold temperatures. Thus, a suitable combination of pressure and temperature can maximize the effectiveness of pressure-induced starch gelatinization (Kim et al., 2012; Pei-Ling et al., 2010).

Pressure holding time is another important parameter for pressure induced gelatinization. The degree of gelatinization of starch granules generally rises with pressure holding time at a given pressure and temperature (Kim et al., 2012).

The degree of gelatinization increases as the starch concentration decreased. Heat causes the granules suspended in water to swell, and the degree of swelling varies based on the amount of starch present (Pei-Ling et al., 2010).

Besides these parameters, starch crystalline structure also affects the starch gelatinization under pressure. The B-type crystalline structure is more resistant to HHP treatment than C-type and the A-type crystalline structure. This difference may

be attributed to having helical column of organized water molecules of B-type crystalline structure which have a reduced compressibility than A-type crystalline structure which have water molecules randomly dispersed within amylopectin double helices. Furthermore, the differences between pressure resistances of A-type and B-type starch granules may be also attributed to the variations in the amylopectin branch chain structures. In comparison to B-type starch granules, A-type starch granules have more distributed amylopectin branch structures, increasing the flexibility of the crystalline structures. As a result, the A-type crystalline structure appears to be more vulnerable to HHP treatment than the B-type crystalline structure. HHP treatment changes the polymorphism of the starch from A-type to B-type which is more stable to pressure (Kim et al., 2012).

1.3.2 Ultrasonication (US)

Ultrasound has lately emerged as a novel food processing technology, over the several accessible traditional technologies. The reason of this interest is related with the non-thermal nature, nondestructive characterization, low energy consumption, minimum degradation of food and production of less toxic compounds (Malik, Erginkaya, & Erten, 2019; Rahman, 2007).

Ultrasound is based on the cavitation, which occurs during compressions and rarefactions of ultrasonic waves. Various chemical and mechanical reactions in food matrix are caused by the production of implosive bubbles at the microstructural level, as well as in the bulk (Malik et al., 2019).

Ultrasound waves are sound waves produced in certain frequency ranges. Ultrasonic waves are comparable to sound waves; however, their frequencies are much higher than the upper limit of the human ear, above 18 kHz. The fundamental parameters of ultrasound are wavelength, frequency, and velocity. Wavelength is the distance of wave which travels in the medium, frequency is the number of oscillations per unit

time and velocity is dependent on the physical properties of the medium (density, etc.) (Malik et al., 2019)

Ultrasound is usually separated into three frequency bands. High power ultrasound operates at frequencies ranging from 16 to 100 kHz (1 Hz equals 1 cycle/s), high-frequency ultrasound operates at frequencies ranging from 100 kHz to 1 MHz, and diagnostic ultrasound operates at frequencies ranging from 1 to 10 MHz (Jambrak et al., 2010; Mason, Paniwnyk, & Lorimer, 1996).

High power ultrasound employs at low frequency, 16-100 kHz. It is used for food operations such as freezing, emulsification, extraction and drying to estimate the physical, chemical, and biochemical changes by cavitation and mainly for cleaning purposes. Low power ultrasound employs at high frequency, higher than 100 kHz. It is used for food operations such as dispersing aggregated materials, generating emulsions and disrupting cells (Malik et al., 2019).

Ultrasound spreads as vibrations through wave direction. These vibrations result in molecules to shift and oscillate from their original positions. Ultrasound waves go through a series of compression and rarefaction cycles, causing physical and chemical changes in the medium they propagate. Wave motion transmits energy from one location to another without transmitting material. The major factor that causes changes in the medium is frequency. Other elements that determine the nature of the ultrasonic wave are wavelength (m), frequency (Hz), amplitude (m), velocity (m/s), and intensity (W/cm^2) (Malik et al., 2019).

The most well-known consequence of ultrasound in liquid media is cavitation. When a powerful sound wave propagates through a liquid, it causes compression (positive pressure) and rarefaction (negative pressure). A cavity or bubble can grow in the liquid if the negative pressure during rarefaction is strong enough. Cavities are divided into two categories: transient (also known as "inertial") and stable (also known as "noninertial"). Each one shows a different form of gas bubble activity when it is exposed to an ultrasonic field. These bubbles formed during cavitation collapse and triggers physical, chemical, and thermal changes. Physical changes

include pressure, turbulence, and shear forces. The chemical effects, however, comprises free radical generation. including shear, turbulence, and formation of reactive radicals. Shock waves, produced because of the pressure change, cause bacterial cell membranes to disrupt, resulting in cell lysis. In Figure 1.10, cavitation phenomenon is demonstrated (Malik et al., 2019; Rahman, 2007).

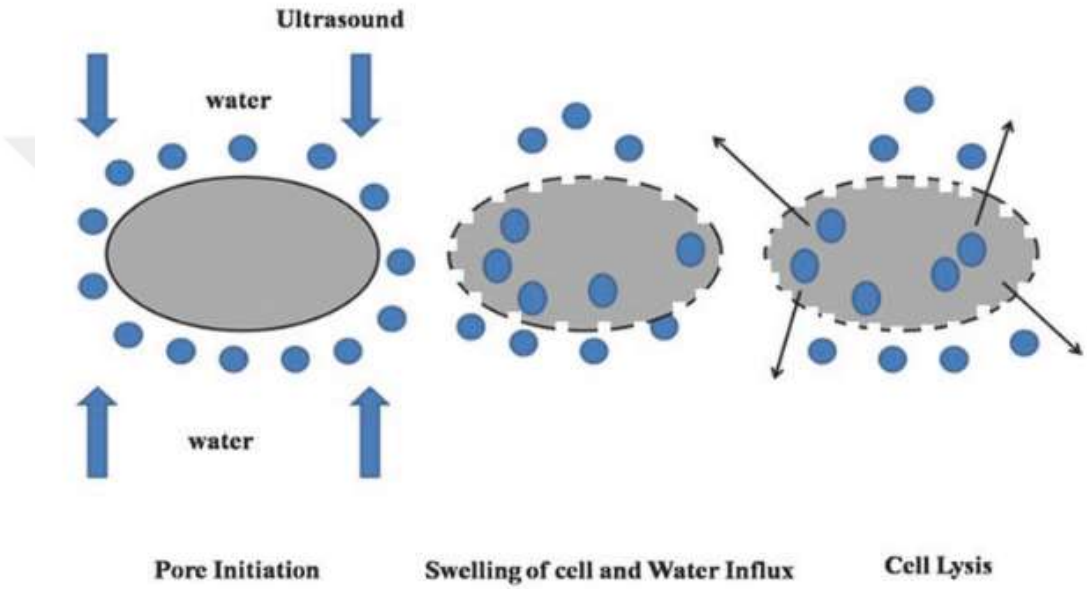

Figure 1.10. Cavitation phenomenon (Malik et al., 2019)

Ultrasound energy is generated by a system consisting of a transducer and a processor. Electrical energy is converted to mechanical energy by the transducer and the ultrasonic processor converts the received mechanical signal back to an electrical signal, which is then digitized. There are mainly three types of transducers which are fluid-driven, magnetostrictive and piezoelectric transducers. The vibrations created by the transducer are enhanced and sent to a sonotrode or probe in direct contact with the fluid (Jambrak et al., 2010; Malik et al., 2019).

There are three ways that ultrasound can be used on food: direct application, coupling with device and submerge in an ultrasonic bath. Ultrasound can be utilized to improve the inactivation performance of food preservation when combined with other methods. The main ultrasound application methods are ultrasonication, thermosonication, manosonication and manothermosonication (Malik et al., 2019).

Ultrasound treatment has used in food industry for many purposes such as microbial inactivation, sterilization/pasteurization, spore inactivation (in combination with pressure), enzyme inactivation, extraction of bioactive, degassing, crystallization, freezing, thawing, cooking, filtration, starch polymerization, fat separation, emulsification/homogenization, brining, pickling, marinating, extrusion. In Table 1.3, type of ultrasound effect in food industry and the possible results are reviewed (Mason et al., 1996).

Table 1.3. Ultrasound in food technology (Mason et al., 1996)

Type of Effect	Result
Effect on living cells	Stimulation of cell activity Sonochemical cell destruction (microbial inactivation)
Effect on enzymes	Stimulation of cell activity Controlled denaturation
Effect of 'jet' impact on surface	Improved impregnation Improved extraction
Other applications	Meat processing Crystallization and freezing Emulsification Filtration and drying Rice grain treatment

Ultrasound treatment can alter the starch granule structure due to cavitational forces. As compared to conventional procedures, ultrasound treatment causes to a milder temperature increase in the medium. The intense shear force encountered by the starch molecule in the shearing valve is primarily responsible for the ultrasound-induced breakdown of starch. Ultrasound treatment disrupts the crystalline region of the starch granule before reversible swelling of the amorphous phase. This leads to destruction of the granular structure. Thus, ultrasound treatment is used for the starch modification purposes (Jambrak et al., 2010).

1.3.3 Osmotic Stress (OS)

Osmotic stress is a physiologic malfunction induced by osmotic dehydration. Osmotic dehydration is an operation of water removal from plant tissues by immersing in a concentrated aqueous solution (hypertonic solution). In osmotic dehydration, mass transport of water and solute are observed in combination. The driving force for mass transfer is the concentration gradient between the aqueous solution and the intracellular fluid. Water is removed from a lower concentration of solute to a higher concentration through a semipermeable membrane, ensuring equilibrium in both sides of the membrane (Fig.1.11). The solutes used in osmotic dehydration are mainly sugar syrup, salt (sodium chloride) or brine (Kumar, Satya, & Singh, n.d.; Rahman, 2007).

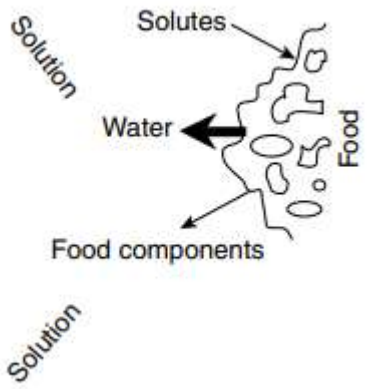

Figure 1.11. Transfer of water and solutes in osmotic process (Rahman, 2007)

During osmotic dehydration, water removal from the vacuole of plant cell leads to separation of semi-permeable membrane, plasma membrane and tonoplast of plant tissue resulting in a process known as plasmolysis. Plasmolysis occurs as a result of loss of turgor pressure. There are two types of plasmolysis: partial and total plasmolysis. When the plasma membrane begins to separate from the cell wall, partial plasmolysis occurs, and total plasmolysis appears when the protoplast is completely separated (Traffano-Schiffo et al., 2017).

Osmotic dehydration is used as a pretreatment method for canning, freezing and other minimal processes for food preservation (Rahman, 2007).

1.4 Analytical Techniques Used to Assess the Effect of Physical Treatments on Seeds and Grains

There are various methods that have been used to characterize starch especially for gelatinization purposes. On this subject, the differential scanning calorimeter (DSC) has been widely used. Other methods commonly used in starch gelatinization include X-ray diffraction, scanning electron microscopy (SEM), transmission electron microscopy (TEM), optical microscopy, Fourier transform infrared spectroscopy

(FTIR), particle size analysis, and rheology tests. However, they do not provide detailed information about the state of the dynamic water and starch-water interactions in the granule. In this field, nuclear magnetic resonance (NMR) is one of the leading successful techniques to analyze state of dynamic water, its distribution and interaction with the surroundings (Kirtil & Oztop, 2016).

1.4.1 Nuclear Magnetic Resonance (NMR) Relaxometry

Nuclear Magnetic Resonance (NMR) relaxometry is widely used for the analysis of physiological and biochemical changes in a huge variety of samples including fruits and vegetables. It is a rapid, non-destructive, and non-invasive method. NMR relaxometry provides both qualitative and quantitative data so that it gained much attraction especially in the food industry. Quantification of water absorption and analyzing its distribution can be carried through NMR instruments successfully (Kirtil & Oztop, 2016).

The main concept of NMR technology is based on nuclear magnetism. Signals are obtained through the alignment of protons (spins) present in the sample. For that purpose, generally hydrogen is used because it is abundant in organic samples such as water and oil and gives the highest signal in NMR (Kirtil & Oztop, 2016; Konez, 2011). In Figure 1.12, the schematic view of the stages of signal acquisition is demonstrated (Kirtil & Oztop, 2016). Protons within the sample are randomly aligned without the presence of an external magnetic field. When the sample is placed into an external static magnetic field (B_0), protons within the sample align with the external magnetic field in z-direction referring to longitudinal magnetization and start to spin at a frequency, which is proportional to the magnetic field strength of the magnet. The protons make a spinning motion called precession in an external magnetic field. When a radio frequency (RF) pulse is applied, some protons align themselves in the opposite direction with B_0, resulting in a decrease in longitudinal magnetization. However, the precessional movement of protons becomes synchronized with one another, resulting increase in transverse magnetization. After

RF pulse is turned off, the protons will turn back to their previous state and a relaxation and a recovery signal is obtained. This process is named as relaxation. To acquire information about the sample, the relaxation of longitudinal and transverse magnetization is examined (Kirtil & Oztop, 2016).

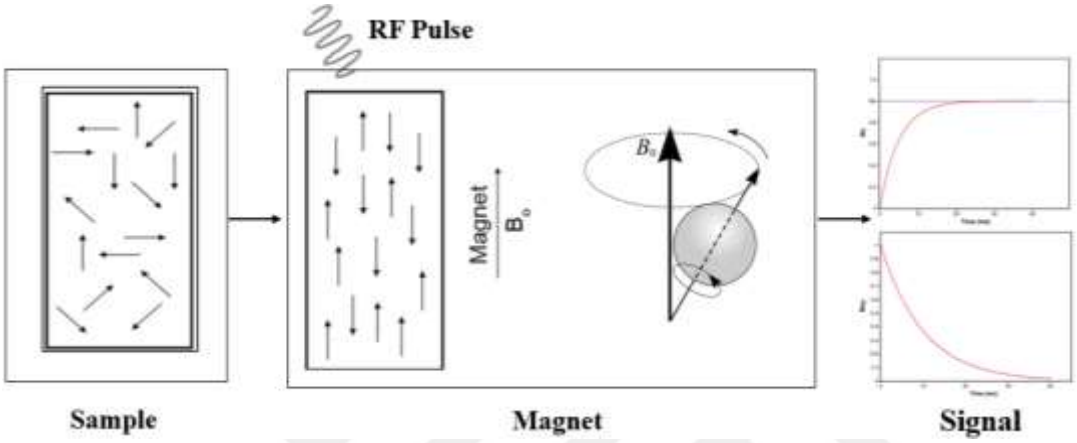

Figure 1.12. Schematic representation of acquiring signal from a sample (Kirtil & Oztop, 2016)

NMR relaxometry provides information about longitudinal (T_1) and transverse (T_2) relaxation times. T_1 is longitudinal relaxation time (spin-lattice relaxation time) is defined as the time of realigning of spins along the external magnetic field axis and derived from the recovery curve of z-component of the magnetization vector. T_2 is transverse relaxation time (spin-spin relaxation time) is defined as the time for decay of transverse magnetization to zero (Fig.1.13) (Kirtil & Oztop, 2016).

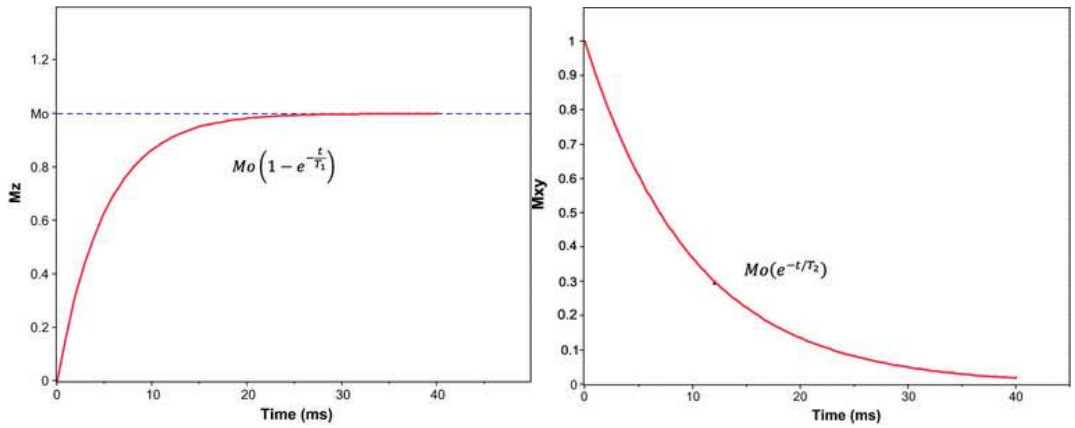

Figure 1.13. Representation of exponential relaxation curve of longitudinal magnetization-T_1 (left), exponential relaxation curve of transverse magnetization-T_2 (right)

When these T_1 and T_2 relaxation curves are analyzed with Non-Negative-Least-Square (NNLS) method, proton pools could be identified which gives knowledge about the mobility of hydrogen molecules in the sample (Kirtil & Oztop, 2016; Ozel, Dag, Kilercioglu, Sumnu, & Oztop, 2017). NNLS is an inverse Laplace transformation provides transformation of the transverse relaxation curves to continuous distributions of T_2 relaxation times, as presented in Figure 1.14 (Hemdane et al., 2017; Unal, Alpas, Aktas, & Oztop, 2020).

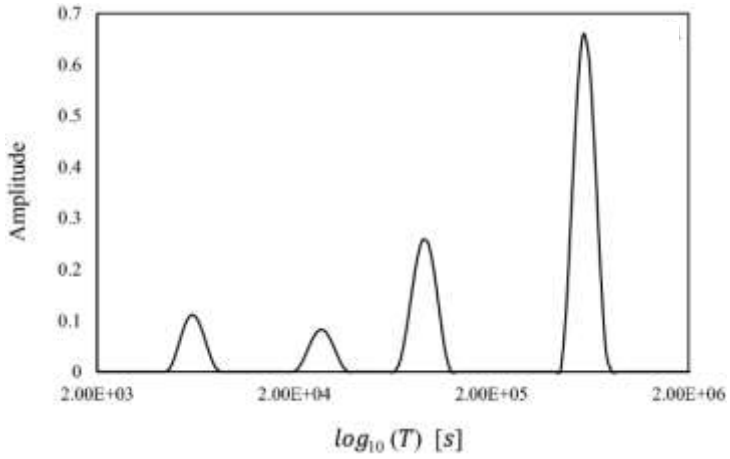

Figure 1.14. T_2 relaxation spectrum of tomato seeds 1 h after soaking with distilled water (Unal et al., 2020)

In the study of plants and plant-based foods, the application of NMR imaging and relaxometry has been demonstrated to be a valuable technique. In plant tissues, the proton signals are dominated by water protons and the proton density of the tissue is proportional to the NMR signal intensity, and accordingly NMR relaxation signals coming from plant tissues provides information about water environments (Unal et al., 2020; Van der Weerd et al., 2001; Westbrook, 1993). It provides the study of physiological changes in plant tissues exposed to natural or artificial stresses by displaying anatomic information of the whole tissue, spatial distribution, and physical properties of water. Physiological changes in plant tissues results variations in cell compartmentalization and water distribution. These variations are investigated by obtaining the relaxation time parameters, T_1 (spin–lattice or longitudinal relaxation) and T_2 (spin–spin or transverse relaxation) (Snaar & Van As, 1992; Van der Weerd et al., 2001; Van, Van Der Weerd, Claessens, Efdé, & Van As, 2002). In compartmentalized systems such as plant cells, proton relaxation is usually a multiexponential process that indicates the existence of numerous water compartments with different relaxation times in a plant tissue (P. S. Belton & Ratcliffe, 1985; B. P. Hills & Clark, 2003). This multiexponential behavior of the relaxation provides investigation of cellular compartmentalization and water

distribution within the plant tissue (Ersus & Barrett, 2010; B. P. Hills & Remigereau, 1997; Marigheto, Vial, Wright, & Hills, 2004; Raffo, Gianferri, Barbieri, & Brosio, 2005). In the plant tissues, researchers have been identified mostly three or four proton relaxation peaks previously. The vacuole, the cytoplasm, and the cell wall were attributed to the first three peaks respectively. The last peak was generally assigned to the protons of starch or non-exchangeable macromolecular protons or extracellular water in plant cells (Musse et al., 2009; Raffo et al., 2005; Sibgatullin, 2005). When the cellular compartmentalization is disrupted, an exchange of water protons occurs between the more mobile intracellular water and the less mobile extracellular water as well as the hydration water of tissue, causing decrease in the T_2 relaxation time (B. P. Hills & Remigereau, 1997; Maheswari, Joshi, Saha, Nagarajan, & Gambhir, 1999). Some of the stresses causing the loss of cellular compartmentalization includes high hydrostatic pressure (HHP), ultrasonication (US) and osmotic stress (OS), as discussed earlier.

NMR relaxometry also used as a characterization measurement tool to analyze the changes occurred during starch-water interactions so that it can be used to investigate starch modification. A variety of studies is employed that analyze starch gelatinization through NMR. One of them studied the effect of different water content, heating temperature and different type of starch with varying crystallinity of amylopectin on starch gelatinization by using NMR and DSC technique. It was observed that water-starch mixtures of ungelatinized samples display two distinct water populations, which are assigned to the water present in the interior and exterior part of the granule. The mass transfer barriers between the two populations weakened by gelatinization, leading to fast water exchange between populations. As temperature increases above gelatinization temperature, the two-water population merge gradually and display one water compartment indicating complete starch gelatinization (Tananuwong & Reid, 2004).

NMR technology has been used extensively in the industry for varying purposes. Postharvest physiology of fruits and vegetables, postmortem muscle, cereals, dough,

and baking processes are investigated by NMR measurements. In dairy industry, it is also used extensively (Kirtil & Oztop, 2016).

1.4.2 Fourier Transform Infrared (FTIR) Spectroscopy

Fourier transform infrared (FTIR) spectroscopy is a technique, which brings out infrared spectrum of absorption, emission, and photoconductivity of solid, liquid, and gas. It is used to identify functional groups in organic and inorganic compounds (Berna, 2016; Sindhu, Binod, & Pandey, 2015)

FTIR spectrum gives bands between 4000 and 400 cm^{-1} and the peaks observed in that region are associated with specific functional groups. In Table 1.4, there is relevant information about bands found in FTIR spectra of starches and their assignments (Torrenegra, Solano, Herrera, León, & Pajaro, 2018).

Table 1.4. Band assignments in FTIR spectra of starches (Torrenegra et al., 2018)

Band (cm^{-1})	**Assignment**
3300	O-H stretching vibration
2947	−CH2 stretching vibrational modes
1740	carbonyl (C=O) stretching vibration
1690	Angular O-H bending of water molecules
1152	Anti-symmetric stretching of the C-O-C
1080	Stretching vibration of the C-O
1010	Anhydroglucose ring O-C stretch

1.4.3 Differential Scanning Calorimetry (DSC)

Differential Scanning Calorimetry (DSC) is a thermal analytical technique that is used to determine the thermal properties of a sample by measuring the heat capacity

change by temperature. It provides the evaluation of properties such as glass transition temperature, melting, crystallization, specific heat capacity, cure process, purity, oxidation behavior, and thermal stability (Elmer, 2014; Gill, Moghadam, & Ranjbar, 2010; Spink, 2008).

Differential Scanning Calorimetry (DSC) is the most common thermal analytical method used on a large scale in different areas such as polymers, food, pharmaceuticals, agriculture, and manufacturing for research and development, quality control and testing (Karoui, 2012)(Elmer, 2014; Spink, 2008).

In a typical DSC experiment, energy is supplied to the sample and reference simultaneously. As the temperatures of the sample and reference increases over time, energy input is required to match the temperature of the sample to that of the reference. The difference in the input energy provides the amount of heat absorbed or released by the sample, which result in endothermic or exothermic process, respectively. As in Figure 1.15, excess heat is required to match the same temperature of the reference (Gill et al., 2010). The area under the peak is refers to the enthalpy change (ΔH) and its direction specifies the kind of the thermal event whether it is endothermic or exothermic.

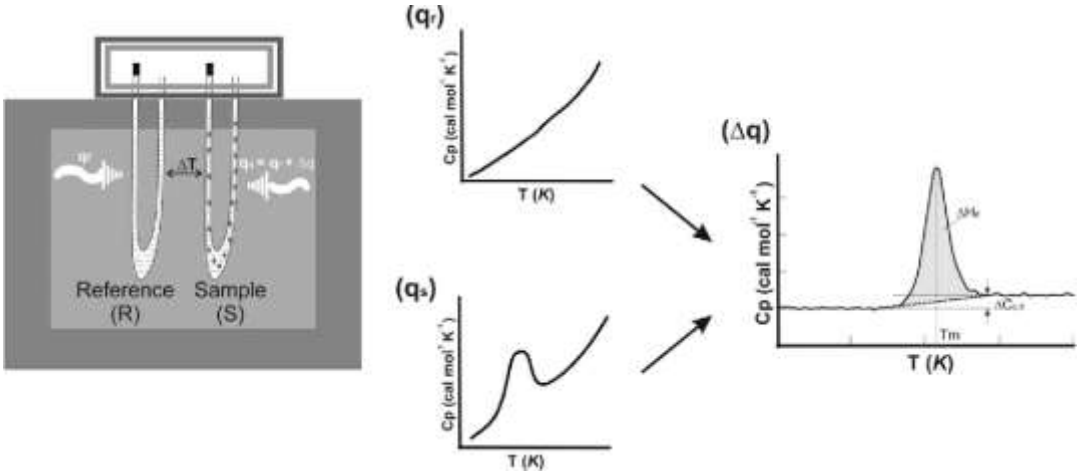

Figure 1.15. Experimental setup for a DSC experiment. T(K) for temperature, kelvin; ΔH_d for change in enthalpy; $\Delta C_{p,d}$ for change in C_p; T_m for transition and melting point; d for denatured (Gill et al., 2010)

DSC also provides information of the transition temperatures such as onset temperature (To), peak temperature (Tp), conclusion temperature (Tc), glass transition temperature (Tg) and enthalpy of gelatinization (ΔHgel). Tg is a thermal transition from rubbery to glassy state of amorphous materials. It is identified as a shift of the baseline on the DSC curve (Gill et al., 2010; Yrjö H., 2010).

DSC is well established technique utilized to investigate the starch gelatinization process. Gelatinization degree of the samples were calculated by using the following formula (Bitik, Sumnu, & Oztop, 2019):

$$\text{Degree of gelatinization } (\%) = \left(1 - \frac{\Delta H_{treated}}{\Delta H_{native}}\right) * 100$$

where ΔH_{native} is the enthalpy of native untreated sample, $\Delta H_{treated}$ is the enthalpy of treated sample.

1.4.4 X-Ray Diffraction (XRD)

X-ray diffraction (XRD) is a nondestructive analytical technique used to characterize crystalline materials. It provides information about structure, crystallinity or texture of the sample. The principle of X-ray diffraction is based on Bragg's Law. X-ray beams are sent through the sample, so the angle of the diffraction will be changed by change in the spacing of the atoms in the molecule. Thus, diffraction patterns are created and these diffraction patterns act as a fingerprint since they are special to that crystal (Kohli, 2012; LibreTexts, 2020)

The result of X-ray diffraction is obtained as a plot of signal intensity for different angles of diffraction, namely diffractogram. The intensity of the peak is associated with the amount of crystals in that phase or with that spacing. The peak with high intensity means that there is high amount of crystals or molecules within that distinct spacing. The width of the peaks is inversely correlated with the crystal size. While a sharp/thin peak structure indicates the existence of bigger crystals or molecules, a broader peak indicates smaller crystals, deformity in the crystal or amorphous structure within that distinct spacing (Eliasson, 2010; LibreTexts, 2020). X-ray diffraction is used for starch characterization in the literature. Figure 1.16 displays an X-ray diffractogram of lentil, corn and potato starches in native state as an example (Joshi et al., 2013).

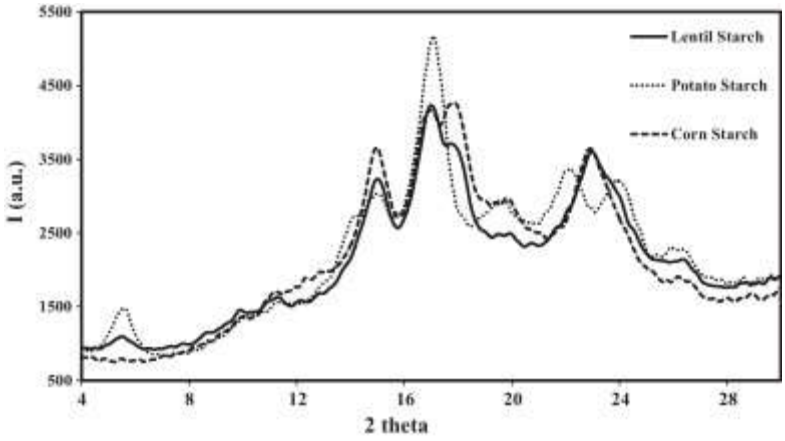

Figure 1.16. X-Ray diffractogram of lentil, corn and potato starches in native state (Joshi et al., 2013)

1.4.5 Scanning Electron Microscopy (SEM)

Scanning electron microscopy (SEM) is a technique, which provides images of a sample by scanning the surface of the sample with a focused beam of electrons. It is a widely used analytical method in the study of the granulate microstructure and starch (Horovitz et al., 2011).

1.5 Patents

When a patent search is conducted in the field of NMR Relaxometry relevant to the samples examined under this topic, some applications related with the use of NMR Relaxometry were encountered. The cooperative patent classification (CPC) in this field is:

G01N 24/08: investigating or analyzing materials by determining their chemical or physical properties, by using nuclear magnetic resonance (G01N 24/12 takes precedence).

AU2012281017A1 discloses an invention that monitor the blood clotting process by measuring the signal of NMR relaxation of water in a blood sample that go through clotting. It characterizes a method for monitoring blood clot formation by following the rheological change in the aqueous blood sample. The application date was 13/07/2012 with a priority date of 13/07/2011. It was published at 30/11/2014. The application was granted and its anticipated expiration date is 13/07/2032.

CN110618159A discloses a method to measure the moisture content of nanmu seed by using LF-NMR (low-field nuclear magnetic resonance). The method includes sampling nanmu seeds, rinsing the seeds, testing nanmu seeds by using LF-NMR technology, and obtaining a linear relationship between the seed moisture content and total signal value obtained from the seed and obtaining seed moisture content by summing up the three NMR relaxation peaks as free water relaxation signal value, non-easy flowing water relaxation signal value and bound water relaxation signal value. The application date was 05/11/2019. It was published at 27/12/2019 and its status is pending.

EP1813936A1 describes a magnetic resonance imaging device and method for determining physical and chemical qualities of agricultural product, such as seeds. The application date was 19/12/2001 with a priority date of 20/12/2000. It was published at 01/08/2007. The application was granted and its lifetime was expired at 19/12/2021.

CN107300565A is about a nuclear magnetic resonance wave spectrum method in order to rapidly identifying any rice syrup mixing present in honey. A honey sample is prepared with a solution of heavy water, an internal marker solution containing 3-trimethylsilyl-1-propyl sodium sulfonate and a sodium azide phosphate buffer solution. Nuclear magnetic resonance spectrum is obtained through nuclear magnetic resonance spectroscope. If the relative intensity error range exceed 10%, it can be said that the honey sample does not contain rice syrup.; otherwise honey sample is mixed with rice syrup. The approach may be used to analyze a large number of samples in a short amount of time, and it can quickly determine whether rice syrup

has been blended into the honey. The application date was 25/08/2017 with a priority date of 25/08/2017. It was published at 27/10/2017. The application was granted and its anticipated expiration date is 25/08/2037.

CN104764764A relates to a low-field nuclear magnetic resonance method for determining the gel swelling ratio. This method comprises determination of NMR attenuation curve of gel during swelling, obtaining T_2 distribution curve, identifying a T_2 distribution peak relating to the internal water of gel, evaluating the integral area of the peak related to gel internal water, computing the swelling ratio in terms of peak area associated with gel internal water before and after swelling. The application date was 05/03/2015. It was published at 08/07/2015 and its status is pending.

In the field of quinoa and seed related products, the cooperative patent classifications (CPC) are:

A23L 25/00: Foods consisting mainly of nutmeat or seeds and preparation or treatment methods

A21D 13/06: Finished or partly finished bakery product, products with modified nutritive value, e.g. with modified starch content

A23L 7/152: Cereal-derived products; Malt products; Preparation or treatment thereof (preparation of malt for brewing, cereal-derived products, cereal germ products

C08B 30/00: Preparation of starch, degraded or non-chemically modified starch, amylose, or amylopectin

US3770472A is about the process for preparation of modified starch dispersions. The application date was 09/05/1972 with a priority date of 09/05/1972. It was published at 06/11/1973. The application was granted and its lifetime was expired at 06/11/1990.

CN111184178A relates a product that includes resistant starch and preparation and application method of it. In the product, resistant starch is obtained by applying quinoa powder with the ultrahigh pressure treatment at 400-600 MPa. It is aimed to widen the use of quinoa in the fields of low glycemic index foods. The application date was 18/03/2020 with a priority date of 18/03/2020. It was published at 22/05/2020 and its status is pending.

CN102585018A relates modification method of lotus-seed starch under ultrahigh pressure. The process comprises preparation of raw material, applying ultrahigh pressure, drying, grinding and sieving, respectively. This pressure application improves the structure, physicochemical property and eating quality of the starch. The application date was 09/04/2012 with a priority date of 09/04/2012. It was published at 18/07/2012 and its status is pending.

WO2019049168A1 discloses preparation of ready to eat quinoa flakes. The preparation method of ready to eat quinoa flakes includes soaking, drying, and roasting of quinoa seeds, respectively and flattening them to form quinoa flakes, drying, coating with edible oil, coating with edible starch and coating with flavor, respectively. The application date of this PCT application was 04/09/2018 with a priority date of 06/09/2017. It was published at 04/03/2019. It has two national phase entries in Canada and United states of America.

CN106720058A discloses a processing method of quinoa biscuit. The application date was 23/01/2017 with a priority date of 23/01/2014. It was published at 31/05/2017 and its status is pending.

In the field of HHP and the products related to its use, the cooperative patent classifications (CPC) are:

A23L 3/015: Preservation of foods or foodstuffs, in general, e.g. pasteurizing, sterilizing, specially adapted for foods or foodstuffs (preserving foods or foodstuffs in association with packaging by treatment with pressure variation, shock, acceleration or shear stress (or cavitation).

A23C 2210/15: Physical treatment of dairy products, High pressure treatment

WO03007724A1 relates to methods for manufacturing yogurt using high hydrostatic pressure and thermal processing and for milk products prepared by those methods. The application date of this PCT application was 07/17/2002 with a priority date of 07/17/2001. It was published at 30/01/2003.

EP3424344A1 relates to the field of high pressure processing of foods, in particular a method of pasteurization. The application date was 24/08/2017 with a priority date of 07/07/2017. It was published at 09/01/2019. The application was withdrawn.

CN102585018A provides a method for modifying lotus-seed starch under ultrahigh pressure. The application date was 09/04/2012 with a priority date of 09/04/2012. It was published at 18/07/2012 and its status is pending.

1.6 Objectives of the Study

Time domain (TD)-NMR relaxometry has been demonstrated to be a valuable technique as being fast, non-invasive and non-destructive. It is used extensively in the food applications. However, there is limited research about investigation of cell integrity of treated plant tissues by TD-NMR Relaxometry. In addition, in the literature, there are studies in the field of HHP and US induced starch modification, but a little information is available in the field of HHP and US treated quinoa starch, which is analyzed by TD NMR Relaxometry.

In the first part of this dissertation, the aim is to investigate the effect of osmotic stress (OS), ultrasonication (US) and high hydrostatic pressure (HHP) on the cell membrane integrity of tomato seeds using variations in T_2 relaxation times and to analyze the use of H-NMR relaxometry as a tool for the identification of physiological changes in tomato seeds.

In the second part of this dissertation, the goal is to analyze the functional and rheological properties of HHP and US treated quinoa starch and associate the results

with TD NMR Relaxometry. For this purpose, swelling/solubility, rheology, particle size, FTIR and SEM measurements were conducted to confirm the results. In addition to HHP and US treated quinoa starch samples, the starch was fully gelatinized by heat treatment and considered as control gelatinized starch.

CHAPTER 2

MATERIALS AND METHODS

In this dissertation , TD-NMR Relaxometry was utilised for 2 group of samples. Part I focused on Time Domain (TD)-NMR relaxometry as a tool to investigate the cell integrity of tomato seeds exposed to osmotic stress (OS), ultrasonication (US) and high hydrostatic pressure (HHP). Part II examined the use of NMR Relaxometry to assess physicochemical characteristics of quinoa starch exposed to high hydrostatic pressure (HHP) and ultrasonication (US).

Table 2.1. Experimental design of the study

	Factors	**Levels**	**Responses**
Part I	Physical Treatments	HHP (300, 400 and 500 MPa for 20 °C for 15 min) US (at 75% amplitude for 5, 10 and 20 min) OS (10 (w/w), 20 (w/w) and 30% (w/w) NaCl solution)	NMR relaxometry measurements SEM
Part II	Physical Treatments	HHP (250, 350 and 500 MPa at 20 and 40°C for 5 min) US (100% power with constant pulse for 15 min)	Swelling & Solubility Particle size measurements Rheological measurements FTIR NMR relaxometry measurements DSC X-ray diffraction (XRD) SEM

2.1 PART I – Cell Integrity of Tomato Seeds

In Part I, use of time domain (TD)-NMR relaxometry as a tool to investigate the cell integrity of tomato seeds exposed to osmotic stress (OS), ultrasonication (US) and high hydrostatic pressure (HHP) was studied. Flow chart of the experiments which are carried in this section is given in Figure 2.1.

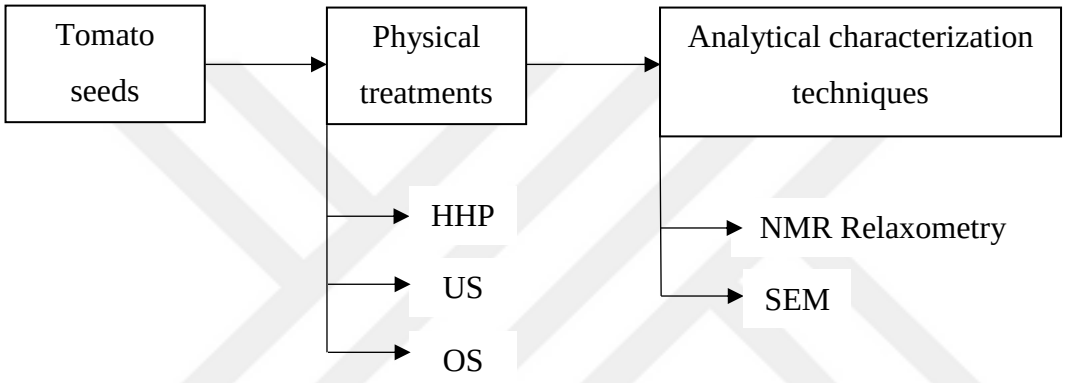

Figure 2.1. Flow chart of Part I

2.1.1 Materials

Tomato seeds were provided by the Department of Plant Protection Faculty of Agriculture Science and Technology of Isparta University in Isparta, Turkey. The seeds with an average weight and diameter of 0.004 g and 1.25 mm, respectively were stored in a refrigerator at 4 °C prior to experiments. The initial moisture content of these tomato seed samples was found to be 9 ± 0.5%. The number of tomato seeds required for one NMR measurement is approximately around 25–30. Thus, for all the experiment including OS treatment, US treatment, HHP treatment and control, approximately 250–300 tomato seeds are required.

2.1.2 Ultrasonication (US)

Tomato seed samples were soaked with distilled water at a ratio of 1:4 between the seed and the solution to increase the moisture content of the seeds. After 1-day period, samples were subjected to probe type ultrasonicator using MS73 probe (Bandelin Sonoplus HD 3100, Bandelin electronic GmbH & Co. KG, Berlin Germany) at 75% amplitude for 5, 10 and 20 min. Each system was prepared with triplicates for the three-ultrasonication time.

2.1.3 High Hydrostatic Pressure (HHP)

HHP treatment was carried out with 760.0118 type high hydrostatic pressure equipment as shown in Fig. 2.2 and Fig. 2.3 (supplied by SITEC, Zurich, Switzerland). The equipment comprises a cylindrical design pressurization chamber with two end closures, a tool for limiting the end closures, a hydraulic unit, a device for temperature control and a pressure pump. The pressurization chamber had a capacity of 100 mL with length of 153 mm and an inner diameter of 24 mm. A built-in heating–cooling system (Huber Circulation Thermostat, Offenburg, Germany) was used to maintain the required temperature. A type of K thermocouple was used to monitor the temperature in the chamber. The pressure- transmitting medium which is composed of a mixture of water and glycol was filled in the chamber. By built-in system, before applying pressure, the medium was heated up to the required temperature. Tomato seed samples were soaked with distilled water with a ratio of 1:4 between the seed and the solution, and pressurized in 20 mL sterile cryotubes at pressure levels of 300, 400 and 500 MPa for 20 °C for 15 min.

Figure 2.2. HHP equipment

Figure 2.3. Pressurization chamber

2.1.4 Osmotic Stress (OS)

The osmotic stress was performed with three different aqueous solutions: 10 (w/w), 20 (w/w) and 30% (w/w) NaCl solution, which was prepared with NaCl (Sigma-Aldrich, 746398) at 25 °C. Tomato seed samples were weighed and immersed into solutions containing NaCl with a ratio of 1:4 (w/w) between the seed and the solution. Soaking of tomato seeds with NaCl solution was performed for a 1-day period with three replicates.

2.1.5 Nuclear Magnetic Resonance (NMR) Relaxometry

T_2 relaxation times were measured for tomato seeds exposed to OS, US and HHP treatments and for the untreated control samples. Samples were placed into a 10 mm NMR tube and analyzed. H-NMR Relaxometry experiments were carried out by using 0.5 T (22.40 MHz) low-field bench top 1H Nuclear Magnetic Resonance (LF-NMR) instrument (SpinCore Technologies, Inc., Gainesville, USA) with 10 mm r.f. coil (Fig 2.4). The spin–spin relaxation times (T_2) of tomato seed samples were measured using Carr–Purcell–Meiboom–Gill (CPMG) sequence with an echo time (TE) of 1000 μs, 512 points, spectral width of 300 kHz, 1000–5000 number of echoes, repetition delay of 3 s, and 24 scans. T_2 signals were analyzed with MATLAB. A mathematical transformation PROSPA software (Magritek Inc., Wellington, New Zealand), which uses Non-Negative Least Square (NNLS), was conducted to analyze the multiexponential decay of T_2 relaxation curves. 1D-NNLS analysis by PROSPA software revealed T_2 relaxation spectrum. All measurements were performed in triplicate.

Figure 2.4. 1H Nuclear Magnetic Resonance (LF-NMR) system

2.1.6 Scanning Electron Microscopy (SEM)

Scanning electron microscopy (SEM) images were obtained at the Scanning Electron Microscopy Laboratory, Metallurgical and Materials Engineering Department, Middle East Technical University (METU), Turkey. Since the SEM works under a vacuum, it is essential that the specimen is completely dry to obtain an image (Karcz 2009). Tomato seeds had a moisture content of between 4 and 8% naturally. For that reason, untreated tomato seeds, and seeds treated with OS with 10%, 20% and 30% NaCl solution, seeds exposed to US for 5, 10 and 20 min, exposed to HHP at 20 °C and 15 min at 300 MPa, 400 MPa and 500 MPa were freeze dried in the freeze dryer (Christ Alpha 2-4 LO Plus Freeze Dryer, Ankara, Turkey) before getting the SEM images. After freeze drying, samples were coated at room temperature with a thin layer of Au–Pd (6–11 nm; 10 mA; 40 s) and the analysis was carried out with a scanning electron microscope (SEM, Quanta SC7620, England).

2.1.7 Statistical Analysis

Analysis of variance (ANOVA) with Tukey's multiple range test was used to compare the means of the relaxation times. Differences were considered significant

for $p < 0.05$. T_2 relaxation times of peaks were not analyzed statistically since some peaks disappeared after applied treatments.

2.2 PART II- Physicochemical Characteristics of Modified Quinoa Starch

In Part II, the use of NMR Relaxometry to assess physicochemical characteristics of quinoa starch exposed to high hydrostatic pressure (HHP) and ultrasonication (US) was studied. Flow chart of the experiments which are carried in Part II is represented in Figure 2.5.

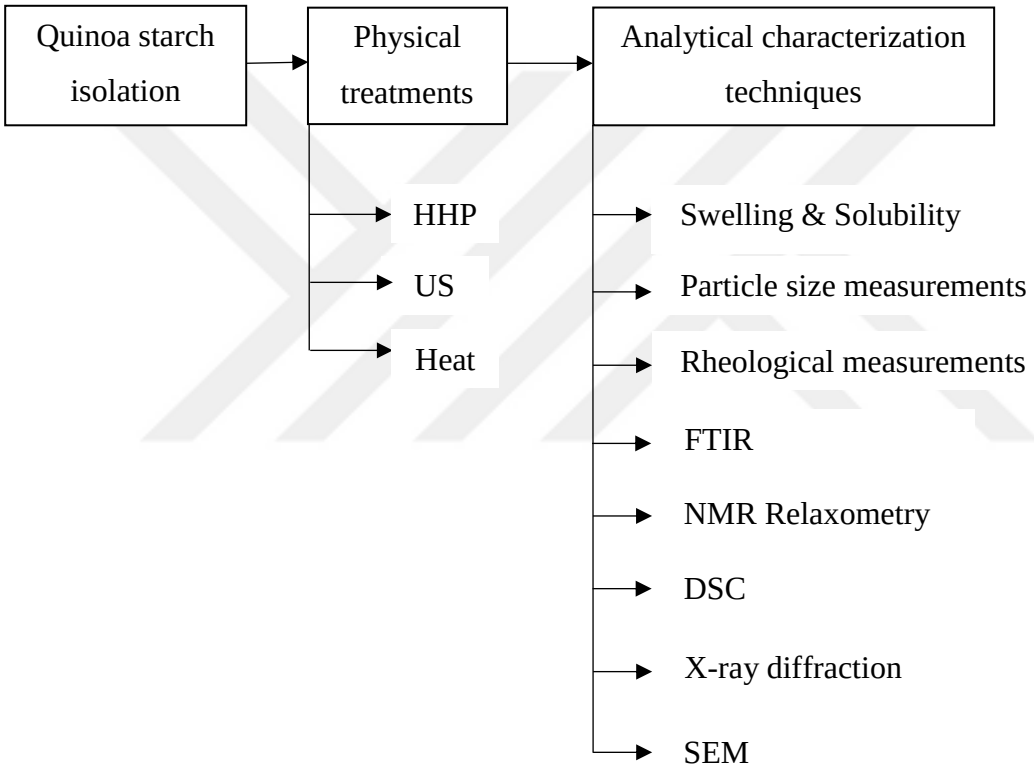

Figure 2.5. Flow chart of Part II

2.2.1 Materials

Quinoa seeds were purchased from the local market in Ankara, with the brand name as “Ala Çiftçi – White Quinoa” with the origin of Peru.

2.2.2 Starch Isolation

For the isolation of quinoa starch, water steeping method was used described in the literature (Jan, Panesar, & Singh, 2017). Quinoa seeds were steeped in water with a ratio of 1:6 at room temperature for 24 h with intermittent stirring. Then, using a lab scale blender, wet milling was applied for 2 min. Following wet milling, the slurry was filtered, and the obtained filtrate was centrifuged at 5500 rpm for 15 min by MF 80 General Centrifuge (Hanil, Incheon, South Korea). The supernatant and the yellowish layer occurred above the starch cake was removed carefully. The obtained starch cake was re-suspended in water, centrifuged and the yellowish layer was removed again after each centrifugation by repeating this procedure four times for the purification of starch. The recovered purified starch was dried at 40°C in a hot air oven for 6 h. Then, powder quinoa starch (QS) samples were obtained by grinding and stored in an airtight container for further analysis (Fig. 2.6) (Jan et al., 2017).

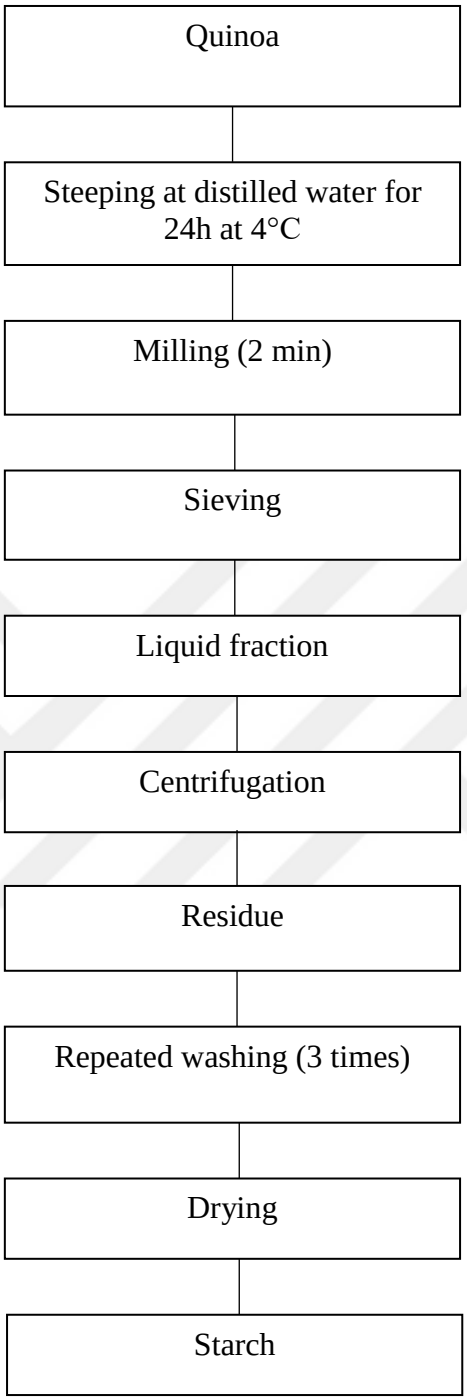

Figure 2.6. Standard process for isolation of quinoa starch

2.2.3 Modification of Starch

Isolated quinoa starch was modified by high hydrostatic pressure and ultrasonication treatments by using the parameters based on the preliminary studies.

2.2.3.1 High Hydrostatic Pressure (HHP)

Quinoa starch suspensions were prepared by mixing appropriate amount of quinoa starch with required volume of distilled water with a concentration of 10% (w/v) based on the preliminary studies (Li & Zhu, 2018). The suspension was stirred gently using a magnetic stirrer (Multi Hotplate Stirrer, Wisd, DAIHAN Scientific Co., Ltd., Korea) at 450 rpm for 5 min and were sealed in 25 ml sterile polyethylene cryotubes so that no gas left in the tube. HHP treatment was carried out with 760.0118 type high hydrostatic pressure equipment (supplied by SITEC, Zurich, Switzerland). The equipment comprises a cylindrical design pressurization chamber with a pressure-transmitting medium which is composed of a mixture of water and glycol which was filled in the chamber. The pressurization chamber had a capacity of 100 mL with length of 153 mm and an inner diameter of 24 mm. Prepared QS suspensions were pressurized at pressure levels of 250, 350 and 500 MPa at 20 and 40°C for 5 min. The pressurization time reported in this study did not include the pressure increase and release times because of short pressure release time (less than 20 s). After HHP treatment, samples were centrifuged at 4000 rpm for 5 min (MF 80 General Centrifuge, Hanil, Incheon, South Korea), freeze dried for about 48 h and ground to powder form for further analyses.

2.2.3.2 Ultrasonication (US)

Quinoa starch suspensions were prepared at a concentration of 5% (w/w) based on the preliminary studies (Manchun, Nunthanid, Limmatvapirat, & Sriamornsak, 2012). The suspension was stirred gently using a magnetic stirrer (Multi Hotplate

Stirrer, Wisd, DAIHAN Scientific Co., Ltd., Korea) at 450 rpm for 5 min. US treatment was conducted by a probe type ultrasonicator using MS73 probe (Bandelin Sonopuls HD 3100, Bandelin electronic GmbH & Co. KG, Berlin Germany) at 100% power with constant pulse for 15 min in an ice bath. After US treatment, samples were centrifuged at 4,000 rpm for 5 min (MF 80 General Centrifuge, Hanil, Incheon, South Korea), freeze dried for about 48 h and ground to powder form for further analyses.

2.2.3.3 Fully Gelatinized Starch Preparation

Conventional heat treatment was used to obtain the fully gelatinized (control gelatinized) quinoa starch samples, which were prepared by heating 10% quinoa starch suspension in water bath (GFL 1086, Burgwedel, Germany) at 90°C for 30 min. Following heat treatment, sample was centrifuged at 4,000 rpm for 5 min (MF 80 General Centrifuge, Hanil, Incheon, South Korea), freeze dried for about 48 h and ground to powder form for further analyses.

2.2.4 Swelling Power (SP) and Water Solubility Index (WSI)

Swelling power (SP, g/g) and water solubility index (WSI, %) were determined using a method modified from (Li, Wang, & Zhu, 2016). Quinoa starch suspensions of 4% were prepared in a centrifuge tube and heated in a shaking water bath (GFL 1086, Burgwedel, Germany) at 90°C for 30 min. Each suspension was then cooled and centrifuged at 3000 rpm for 30 min (MF 80 General Centrifuge, Hanil, Incheon, South Korea). After centrifugation, the precipitate was weighed (W_s), and the supernatant was dried at 100°C for 24h until reaching to a constant weight (W_1). WSI and SP were described by the following equations:

$$WSI\ (\frac{g}{100\ g}) = \frac{Weight\ of\ the\ soluble\ material\ in\ the\ supernatant\ ,W_1\ (g,dry\ basis)}{Weight\ of\ the\ starch\ sample\ ,W_0\ (g,dry\ basis)} * 100 \qquad (1)$$

$$SP = \frac{Weight\ of\ the\ precipitate, W_s\ (g, dry\ basis)}{Weight\ of\ the\ starch\ sample, W_0\ (g, dry\ basis) * (100 - WSI)} * 100 \quad (2)$$

2.2.5 Rheological Measurements

Rheological measurements were carried out using the cup and bob geometry of the rheometer (Kinexus lab+, Malvern Instruments Ltd., Worcestershire, UK). For analysis, 10% (w/w) quinoa starch suspensions were prepared, and the rheometer was filled with 20 ml of the prepared suspension (Jambrak et al., 2010). The shear stress values of the samples with increasing shear rate (from 0.1 to 100 s^{-1}) were recorded and fitted to the power law by using the following formula:

$$\tau = k * \gamma^n$$

$$ln\tau = lnk + nln\gamma$$

where;

n: flow behavior index, k: consistency index ($Pa.s^n$), τ: shear stress (Pa), γ:shear rate (s^{-1})

2.2.6 Particle Size Measurements

Particle size distributions of quinoa starch samples were analyzed by a particle analyzer based on a laser diffraction (Mastersizer 3000, Malvern Instruments Ltd, Malvern, UK). Samples were subjected to 2,500 rpm stirring. Measurements were done under 1% to 25% obscuration range and selected irregular shape. The starch refractive and absorption index values were taken as 1.51 and 0.1, respectively. The refractive index of water used was 1.33 (Devi, Fibrianto, Torley, & Bhandari, 2009). D[4,3] values were calculated from the instrument software.

2.2.7 Nuclear Magnetic Resonance (NMR) Relaxometry Measurements

TD-NMR Relaxometry experiments were carried out by using 0.5 T (22.40 MHz) low-field bench top 1H Nuclear Magnetic Resonance (LF-NMR) instrument (SpinCore Technologies, Inc., Gainesville, USA) with 10 mm radio frequency coil. Quinoa starch suspension with 10% (w/w) were placed into the cylindrical 10 mm tubes. The spin-spin relaxation times (T_2) of quinoa starch samples were measured using Carr-Purcell-Meiboom-Gill (CPMG) sequence with an echo time (TE) of 1000 μs, 512 points, spectral width of 300 kHz, 1000-5000 number of echoes, repetition delay of 3 s, and 32 scans. In order to obtain T2 relaxation curves, obtained T_2 signals were analyzed with MATLAB and fitted to mono and bi-exponential models. Non-Negative Least Square (NNLS) was also conducted to analyze the multiexponential behavior of T_2 relaxation curves (PROSPA, Magritek Inc., Wellington, New Zealand). 1D-NNLS analysis yielded T_2 relaxation spectrum (Unal, Alpas, Aktas, & Oztop, 2020).

2.2.8 Fourier Transform Infrared (FTIR) Spectroscopy

The Fourier Transform Infrared (FTIR) spectra of the quinoa starch samples were obtained using an IR Affinity-1 spectrometer with attenuated total reflectance (ATR) attachment (Shimadzu Corporation, Kyoto, Japan). The measurements were collected over a wavelength range of 500-4000 cm^{-1} with 32 scans. The mean of the scans of each sample were reported in the spectrum including absorbance vs wavenumber plots of quinoa starch samples.

2.2.9 Differential Scanning Calorimetry (DSC)

The gelatinization properties of the quinoa starch samples were analyzed by using Differential Scanning Calorimeter DSC 4000 (Perkin Elmer, Waltham, MA, U.S.A.) at METU Central Laboratory (Ankara, Turkey). DSC 4000 was used by applying

pure nitrogen gas through the system with a flow rate of 19.8 ml/min in hermetically sealed aluminum pans. An empty aluminum pan was used as the reference for all measurements. The samples were heated from 20℃ to 80℃ with a heating rate of 10℃/min. Gelatinization degree of the samples were calculated by using the following formula (Bitik et al., 2019):

$$\text{Degree of gelatinization } (\%) = \left(1 - \frac{\Delta H_{treated}}{\Delta H_{native}}\right) * 100$$

where ΔH_{native} is the enthalpy of native untreated sample, $\Delta H_{treated}$ is the enthalpy of treated sample.

2.2.10 X-ray Diffraction (XRD)

X-Ray Diffraction experiments were carried out by using a Rigaku Ultima-IV X-Ray Diffractometer (Japan) at 40kV and 30 mA at METU Central Laboratory. Data were collected between 4-70°C with the 2θ range. Crystalline peaks were analyzed using Origin software (Version 9.0) by separation and integration of the areas under crystalline and amorphous regions. The crystallinity degree (CD) of the samples was determined based on the following formula described by (Demirkesen et al., 2014b; Ribotta et al., 2004a)

$$CD = \frac{I_c}{I_c + I_a}$$

where Ic is the integrated intensity of crystalline phase, and Ia is the integrated intensity of the amorphous phase.

2.2.11 Scanning Electron Microscopy (SEM)

Scanning electron microscopy (SEM) images were obtained at the Scanning Electron Microscopy Laboratory, Metallurgical and Materials Engineering Department, Middle East Technical University (METU), Turkey. Quinoa starch samples were

coated at room temperature with a thin layer of Au-Pd (6–11 nm; 10 mA; 40 s) and the analysis was carried out with a scanning electron microscope with various magnifications (SEM, Quanta SC7620, England).

2.2.12 Statistical Analysis

Analysis of variance (ANOVA) with Tukey's multiple range test was used to compare the means of the relaxation times. Differences were considered significant for $p < 0.05$.

CHAPTER 3

RESULTS AND DISCUSSION

3.1 PART I

3.1.1 NMR Relaxometry Measurements for Tomato Seeds

3.1.1.1 1D T2 Relaxation Spectra

One dimensional T_2 relation measurements provide information on water content, interaction of water with the surrounding macromolecules and physical properties of water (L. Zhang & McCarthy, 2012). The changes in relaxation spectrum give information about changes within food systems related to proton such as change in water content, proton exchange between compartments and physiological events that result in occurrence of new proton pools (P. Belton & Capozzi, 2011). The measured signal in a CPMG (Carr–Purcell–Meiboom–Gill) experiment is the weighted sum of the T_2 relaxation decay of water protons in each compartment. The relative water content in each compartment specifies the contribution of T_2 relaxation behavior of water to the observed signal. Therefore, multiexponential inversion of the T_2 relaxation data was obtained as shown in Figure 3.1.

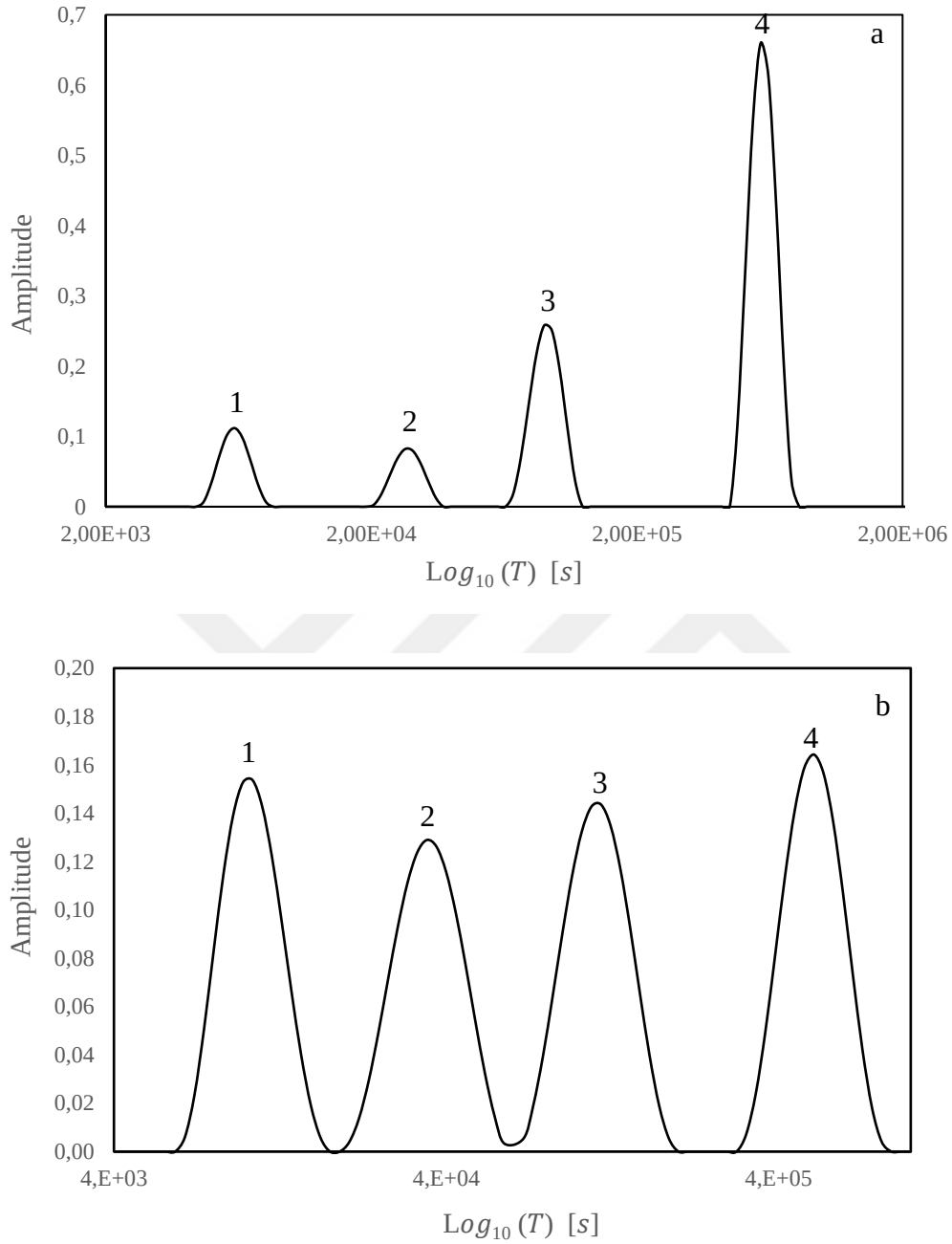

Figure 3.1. T_2 relaxation spectrum of tomato seeds 1 hour (a) and 1 day (b) after soaking with distilled water

Figure 3.1 shows T_2 relaxation spectra of an untreated tomato seed sample revealing several components having different relaxation times. In untreated tomato seeds, four peaks were observed. When the relaxation spectra obtained from previous studies, which analyzed the fruit and vegetable tissues by using T_2 relaxation spectra, were compared with those obtained from this study, consistency was observed in the peak numbers (Hernández-Sánchez, Hills, Barreiro, & Marigheto, 2007). Each peak relates to a relaxation component that is associated with a water-proton compartment within the sample. The multicompartment nature of the plant cellular tissue leads to the multiexponential relaxation behavior in the T2 relaxation spectra of the plant cell (B. P. Hills & Clark, 2003).

According to Figure 3.1 (a) and Table 3.1, the peak having the smallest relative area, peak 2, may be associated with the signals coming from the water in the cell wall. The water in cell wall tightly held by strong water-binding sides and surrounding matrix and exists in very small pores (Taiz & Zeiger, 2006). This feature of cell wall water restricts the water mobility and thus increases proton exchange between water and surrounding macromolecules. Thus, the smallest T_2 relaxation time was supposed to belong to the water in the cell wall. Peak 3 is associated with the cytoplasm. A part of the water in cytoplasm forms hydrogen bonds with the side chains of the proteins, setting the gel-like framework of cytosol (Kramer, 1983; Raffo et al., 2005) and an intermediate T_2 relaxation time is expected to be displayed. Peak 4, having the longest T_2 relaxation time and relative area could be assigned to the vacuole. In plant cells, the majority of water is stored in the vacuoles by containing 50–80% or more of cellular water (Kramer, 1983). The vacuole water is in a remarkably mobile liquid state since it does not include intensive amount of water binding molecules (L. Zhang & McCarthy, 2012). Thus, water in vacuole should reveal the longest T_2 relaxation times. Peak 1 with the smallest T_2 relaxation time has a short average T_2 relaxation time that is appropriate for T_2 values of solids rather than water (Hashemi, R.H., Bradley, W.G., & Lisanti, 2010). Thus, Peak 1 may be associated with the protons of sugar and protein molecules.

Figure 3.1 (b) shows the relaxation spectrum of tomato seeds one day after soaking with distilled water. It was observed that the relative areas of the four peaks became equal with each other. This may be due to water diffusion through the cells. Water influx continues until the osmotic pressure reaches equilibrium with the turgor pressure. The cell is still intact at this stage since the cell wall and semi permeable membrane prevents the cell lysis in the plant cell (Dellarosa et al., 2016).

The identification of several peaks in the untreated tomato seed sample demonstrated that, on the time scale of NMR acquisition, the exchange of water between compartments is slow, since the cell membranes, plasma membrane and tonoplast acted as barriers by separating plant cell into subcellular compartments. The compartments, consisting of different content and structure, influence the molecular movement of water protons and resulting in different T_2 relaxation times (Snaar & Van As, 1992; Vandusschoten, Dejager, & Vanas, 1995). In case of deterioration of the subcellular membranes, serving as permeability barriers to proton exchange, fast diffusive exchange occurs resulting in loss of cell integrity. This causes merging in the distinct peaks of slow diffusive exchange regime and decrease in the number of peaks in the relaxation spectrum indicating a physiological alteration in the cellular structure of the sample tissue (B. P. Hills, 1998; B. P. Hills & Clark, 2003).

Table 3.1. Average T_2 relaxation times and percent relative areas (RA) of tomato seed samples after different treatments. Untreated (Control); OS (10%), OS (20%), OS (30%), US (5 min), US (10 min), US (20 min), HHP at 300 MPa and 20°C, HHP at 400 MPa and 20°C, HHP at 500 MPa and 20°C

Treatment	**T_2 (ms)**		**T_2 (ms)**	**RA(%)**
Untreated	952.333±32.62[a]	peak 1	4.4	13.85
		peak 2	35	23.13
		peak 3	140	29.68
		peak 4	1200	33.34
OS 10%	619.203±64.97[b]	peak 1	3.8	14.67
		peak 2	33.7	19.19
		peak 3	126.7	31.57
		peak 4	900	34.15
OS 20%	741.333±84.76[b]	peak 1	24.7	18.79
		peak 2		
		peak 3	113.3	38.81
		peak 4	1046,7	42.40
OS 30%	764.667±76.97[b]	peak 1	35.3	21.26
		peak 2		
		peak 3	136.7	33.49
		peak 4	963.3	39.97
US 5 min	710.423±2.08[b]	peak 1	29	12.50
		peak 2		
		peak 3	260	25.33
		peak 4	880	62.10
US 10 min	698.767±9.64[b]	peak 1	28	12.03
		peak 2		
		peak 3	270	37.52
		peak 4	730	50.45

Table 3.1. (Cont'd)

US 20 min	712.455±9.17[b]	peak 1		
		peak 2		
		peak 3	290	60.53
		peak 4	360	42.67
HHP 300 MPa	650.351±12.5[b]	peak 1	290	15.19
		peak 2		
		peak 3	69	29.87
		peak 4	53	23.45
HHP 400 MPa	590.623±53.02[b,c]	peak 1	420	16.50
		peak 2		
		peak 3	90	29.15
		peak 4	29	17.09
HHP 500 MPa	585.307±8.74[c]	peak 1		
		peak 2		
		peak 3	290	16.68
		peak 4	28	40.90

3.1.1.2 Effect of OS Treatment on Tomato Seed Samples

In tomato seed samples, exposed to osmotic stress, a decrease in the T_2 relaxation time of tomato seeds as shown in Table 3.1 was observed. This can be explained by the process known as plasmolysis. When the seed contacts with the osmotic solution, water loss occurs and the semipermeable membrane, plasma membrane and tonoplast start to separate. This water loss causes decrease in the T_2 value of the sample. The T_2 distributions obtained from CPMG experiments of OS treated tomato seeds revealed almost all four peaks in the relaxation spectrum with only minor changes in T_2 relaxation times and relative areas as shown in Figure 3.2 The osmotic dehydration caused by OS treatment caused to removal of water partially from inner parts of the cell towards the extracellular space (cytoplasm) thereby, the T_2 value of vacuole was slightly decreased and the T_2 value of cytoplasm was slightly increased. The peak assigned to the cell wall was disappeared in tomato seeds treated with 20% NaCl solution and 30% NaCl solution. This suggests that OS treatment with 20 and 30% NaCl solutions have caused the cell wall disruption resulting in the release of the water that was bounded in rigid cell wall compartments. Peak 1 which is attributed to the protons of starch or non-exchangeable macromolecular protons remained intact implying the rupture of internal cellular membranes.

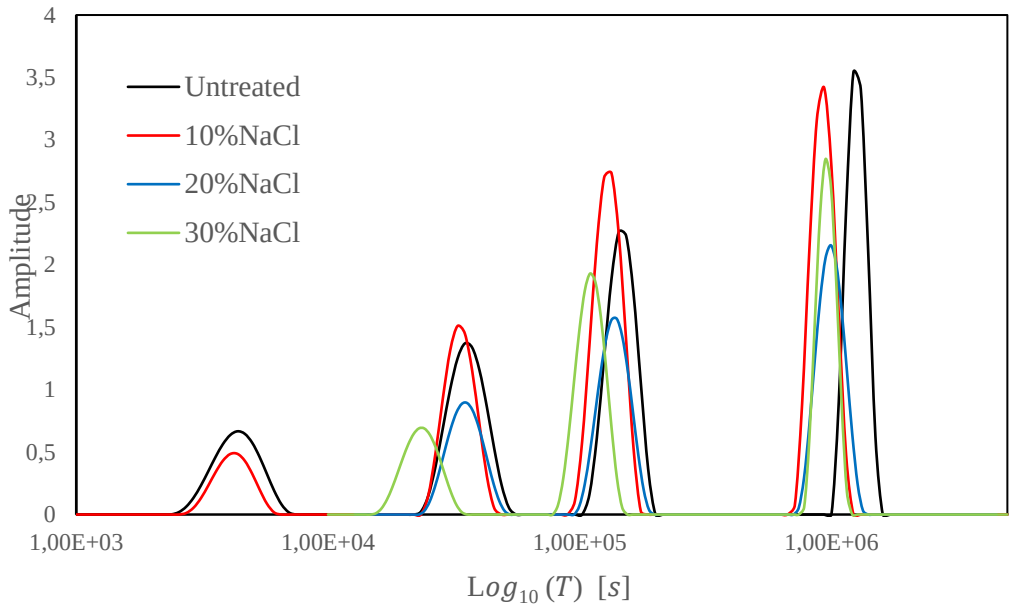

Figure 3.2. T_2 relaxation spectrum of tomato seeds soaked with 10% NaCl (a), 20% NaCl (b) and 30% NaCl (c) solutions

3.1.1.3 Effect of US Treatment on Tomato Seed Samples

The effect of US was investigated by NMR relaxometry technique and the results were shown in Table 3.1 and Figure 3.3 When T_2 relaxation times of untreated tomato seeds and US treated tomato seeds were compared, a significant decrease ($p<0.05$) was seen. In Fig.3.3, partial merging was observed between the peaks. This can be explained by fast water exchange between compartments which equals the water proton relaxations to an average in response to the disruption of the cell. The merged peaks in a relaxation spectrum is an indication of this water diffusive averaging effect. Cell disruption as result of US treatment causes the increase in permeability or loss of tonoplast integrity. According to Table 3.1, relative area and T_2 value of the vacuole were decreasing, and relative area and T_2 of extracellular space/cytoplasm were increasing as US treatment duration increased from 5 to 20 min. These results suggested a partial removal of water from inner cellular compartments towards the extracellular space.

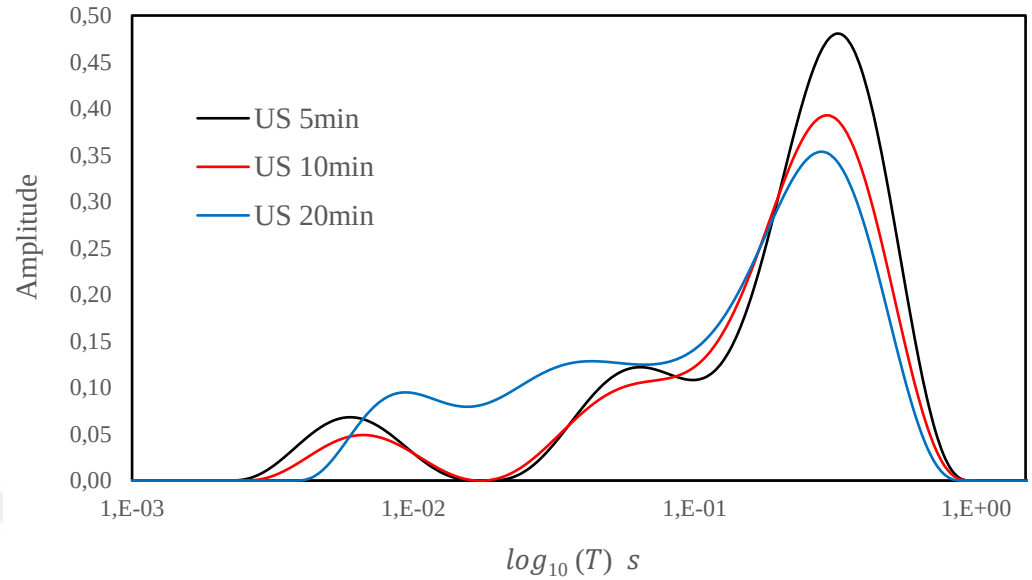

Figure 3.3. T_2 relaxation spectrum of tomato seeds exposed to ultrasonication for 5 min (a), 10 min (b) and 20 min (c)

3.1.1.4 Effect of HHP Treatment on Tomato Seed Samples

NMR measurement results of tomato seeds treated with HHP are shown in Table 3.1 and Fig.3.4. T_2 values of HHP treated tomato seeds were significantly ($p<0.05$) lower compared to the untreated samples and OS and US treated tomato seeds, which supported water loss. After HHP treatment, T_2 relaxation spectrum gave fewer peaks as compared to the untreated tomato seeds. 300 MPa pressurization resulted in three peaks with lower T_2 relaxation time of vacuole and higher T_2 relaxation time of the cytoplasm. As pressurization level increased to 400 MPa, partially merging between peak 1 and peak 2 was observed. 500 MPa pressurization led to only two peaks in the relaxation spectrum with a lower T_2 relaxation time of vacuole and a higher T_2 relaxation time of cytoplasm. These changes in the relaxation spectrum could be explained by the detrimental effect of high hydrostatic pressure to the cell structure of tomato seed. As previous investigators proved, HHP treatment could cause changes in the functionality of proteins, polysaccharides and lipids that might result in functional and structural changes in the plant tissue (Fister, Merkel, & Tauscher,

2002). HHP caused disruption of the cellular compartmentalization that would lead to partial removal of water from inner cellular compartments towards to the extracellular space. When the applied pressurization levels were compared according to the NMR relaxometry measurements (Table 3.1), it was observed that 500 MPa caused the most detrimental effect in the cell structure since T_2 relaxation spectrum gave two peaks (proton pools) due to the disruption the cell compartmentalization.

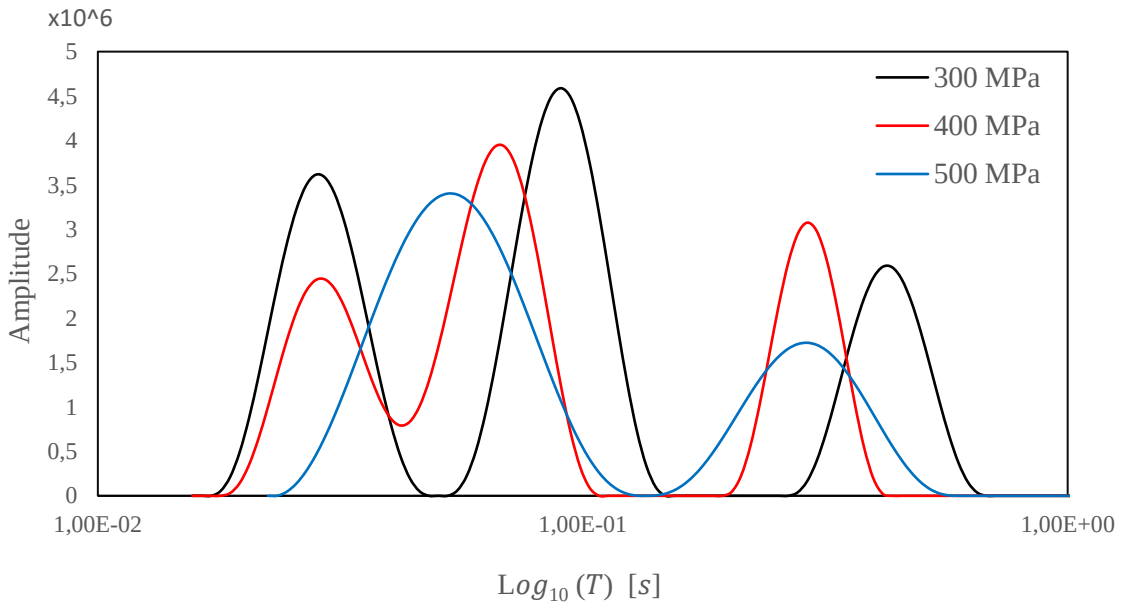

Figure 3.4. T_2 relaxation spectrum of tomato seeds exposed to HHP at 300MPa, 400MPa and 500MPa at 20°C, 15min

3.1.2 Scanning Electron Microscopy (SEM)

Scanning electron microscopy (SEM) provides an opportunity to view the interior and three-dimensional structure of the cell surrounded by the cell membrane. Untreated, OS, US and HHP treated tomato seed samples were analyzed by SEM. Figure 3.5 shows the SEM image of untreated tomato seed with testa, embryo, endosperm and endosperm cap. Figure 3.6 (a) shows the SEM image of untreated tomato seed and Fig.3.7 (b–d) shows SEM image of OS treated tomato seed, Fig.3.6 (e–g) shows SEM image of OS treated tomato seed and Fig.3.6 (h–k) shows SEM image of HHP treated tomato seed. When the images were analyzed, it could be observed that untreated tomato seed had an organized cellular structure. However, the SEM images of OS, US and HHP treatment revealed the disruption to the parenchyma cell by displaying the damage to the tonoplast and cell membrane and hereby loss of vacuole structure and cell compartmentalization.

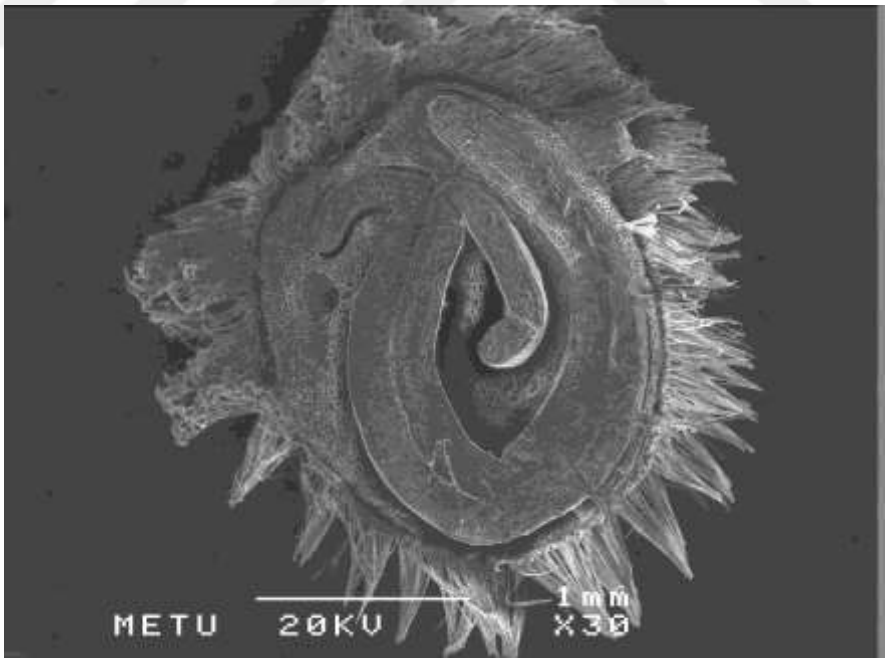

Figure 3.5. Scanning electron microscopy image of untreated tomato seed, Testa (T), embryo (Em), endosperm (End) and endosperm cap (EC).

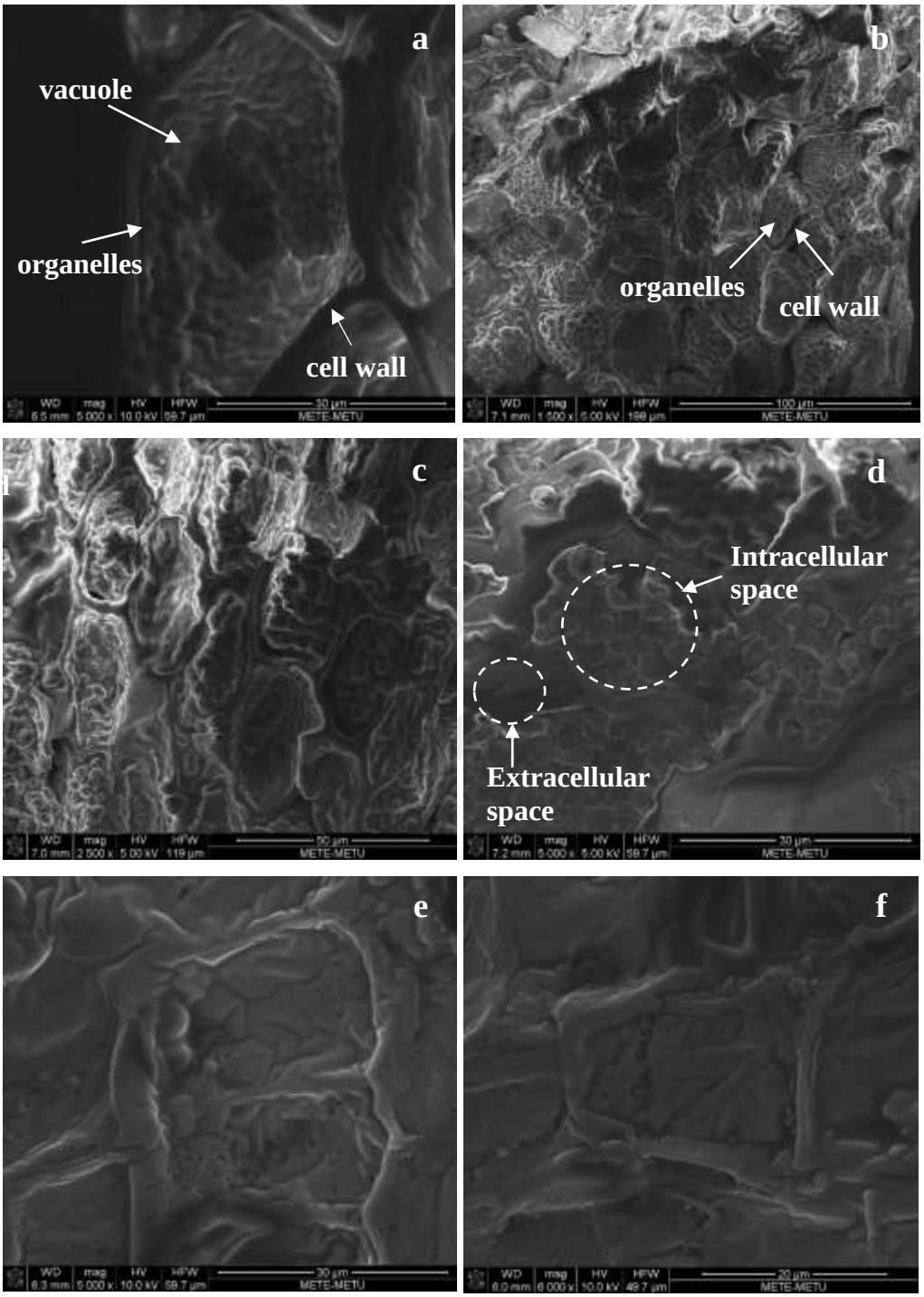

Figure 3.6. SEM images of untreated tomato seeds (a), tomato seeds treated with OS with 10% NaCl solution (b), 20% NaCl solution (c) and 30% NaCl solution (d), tomato seeds treated with US for 5min (e), 10 min (f) and 20 min (g), and tomato seeds treated with HHP at 20℃ and 15 min at 300 MPa (h), 400 MPa (j) and 500 MPa (k)

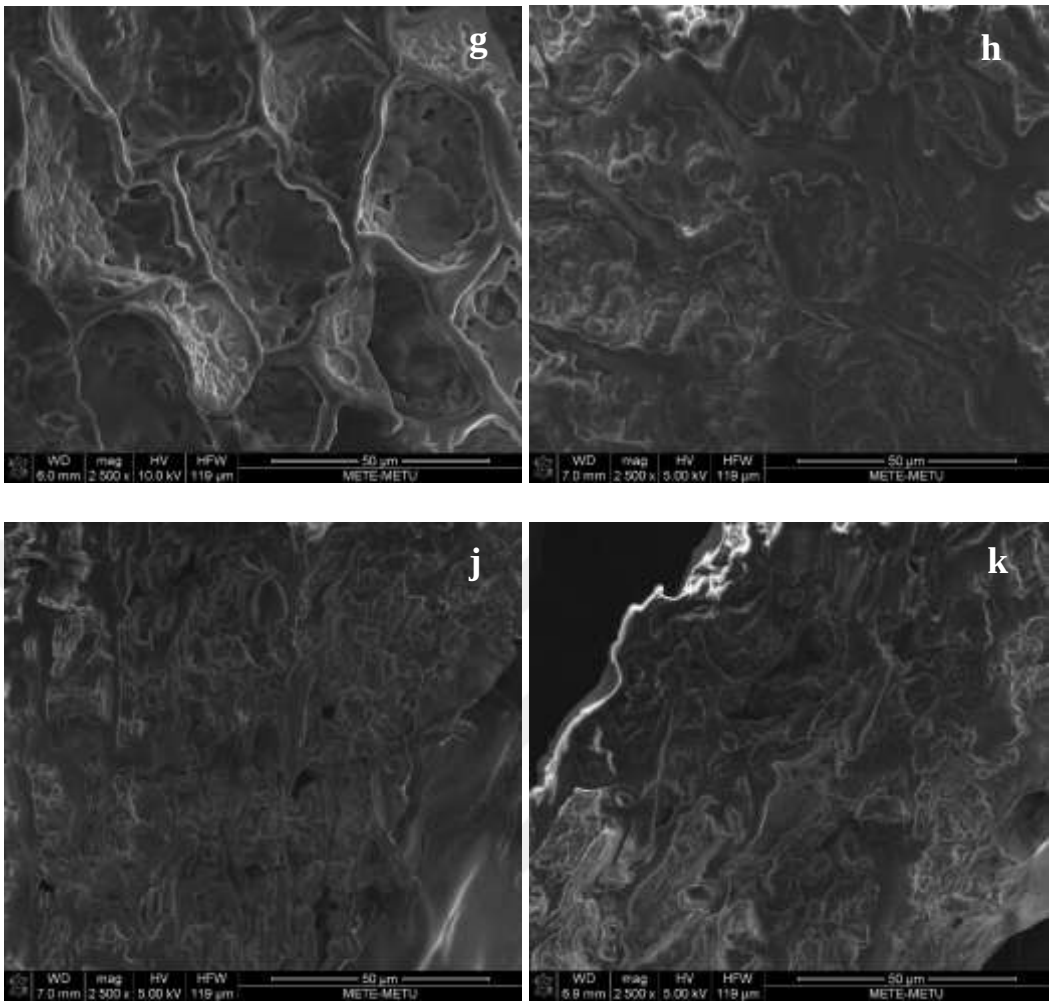

Figure 3.6. (Cont'd)

3.2 PART II

3.2.1 Functional Properties / Swelling Power (SP) and Water Solubility Index (WSI)

SP and WSI values of quinoa starch samples were given in Table 3.2 for the nine types of starches which were exposed to HHP (250, 350 and 500 MPa at 20 and 40℃ for 5 min), US (5 min), heat treatment (control gelatinized) and untreated samples provided as control. The results showed that WSI values of the quinoa starch decreased significantly with HHP and US treatments ($p<0.05$). However, HHP treatment was found to have more effect on the WSI ($p<0.05$). For the HHP treated samples, the results showed that HHP treatment of 250 MPa at 20 and 40℃ did not result in a significant change, while pressure levels above at 350 MPa and 500 MPa showed a significant difference for WSI. This could be explained by the fact that HHP treated starch granules could stay intact or partially disintegrate resulting in restricted amylose leaching and thus decrease in the WSI values of the starch (Yang, Chaib, Gu, & Hemar, 2017a). For quinoa starch samples treated with US, the reason of the decrease in the WSI compared to control sample could be the inadequacy of US treatment time duration to destroy the starch granule completely. This resulted in less amylose leaching and decrease in WSI value of the starch (H. Zhang, Li, Li, & Zhu, 2018). WSI of the quinoa starch gelatinized by heat treatment (90℃) was also found to increase significantly ($p<0.05$) which can be linked to the leaching of water soluble components by complete destruction of the starch granule (Ahmed et al., 2018).

According to Table 3.2, SP values decreased significantly as with HHP and US treatments ($p<0.05$). For the HHP treated samples, the results showed that HHP treatment of 250 MPa at 20 and 40℃ and 350 MPa at 20℃ did not have a significant effect on SP values. Similarly, HPP treatment of 350 MPa at 40℃ and US treatment did not show significant change in SP values ($p<0.05$). However, SP value of the quinoa starch gelatinized by heat treatment (90℃) showed the highest SP value,

which indicates the existence of higher amount of damaged starch than starches treated with HHP and US. This can be attributed to amylose leaching because amylose restricts swelling by strengthening the internal network within the granules (Jan et al., 2017)(Jan et al., 2017). Thus, it was hypothesized that with further HHP application up to 500 MPa, SP and WSI values decrease because of the decrease in leaching of water-soluble components such as amylose with HHP treatment. In addition, formation of amylose-lipid complexes stabilized the granule structure and thus reduced the SP and WSI values. Moreover, US treatment caused less amylose leaching and thus insignificant decrease in SP value of quinoa starch due to inadequacy of US treatment time duration to destroy the starch granule completely (H. Zhang et al., 2018; Zhu & Li, 2019).

Table 3.2. Water solubility index (WSI, %) and swelling power (SP, g/g) of quinoa starches

Treatment	Water solubility index (WSI, %)	Swelling power (SP, g/g)
Control	43.10±0.04^{c}	22.40±0.06^{bc}
HHP - 250 MPa 20°C	44.00±0.25^{b}	23.05±0.91^{b}
HHP - 250 MPa 40°C	43.30±0.04^{bc}	23.24±0.11^{b}
HHP - 350 MPa 20°C	41.00±0.07^{d}	21.70±0.18^{bc}
HHP - 350 MPa 40°C	37.75±0.08^{e}	17.57±0.49^{d}
HHP - 500 MPa 20°C	12.55±0.11^{g}	11.17±2.31^{e}
HHP - 500 MPa 40°C	11.85±0.12^{g}	11.13±1.71^{e}
US - 15 min	36.10±0.35^{f}	19.12±1.15^{cd}
Control Gelatinized (90°C)	58.00±0.72^{a}	38.32±1.54^{a}

Values are an average of triplicate observations and values with different letters are significantly different (*$p < 0.05$); Control (0.01 MPa - 25°C); HHP, high hydrostatic pressure (250 MPa – 20°C and 40°C, 350 MPa 20°C and 40°C, 500 MPa 20°C and 40°C); US, Ultrasonication (100% power - 15 min); Control Gelatinized - Heat Treatment (90°C).

3.2.2 Rheological Measurements

Shear stress/ shear rate profiles for the untreated, HHP and US treated and heat gelatinized (control gelatinized) quinoa starch suspensions are given in Fig. 3.7. Under the current experimental conditions, the quinoa starch samples showed Non-Newtonian and shear thinning behavior as the viscosities of the samples decreased with the increasing shear rate. Shear stress and shear rate data were fitted by power law model. The power law constants k and n were given in Table 3.3. n (Flow behavior index) values of the samples were increased with the increased pressure and did not show any significant change with high hydrostatic pressure (HHP) treatment up to 500 MPa and ultrasonication (US) ($p>0.05$). HHP treatment at 500 MPa-40°C and heat treatment did not result in a significant change in n values of the quinoa starch samples ($p>0.05$). A decrease in k (consistency index) values was observed with increasing pressure and ultrasonication. However, k values did not show any significant change with high hydrostatic pressure (HHP) treatment at 500 MPa at 40°C and heat treatment ($p>0.05$). Apparent viscosity of the starch samples decreased with increasing pressure. Heat treatment also decreased the apparent viscosity. The results showed that HHP treatment at 500 MPa at 20 and 40°C resulted in lower degree of shear-thinning in quinoa starch samples due to the increase in the n value by approaching to n=1. The increase in the n value might be related to the limited amylose leaching and improved granule integrity of HHP treated quinoa starch at 500 MPa (Li & Zhu, 2018). Control gelatinization by heat treatment resulted in increase in the n value of quinoa starch indicating less pseudoplastic behavior. In literature, Xu et al found that the n value increased with increasing temperature indicating reduced pseudoplasticity (Xu et al., 2021), while it was stated in another study that the n value decreased by increasing the heating temperature resulting in more pseudoplastic behavior (Chamberlain, Rao, & Cohen, 1999). In this study, the reason of increase in the n value of control gelatinized quinoa starch might be related to the structure and composition of starch and the ghost structures, which stayed after gelatinization as remnants (Li & Zhu, 2018). The results of rheological

measurements are in agreement with other studies by Li and Zhu who reported that pressure increase (at 500 and 600 MPa) caused decrease in the apparent viscosity and consistency index value of the starch. In another study conducted on ultrasound effect on corn starch (Jambrak et al., 2010), it was reported that ultrasound treatment (at maximum power and intensity (400 W, 73 W cm-2)) decreased the apparent viscosity of the starch samples.

Table 3.3. Rheological properties (flow behavior index (n), consistency index (K) of quinoa starches

Treatment	**n**	**K (Pa.s^n)*10^{-3}**
Control	0.76±0.01^{ab}	1.16±0.00^{a}
HHP - 250 MPa 20°C	0.77±0.03^{ab}	0.86±0.00^{b}
HHP - 250 MPa 40°C	0.78±0.02^{ab}	0.81±0.01^{c}
HHP - 350 MPa 20°C	0.76±0.00^{b}	1.07±0.01^{d}
HHP - 350 MPa 40°C	0.79±0.00^{a}	1.01±0.00^{e}
HHP - 500 MPa 20°C	0.93±0.00^{c}	0.61±0.00^{f}
HHP - 500 MPa 40°C	0.98±0.00^{d}	0.44±0.01^{g}
US - 15 min	0.78±0.00^{ab}	1.09±0.00^{h}
Control Gelatinized (90°C)	0.99±0.00^{d}	0.43±0.00^{g}

Values are an average of triplicate observations and values with different letters are significantly different (*p < 0.05); Control (0.01 MPa - 25°C); HHP, high hydrostatic pressure (250 MPa – 20°C and 40°C, 350 MPa 20°C and 40°C, 500 MPa 20°C and 40°C); US, Ultrasonication (100% power - 15 min); Control Gelatinized - Heat Treatment (90°C).

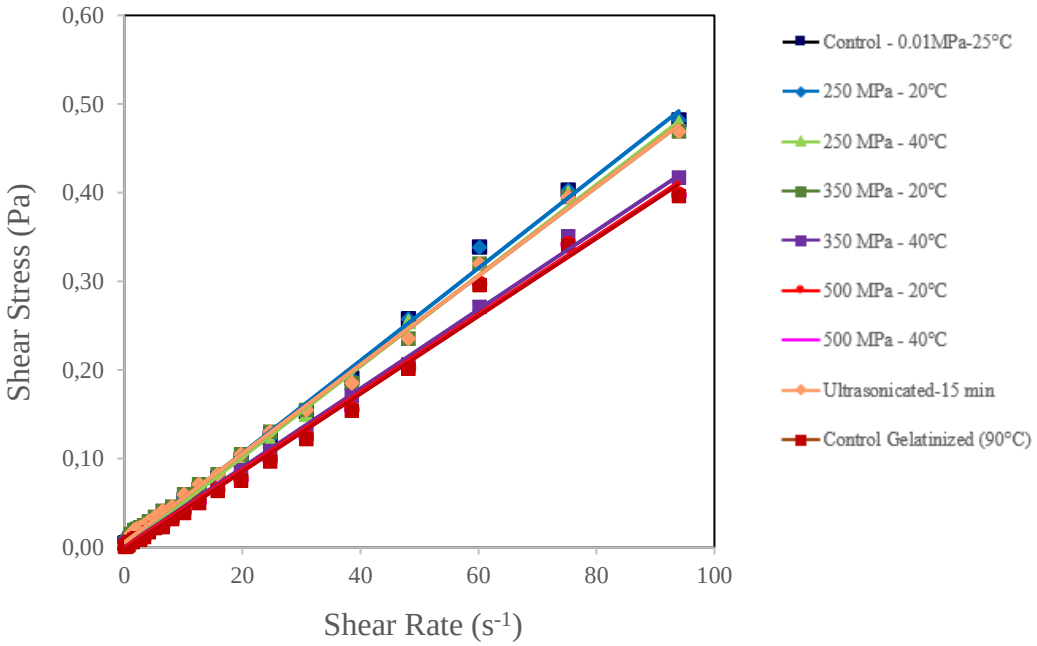

Figure 3.7. Variation of shear stress with shear strain of untreated – control (0.01 MPa - 25°C) and treated quinoa starch with HHP (high hydrostatic pressure) at 250 MPa - 20°C, 250 MPa - 40°C, 350 MPa - 20°C, 350 MPa - 40°C, 500 MPa - 20°C, 500 MPa - 40°C, US (Ultrasonication) at 100% power - 15 min and control gelatinized (by heat treatment at 90°C)

3.2.3 Particle Size Analysis

The average particle size distribution of quinoa starch granules was given in Table 3.4. D [4,3] represent the volume mean diameter. The particle size distribution revealed an apparent increase in the volume mean diameter with HHP treatment ($p<0.05$). The volume mean diameter of the quinoa starch granules was increased from approximately 13,96 µm to 53,53 µm following HHP treatment at 500 MPa-40°C. Heat treatment also resulted in similar particle size distribution with HHP treatment at 500 MPa. Particle size increase after HHP treatment have also been reported in the literature. Guo et al. reported that particle size of lotus seed starch was increased after treatment with ultra-high pressure at 400 MPa (Guo, Zeng, Lu, et al., 2015). This was associated with the aggregation of gelatinized starch. After HHP treatment, the outer shell of the starch granule was destroyed, and the inner section swelled leading to aggregation of the modified granules thus resulting

increase in particle size of starch granules. US treatment did not result any significant increase in the D[4,3] value of the quinoa starch ($p>0.05$).

Table 3.4. Particle size of quinoa starches

Treatment	D [4,3] (µm)
Control	13.97 ± 1.01^{e}
HHP - 250 MPa 20°C	18.40 ± 2.12^{ed}
HHP - 250 MPa 40°C	19.33 ± 3.02^{ed}
HHP - 350 MPa 20°C	17.23 ± 5.21^{dc}
HHP - 350 MPa 40°C	36.37 ± 1.48^{c}
HHP - 500 MPa 20°C	48.40 ± 8.53^{ba}
HHP - 500 MPa 40°C	53.53 ± 5.49^{ba}
US - 15 min	21.00 ± 3.76^{ed}
Control Gelatinized (90°C)	56.9 ± 1.22^{a}

Values are an average of triplicate observations and values with different letters are significantly different (*$p < 0.05$); Control (0.01 MPa - 25°C); HHP, high hydrostatic pressure (250 MPa – 20°C and 40°C, 350 MPa 20°C and 40°C, 500 MPa 20°C and 40°C); US, Ultrasonication (100% power - 15 min); Control Gelatinized - Heat Treatment (90°C); D [4,3], volume-weighted mean diameter.

3.2.4 NMR Relaxometry

3.2.4.1 Spin-Spin T_2 Relaxation Time Measurements

T_2 relaxation time values of quinoa starch samples which were exposed to HHP and US treatment were given in Table 3.5. It was observed that there was an increasing trend in T_2 relaxation time values of quinoa starch samples which were exposed to HHP and US treatment. T_2 value of quinoa starch increased with both treatments, while HHP treatment showed a higher increase on the T_2 values of quinoa starches ($p<0.05$) at 500 MPa. However, the quinoa starch samples that were fully gelatinized by heat treatment had shorter T_2 values. The increase in the T_2 value of HHP treated

quinoa starches could be mainly related to the mechanism of HHP induced starch gelatinization which affect the crystalline and supramolecular structures of starch granules (Yang et al., 2017a, 2016). Application of HHP to starch samples resulted in a conversion of A-type crystalline structure to B-type crystalline structure which favored interhelical water leading to better H-bonds. This caused less double helix dissociation as compared with heat induced gelatinization of starch, resulting in poor amylose leaching and thus less granule swelling of starch (Yang, Gu, & Hemar, 2013). Amylose-fatty acid complexes formed during HHP induced gelatinization could also result in restriction of granule swelling (Katopo, Song, & Jane, 2002). Moreover, another reason behind the increase in the T_2 value of HHP treated quinoa starches was related to the shear force applied during stirring in the conventional heat gelatinization of starch (Yang et al., 2017a). For US treatment, it was observed that there is not a significant increase in the T2 values of quinoa starch samples when compared to HHP treatment up to 350 MPa at 40℃ and control gelatinization with heat treatment, while there is a significant decrease when compared to HHP treatment at 500 MPa at 20 and 40℃. The reason of behind this could be related to the inadequacy of US treatment time duration to destroy the starch granule completely resulting in reduced amylose leaching and thus reduced granule swelling (Manchun et al., 2012; H. Zhang et al., 2018).

Table 3.5. Average T_2 relaxation times and percent relative areas (RA) of control (0.01 MPa - 25℃); HHP, high hydrostatic pressure (250 MPa – 20°C and 40°C, 350 MPa 20°C and 40°C, 500 MPa 20°C and 40°C); US (100% power - 15 min); Control Gelatinized - Heat Treatment (90℃)

Treatment	**T2 (ms)**		**T2 (ms)**	**RA(%)**
Control	65.96±2.29[ab]	peak 1	0.66	20.03
		peak 2	1.7	79.97
HHP 250 MPa-20°C	70.11±2.15[ab]	peak 1	0.48	16.55
		peak 2	1.5	82.61
HHP 250 MPa-40°C	74.12±2.02[ab]	peak 1	0.61	21.02
		peak 2	1.6	78.98
HHP 350 MPa-20°C	90.87±2.98[a]	peak 1	0.43	7.76
		peak 2	1.5	91.27
HHP 350 MPa-40°C	100.86±5.46[a]	peak 1	0.19	23.79
		peak 2	1.5	76.21
HHP 500 MPa-20°C	547.35±43.12[c]	peak 1		
		peak 2	1.5	99.62
HHP 500 MPa-40°C	546.35±32.51[c]	peak 1		
		peak 2	1.7	100
US - 15 min	91.49±4.43[a]	peak 1	0.59	22.42
		peak 2	1.6	7.57
Control Gelatinized (90°C)	22.71±0.88[b]	peak 1		
		peak 2	1.6	99.68

3.2.4.2 Water Proton Transverse Relaxation Time Distributions

To explore the effect of modifications on water compartmentalization in the starch granule, T_2 relaxation spectrums were also analyzed by non-negative-least-squares (NNLS) analysis. Fig.3.8 shows representative T_2 relaxation spectra for the quinoa starch samples. Untreated quinoa starch exhibited mainly two distinct proton populations (peaks). The peak with lower T_2 value was associated with an environment with lower mobility, the interior rigid part of the granule. This could be explained by the slow exchange between the water inside and outside of the granules. The peak with higher T_2 value, on the other hand, was attributed to the more mobile environment, which was the bulk water content in the exterior of the granule. There was a fast diffusive exchange between hydroxyl protons in the amylopectin and amylose molecules in the bulk water of external space (Tananuwong & Reid, 2004; Tang, Godward, & Hills, 2000). HHP treatment up to 500 MPa and US treatment caused only minor changes in the T_2 relaxation spectra. However, the pressure treatment at 500 MPa resulted in significant changes in the proton mobility of the quinoa starch. The area of the peak with higher T_2 value was increased while the area of the peak with lower T_2 value was decreased (a lower fraction) resulting in merging as one peak. This was consistent with high pressure swelling of the starch granule (B. Hills, Costa, Marigheto, & Wright, 2005). HHP treatment at 500 MPa seemed to enhance the mobilization of the amorphous region.

As can be seen in Fig.3.8, fully gelatinized quinoa starch exhibited one peak. Heat induced gelatinization increased the diffusive exchange of water between interior and exterior regions of the granule. The reason behind this phenomenon was related with the destruction in the granule structure during heat treatment. The heat treatment applied for fully gelatinization of starch resulted in destruction of the structural barriers, which led to a faster diffusive exchange of water molecules between compartments in the granule. As a result of this structural change, the area of the peak representing the protons coming from less mobile environment decreased or the peaks merged as one peak, representing one water compartment in the granule

after granule breakdown. These findings were in good agreement with the water fractions in the compartments of the starch granule (Tananuwong & Reid, 2004). NMR Relaxometry results was found consistent with the results obtained from FTIR spectra.

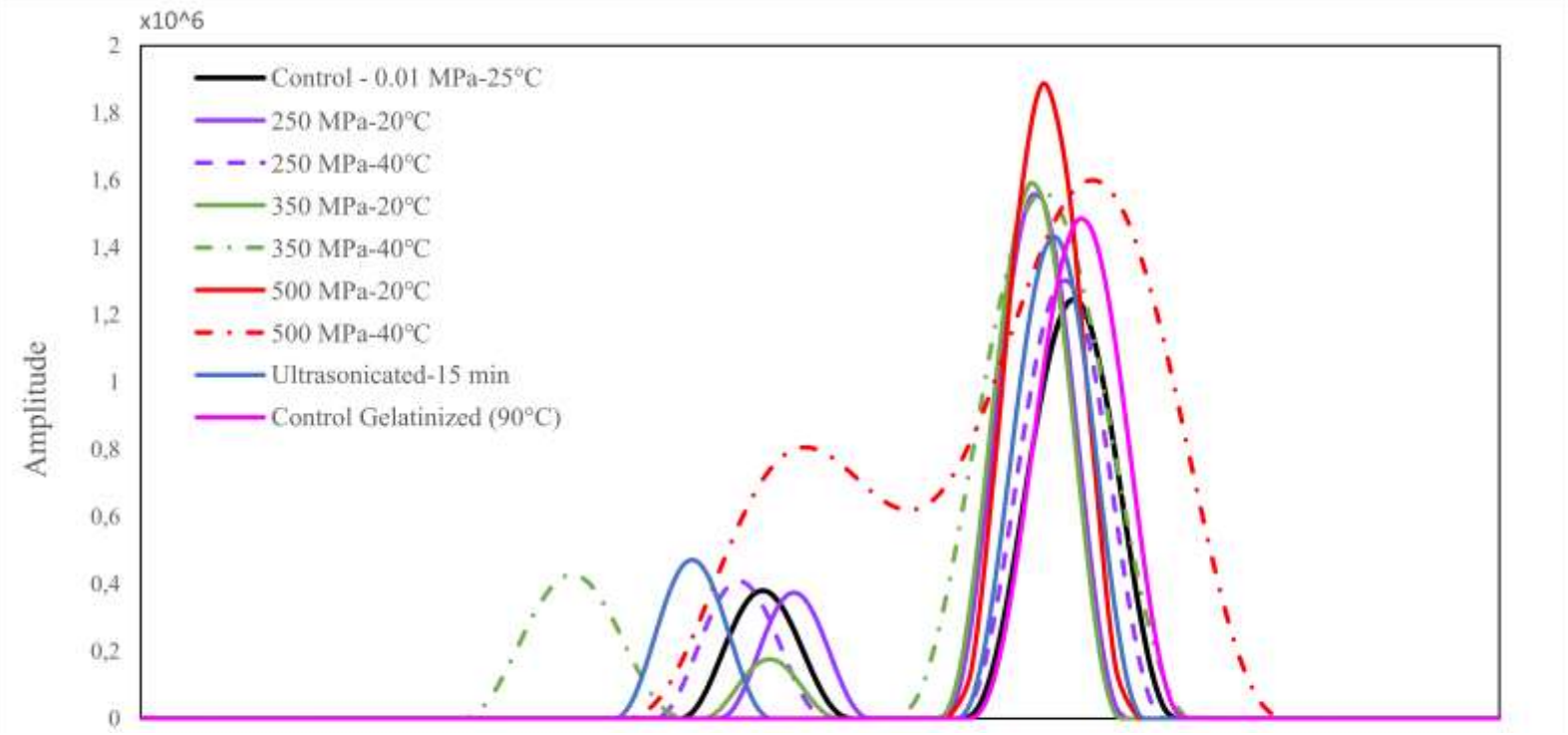

Figure 3.8. T_2 relaxation spectrum of quinoa starch slurries soaked with distilled water for control (0.01 MPa - 25°C) and HHP treated at 250 MPa - 20°C, 250 MPa - 40°C, 350 MPa - 20°C, 350 MPa - 40°C, 500 MPa - 20°C, 500 MPa - 40°C, Ultrasonicated (100% power - 15 min), control gelatinized (by heat treatment at 90°C)

3.2.5 Fourier Transform Infrared (FTIR) Spectroscopy

To identify the major functional groups, present in the untreated, HHP-treated and US-treated quinoa starch samples, Fourier transform infrared (FTIR) spectra are illustrated in Fig.3.9. The starch samples showed strong adsorption bands at 3337, 2940, 1636, 1354, 1153, 1080 and 1011 cm^{-1}. The broadest peak observed at 3337 cm^{-1} was associated with O-H stretching vibration. For the modified starches treated with HHP and US, the intensity of the peak at 3337 cm^{-1} was higher than the untreated quinoa starch. This increase in peak intensity was attributed to the increase in the number of functional groups associated to the peak. It was observed that as the pressure was increased, the intensity of the peak decreased indicating that pressure increase resulted in limited amylose leaching and formation of amylose-lipid complexes that would destroy the ability of the starch to retain bound water (or indicating lower crystallinity of the sample). The results agreed with the previous results. It was stated that increase in pressure caused decrease in the peak intensity at 3330 cm^{-1} (Ahmed et al., 2018). Thus, O-H stretching of the modified starches were higher than untreated starches.

In the obtained FTIR spectra, another peak was detected at 2940 cm^{-1} which was related with C-H stretching (Cruz-Tirado et al., 2018) and the intensity of the peak decreased with pressure increase. Pressure at 500 MPa-40°C decreased the peak intensity suggesting that pressure increase weakened the C-H vibrations. Similar results were stated by Kızıl et al. (Kizil, Irudayaraj, And, & Seetharaman, 2002) and it was stated that the peak between 2800-3000 cm^{-1} was related with CH_2 deformation and the ratio of amylose to amylopectin affected the intensity of the peak.

The intensity of the peak at 1636 cm^{-1} was known to result from O-H bending of water molecules (water absorbed in the amorphous regions of starch) (Kizil et al., 2002). It was stated that peak at 1673 cm^{-1} affected by the change in the crystallinity of the starch and the intensity of this peak became weaker as crystallinity of the starch increased. Fang et al. (Fang, Fowler, Tomkinson, & Hill, 2002) stated that the

peak observed at 1640 cm^{-1} was related with the tightly bound water content of the starch. Therefore, the peaks observed at 1636 cm^{-1} could be considered in relation with O-H group bending. It was observed that the peak intensity decreased with increasing HHP and US treatments. This result also correlated with T_2 values of NMR measurements that will be explored in the latter section.

The intensity of the peak at 1354 cm^{-1} and 1153 cm^{-1} showed an increase up to 350 MPa-40°C and a decrease with 350 MPa-40°C. The peak at 1344 cm^{-1} was related with CH_2 bending modes. It was also stated that the vibrations related to the bending and deformation related to C and H atoms might be tracked between 1500-1300 cm^{-1}. The peak at 1153 cm^{-1} was originated from C-O and CH_2 stretching (Kizil et al., 2002).

A sharper peak was observed at 1011 cm^{-1} indicating C-O-C stretching (Kizil et al., 2002). It was explained the previous study that peak observed between 1060 and 990 cm^{-1} could be associated with the strain deformations of the C-O-C and flexion of the OH and related with the characteristic of the polysaccharides (Ferreira-Villadiego et al., 2018). The peak at 1000 cm^{-1} was stated as water sensitive and attributed to intramolecular H bonding of OH groups (van Soest, Tournois, de Wit, & Vliegenthart, 1995) and attributed to the crystallinity in the starch granule (Warren, Gidley, & Flanagan, 2016). It was also stated that high pressure caused destruction of the crystalline structure of lentil starch granule (Ahmed, Thomas, Taher, & Joseph, 2016). The observations obtained by FTIR spectrum were also consistent with the NMR and SEM results.

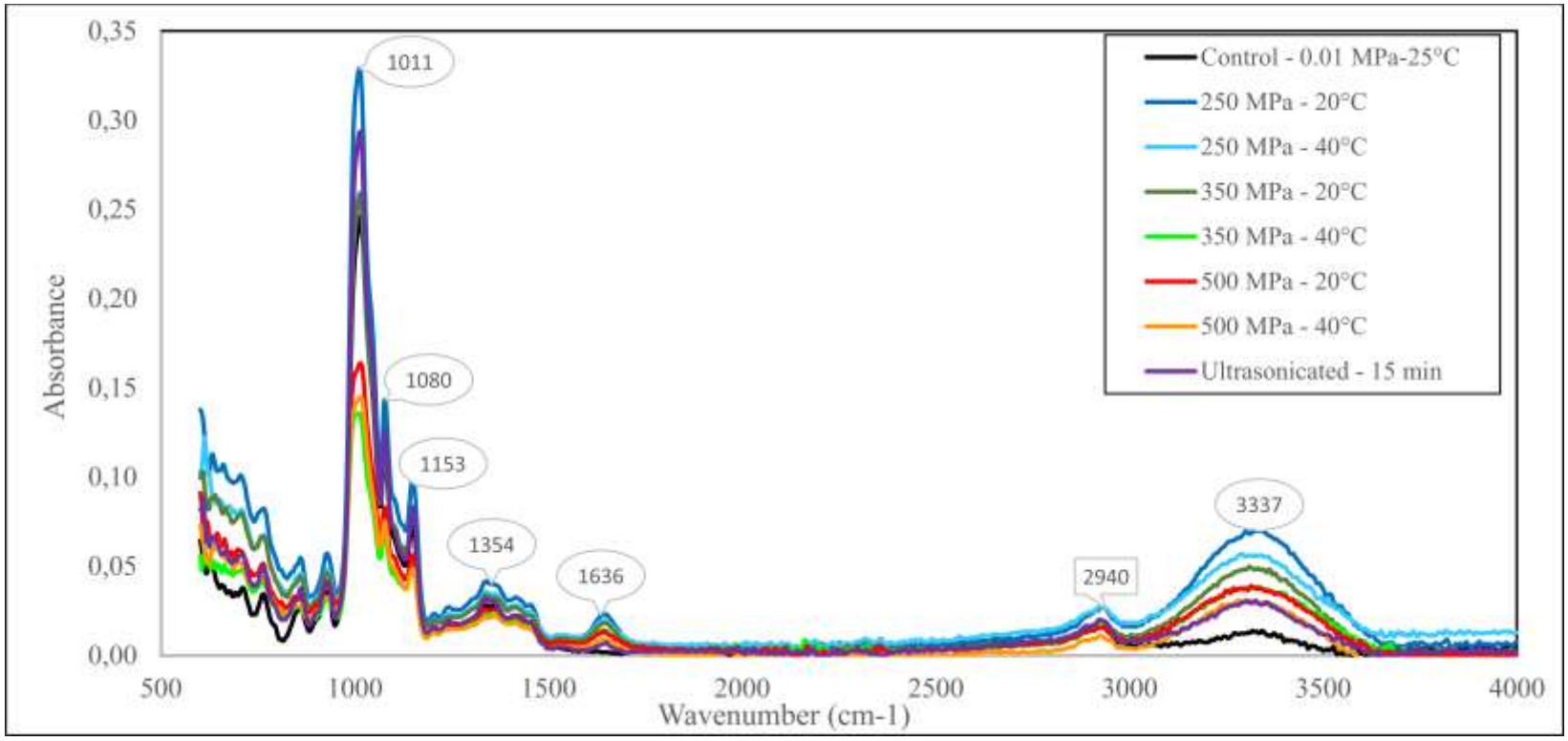

Figure 3.9. FTIR spectra of untreated – control (0.01 MPa - 25°C) and treated quinoa starch with HHP (high hydrostatic pressure) at 250 MPa - 20°C, 250 MPa - 40°C, 350 MPa - 20°C, 350 MPa - 40°C, 500 MPa - 20°C, 500 MPa - 40°C, US (Ultrasonication) at 100% power - 15 min)

3.2.6 Differential Scanning Calorimetry (DSC)

Thermal properties of the native and modified starches are shown in Table 3.6. It was observed that onset temperature of quinoa starch increased with HHP and US treatments. However, it decreased by heat treatment. Several studies in the literature have shown that HHP decreased the gelatinization temperature and the enthalpy change (ΔH) of starch such as lotus seed starch, rice starch, wheat starch and barley starch (Guo, Zeng, Zhang, et al., 2015; Yang, Chaib, Gu, & Hemar, 2017b). On the other hand, HHP has been shown to increase the onset (T_o) and peak temperature (T_p) of potato and high-amylose maize starch (Katopo et al., 2002). It was attributed to the loss of less-stable crystalline structures and the development of amylose-lipid complexes during HHP treatment. It was considered that the amylose-lipid complex possessed a high melting temperature, which resulted in increase in the gelatinization temperature of starch with higher lipid contents treated with HHP (Kugimiya, Donovan, & Wong, 1980). The degree of gelatinization (DG) of native and modified quinoa starches are given in Table 3.6. It increased up to HHP treatment of 350 MPa pressure at 20°C showing the gelatinization of starch at that pressure levels. However, it decreased with HHP treatment of 350 MPa pressure at 20°C. This decrease was associated with the loss of less-stable crystalline structures and the development of amylose-lipid complexes during HHP treatment. It may also be attributed to the retrogradation of starch at HHP treatment of 350 MPa and 500MPa pressure levels due to the unconscious storage of the samples prior to the measurement. HHP treatment at 250 MPa at 20°C and US treatment did not show significant difference in DG values. Heat treatment at 90°C also increased the DG significantly.

Table 3.6. Thermal properties of quinoa starch of control (0.1 MPa - 25℃) and treated with HHP, (250 MPa – 20°C and 40°C, 350 MPa 20°C and 40°C, 500 MPa 20°C and 40°C); US, Ultrasonication (100% power - 15 min); Control Gelatinized - Heat Treatment (90°C); T_0, onset temperature; Tp, peak temperature; ΔH, enthalpy (J/g); DG, degree of gelatinization

Treatment	**T_0 (℃)**	**T_p (℃)**	**ΔH (J/g)**	**DG (%)**
Control	48.19	59.57	0.82	0%
HHP - 250 MPa 20℃	54.48	65.61	0.72	12%
HHP - 250 MPa 40℃	56.62	66.25	0.26	69%
HHP - 350 MPa 20℃	53.12	64.38	0.51	37%
HHP - 350 MPa 40℃	55.08	62.89	0.53	35%
HHP - 500 MPa 20℃	59.03	67.1	1.85	-126%
HHP - 500 MPa 40℃	57.03	64.62	2.18	-166%
US - 15 min	54.11	64.53	0.73	11%
Control Gelatinized (90℃)	45.43	54.39	0.47	43%

3.2.7 X-Ray Diffraction (XRD)

The X-ray diffraction (XRD) patterns of untreated, HHP and US treated and heat gelatinized quinoa starch samples are shown in Figure 3.10. Untreated quinoa starch demonstrated a doublet at 2Θ value of 17.1° and 18° and singlets at 2Θ value of 15.3° and 23.15°, which exhibits an A-type X-ray diffraction pattern. A weak peak was observed at 2Θ value of 20.16°, which was attributed to the amylose-lipid complex. No significant changes in XRD patterns were observed for quinoa starch after HHP treatment of 250 MPa at 20 and 40℃, 350 MPa at 20℃ and US treatment, expressing that starch crystalline structure were not damaged under these conditions. This was consistent with the previous results of functional properties of quinoa starch at these parameters. After HHP treatment of 350 MPa at 40℃, the decrease of the diffraction intensity of quinoa starch started. At HHP treatment of 500 MPa at 20 and 40℃ and heat treatment, the peaks became more broader and larger due to turning of the doublet peak at 2Θ value of 17.1° into a single peak and disappearance of other peaks. It was associated with the conversion of A-type crystalline structure to B-type crystalline structure indicated destruction of the internal crystalline structure and starch gelatinization. Furthermore, as pressure increased, the peak at 2Θ value of 20.16° became more prominent. This could be explained by the high pressure promoting the formation of amylose-lipid complexes.

The degree of crystallinity (CD) values are also demonstrated in Figure 3.10. The results showed that CD values of quinoa starch decreased with HHP, US and heat treatments. It was found that HHP treatment of 250 MPa at 20 and 40℃ and US treatment did not result in a significant change in CD values of quinoa starch, while pressure levels above at 350 and 500 MPa showed a significant difference for CD values of the quinoa starch. CD of the heat-treated quinoa starch was also found to decrease significantly ($p<0.05$). Thus, it was concluded that HHP treatments of 350 MPa at 40℃ and 500 MPa at 20 and 40℃ and heat treatment were sufficient to destroy the internal crystalline structure of the quinoa starch, while HHP treatments

of 250 MPa at 20 and 40℃, 350 MPa at 20℃ and US treatments were inadequate enough (J. Wang et al., 2017).

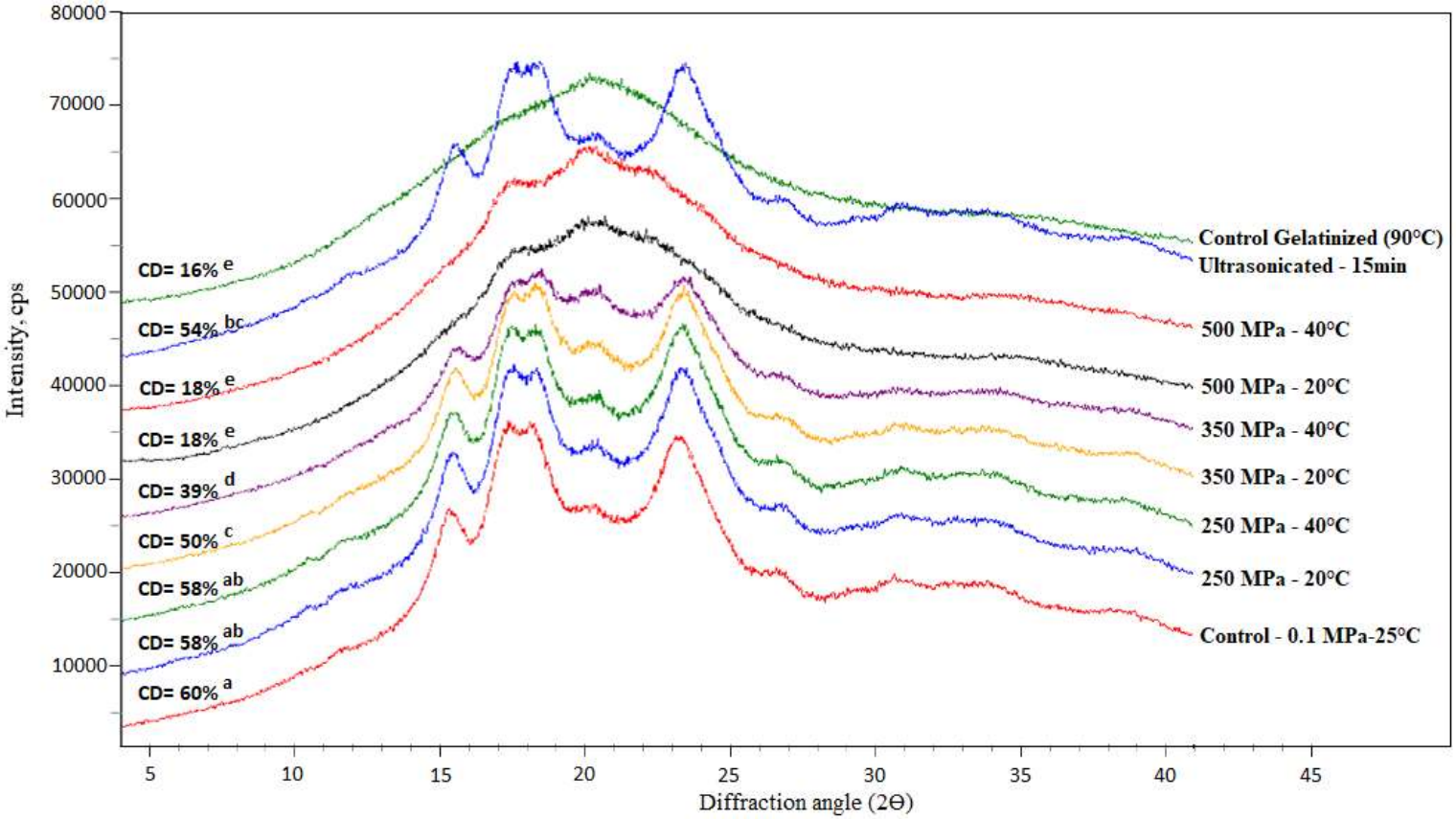

Figure 3.10. X-ray diffraction patterns and degree of crystallinity (CD) of untreated – control (0.1 MPa - 25°C) and treated quinoa starch with HHP (high hydrostatic pressure) at 250 MPa - 20°C, 250 MPa - 40°C, 350 MPa - 20°C, 350 MPa - 40°C, 500 MPa - 20°C, 500 MPa - 40°C, Ultrasonicated at 100% power - 15 min, Control gelatinized (by heat treatment at 90°C).

3.2.8 Scanning Electron Microscopy (SEM)

Scanning electron microscopy images of untreated, HHP and US treated quinoa starches were shown in Fig.3.11. The untreated native starch granules had polygonal shape. The surface of the starch granule was smooth and did not exhibit any cracks. It could be clearly seen that the starches treated at 250 MPa 20°C-40°C and 350 MPa 20°C did not show any significant change as compared to the native starch. The quinoa starch samples treated with US displayed similar surface structure with the native starch. In previous studies, small fissures and depressions were observed on the surface of potato and wheat starch granule treated with US for 30 min at a frequency of 20 KHz and power 170 W (Sujka & Jamroz, 2013). It was consistent to observe smooth surface structure of US treated quinoa starch when compared with US treatment with higher time duration.

At 350 MPa-40°C, morphological changes started to form slowly such as the formation of cracks. HHP treated samples especially at 500 MPa showed the granule destruction due to the gelatinization of quinoa starch. Furthermore, the observations presented in Fig.3.11 were consistent with morphological and FTIR results since gelatinization effect of HHP treatment damaged the starch granule. In literature, similar observations were also reported for different starches (Ahmed et al., 2018; Okur, Ozel, Oztop, & Alpas, 2019).

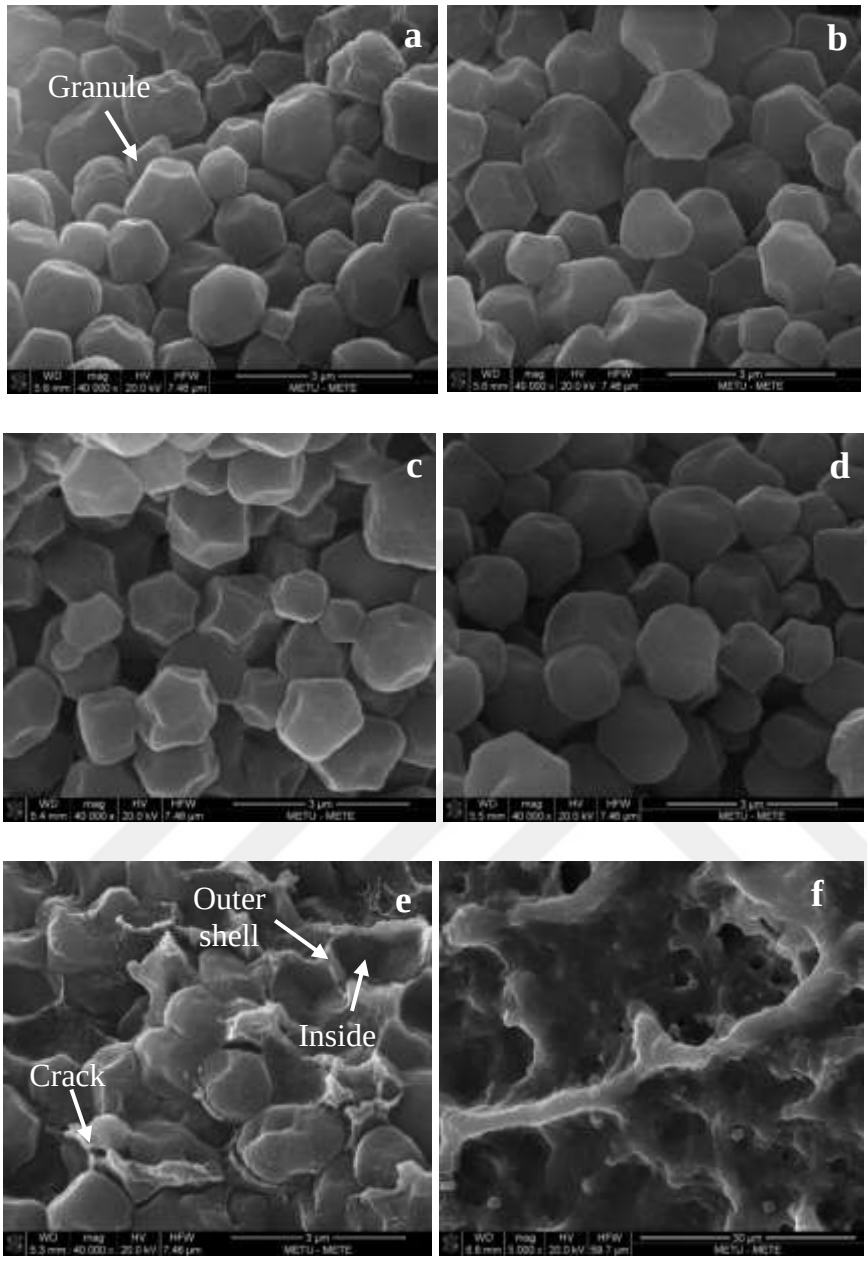

Figure 3.11. Scanning electron microscopy (SEM) images of untreated-control (0.01 MPa - 25°C) (a), quinoa starches treated with high hydrostatic pressure (HHP) at 250 MPa - 20°C (b), 250 MPa - 40°C (c), 350 MPa - 20°C (d), 350 MPa - 40°C (e), 500 MPa - 20°C (f), 500 MPa - 40°C (g), Ultrasonicated (US) at 100% power - 15 min (h)

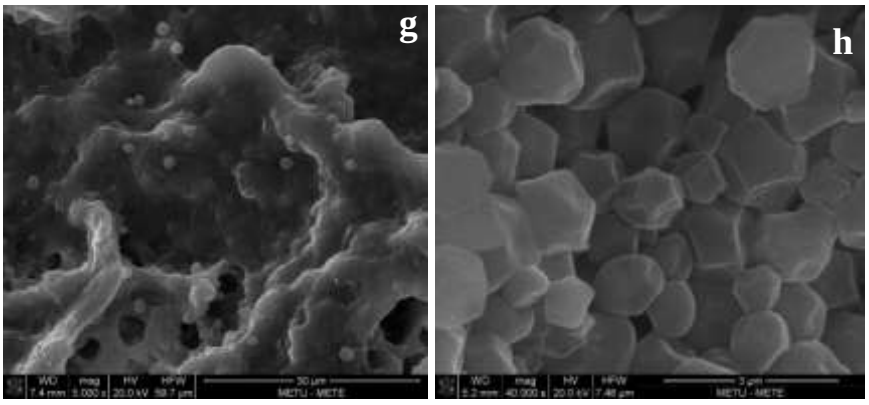

Figure 3.11. (Cont'd)

CHAPTER 4

CONCLUSION

In this study, TD NMR relaxometry was used for investigating the changes in the cell integrity of plant tissues and assessing physicochemical characteristics of starch-water interactions

In the first part of the study, it was used to investigate the changes in the cell integrity of tomato seeds. Osmotic stress (OS), ultrasonication (US) and high hydrostatic pressure (HHP) resulted in cell permeabilization and changes in the plant parenchyma cell structure. After treatments, important information on water redistribution in tomato seeds were obtained using NMR relaxometry, that is indicating the severity of cell disruption effect of applied treatments. It was observed that OS treatment with 10% NaCl solution had caused the least changes in the T_2 relaxation spectrum and OS treatment with 20 and 30% NaCl resulted in minor changes in the T_2 relaxation spectrum. However, US and HHP caused significant alterations in the cell structure of tomato seed and HHP at 500 MPa resulted in the most detrimental effect in the cell structure. SEM measurements further supported the physiological changes observed in relaxation measurement, such as the change in the integrity of the cell membrane. Thus, it was possible to distinguish different degrees of membrane damages caused by different treatments based on changes in the T_2 relaxation spectrum of the sample.

In the second part, physicochemical characteristics of quinoa starch exposed to high hydrostatic pressure (HHP) and ultrasonication (US) were investigated. Swelling power and water solubility index of quinoa starch decreased with both treatments, however HHP caused a significant decrease at 500 MPa. Apparent viscosity of the starch samples decreased with increasing pressure and US treatment. Both treatments resulted in an increase in the D [4,3] value of the quinoa starch, but HHP treatment

caused a significant increase in the volume mean diameter (D [4,3]). FTIR results also revealed consistent results supporting that HHP treatment led to strong changes while US treatment caused minor changes on the quinoa starch. DSC and XRD results revealed the destruction of crystalline structure by HHP treatment of 350 MPa at 40°C, 500 MPa at 20 and 40°C and heat treatment for control gelatinization. SEM results also showed the intense effect of HHP treatment on quinoa starch, especially at 500 MPa pressure level. Time domain (TD) NMR results showed that both treatments resulted with an increase in T_2 values, while HHP treatment caused a strong increase in T_2 values ($p<0.05$) at 500 MPa pressure level. NMR relaxation spectra of quinoa seeds revealed mainly two distinct proton populations. HHP treatment at 500 MPa pressure level caused faster exchange of proton populations compared to US treatment. Thus, it was supported that HHP and US treatments had a modification effect on quinoa starch, while HHP treatment at 500 MPa caused the strongest effect on quinoa starch by providing modified quinoa starch with better quality. Moreover, NMR relaxometry was proved as a useful tool to investigate the quinoa starch water interactions subjected to different treatments.

To conclude, this dissertation has proved that TD-NMR relaxometry is an effective method for characterization of cell integrity of tomato seeds and physiological changes in quinoa starch dispersions. HHP caused the most detrimental effect in the cell structure of tomato seed at 500 MPa. Furthermore, HHP treatment at 500 MPa had the strongest effect on the quality of the quinoa starch by developing modified quinoa starch with better quality.

Based on the findings and analysis, it is possible to conclude that this study provides insight for future research in the seed structure, quinoa starch and use of them. A virus detection method could be designed with a complete experimental design and the elimination of virus with HHP could be analyzed. Furthermore, the changes at different stages of the seed could be analyzed with TD-NMR relaxometry. Moreover, modified quinoa starch could be evaluated for the starch digestibility and effect on resistant starch content and it could be used in a food material for the observation of its properties.

REFERENCES

Abugoch James, L. E. (2009). *Chapter 1 Quinoa (Chenopodium quinoa Willd.)*. https://doi.org/10.1016/S1043-4526(09)58001-1

Ahmed, J., Thomas, L., Arfat, Y. A., & Joseph, A. (2018). Rheological, structural and functional properties of high-pressure treated quinoa starch in dispersions. *Carbohydrate Polymers*, *197*(May), 649–657. https://doi.org/10.1016/j.carbpol.2018.05.081

Ahmed, J., Thomas, L., Taher, A., & Joseph, A. (2016). Impact of high pressure treatment on functional, rheological, pasting, and structural properties of lentil starch dispersions. *Carbohydrate Polymers*, *152*, 639–647. https://doi.org/10.1016/j.carbpol.2016.07.008

Alcázar-Alay, S. C., & Meireles, M. A. A. (2015). Physicochemical properties, modifications and applications of starches from different botanical sources. *Food Science and Technology*, *35*(2), 215–236. https://doi.org/10.1590/1678-457X.6749

Ashogbon, A. O., & Akintayo, E. T. (2014). Recent trend in the physical and chemical modification of starches from different botanical sources: A review. *Starch/Staerke*, *66*(1–2), 41–57. https://doi.org/10.1002/star.201300106

Augusto, P. E. D., Tribst, A. A. L., & Cristianini, M. (2018). High Hydrostatic Pressure and High-Pressure Homogenization Processing of Fruit Juices. *Fruit Juices: Extraction, Composition, Quality and Analysis*, 393–421. https://doi.org/10.1016/B978-0-12-802230-6.00020-5

Bauer, B. A., & Knorr, D. (2005). The impact of pressure, temperature and treatment time on starches: Pressure-induced starch gelatinisation as pressure time temperature indicator for high hydrostatic pressure processing. *Journal of Food Engineering*, *68*(3), 329–334. https://doi.org/10.1016/j.jfoodeng.2004.06.007

Belton, P., & Capozzi, F. (2011). Magnetic resonance in food science - Meeting the challenge. *Magnetic Resonance in Chemistry*, *49*(SUPPL. 1), 47521. https://doi.org/10.1002/mrc.2851

Belton, P. S., & Ratcliffe, R. G. (1985). NMR and compartmentation in biological tissues. *Prog. NMR Spectroscopy*, *17:241-279*.

Berna, F. (2016). Fourier Transform Infrared Spectroscopy (FTIR). *Encyclopedia of Earth Sciences Series*, 285–286. https://doi.org/10.1007/978-1-4020-4409-0_15

Bewley, J. D. (1997). Seed germination and dormancy. *Plant Cell*, *9*(7), 1055–

1066. https://doi.org/10.1105/tpc.9.7.1055

Biliaderis, C. G. (2009). Structural Transitions and Related Physical Properties of Starch. In *Starch* (Third Edit). https://doi.org/10.1016/B978-0-12-746275-2.00008-2

Bitik, A., Sumnu, G., & Oztop, M. (2019). Physicochemical and Structural Characterization of Microfluidized and Sonicated Legume Starches. *Food and Bioprocess Technology*, *12*(7), 1144–1156. https://doi.org/10.1007/s11947-019-02264-4

Buléon, A., Colonna, P., Planchot, V., & Ball, S. (1998). Starch granules: structure and biosynthesis. *International Journal of Biological Macromolecules*, *23*(2), 85–112. https://doi.org/10.1016/S0141-8130(98)00040-3

Buzrul, S. (2014, December 1). Multi-pulsed high hydrostatic pressure inactivation of microorganisms: A review. *Innovative Food Science and Emerging Technologies*, Vol. 26, pp. 1–11. https://doi.org/10.1016/j.ifset.2014.07.004

Carna4. (2015). The Difference Between Grains & Seeds. Retrieved from https://carna4.com/the-difference-between-grains-seeds/

Chamberlain, E. K., Rao, M. A., & Cohen, C. (1999). Shear thinning and antithixotropic behavior of a heated cross-linked waxy maize starch dispersion. *International Journal of Food Properties*, *2*(1), 63–77. https://doi.org/10.1080/10942919909524590

Chiu, C. wai, & Solarek, D. (2009). Modification of Starches. In *Starch* (Third Edit). https://doi.org/10.1016/B978-0-12-746275-2.00017-3

Choi, H. S., Kim, H. S., Park, C. S., Kim, B. Y., & Baik, M. Y. (2009). Ultra high pressure (UHP)-assisted acetylation of corn starch. *Carbohydrate Polymers*, *78*(4), 862–868. https://doi.org/10.1016/j.carbpol.2009.07.005

Cruz-Tirado, J. P., Tapia-Blácido, D. R., Siche, R., Abdullah, A. H. D., Chalimah, S., Primadona, I., & Hanantyo, M. H. G. (2018). IOP Conference Series: Earth and Environmental Science Physical and chemical properties of corn, cassava, and potato starchs Influence of Proportion and Size of Sugarcane Bagasse Fiber on the Properties of Sweet Potato Starch Foams Physical and chemical p. *IOP Conf. Series: Earth and Environmental Science*, *160*, 12003. https://doi.org/10.1088/1755-1315/160/1/012003

Dellarosa, N., Ragni, L., Laghi, L., Tylewicz, U., Rocculi, P., & Dalla Rosa, M. (2016). Time domain nuclear magnetic resonance to monitor mass transfer mechanisms in apple tissue promoted by osmotic dehydration combined with pulsed electric fields. *Innovative Food Science and Emerging Technologies*. https://doi.org/10.1016/j.ifset.2016.01.009

Douzals, J. P., Marechal, P. A., Coquille, J. C., & Gervais, P. (1996). Microscopic study of starch gelatinization under high hydrostatic pressure. *Journal of*

Agricultural and Food Chemistry, *44*(6), 1403–1408. https://doi.org/10.1021/jf950239c

Eliasson, A. C. (2010). Gelatinization and retrogradation of starch in foods and its implications for food quality. *Chemical Deterioration and Physical Instability of Food and Beverages*, 296–323. https://doi.org/10.1533/9781845699260.2.296

Elmer, P. (2014). *DSC*.

Ersus, S., & Barrett, D. M. (2010). Determination of membrane integrity in onion tissues treated by pulsed electric fields: Use of microscopic images and ion leakage measurements. *Innovative Food Science and Emerging Technologies*, *11*(4), 598–603. https://doi.org/10.1016/j.ifset.2010.08.001

Evers, T., & Millar, S. (2002). Cereal grain structure and development: Some implications for quality. *Journal of Cereal Science*, Vol. 36, pp. 261–284. https://doi.org/10.1006/jcrs.2002.0435

Fang, J. M., Fowler, P. A., Tomkinson, J., & Hill, C. A. S. (2002). The preparation and characterisation of a series of chemically modified potato starches. *Carbohydrate Polymers*, *47*(3), 245–252. https://doi.org/10.1016/S0144-8617(01)00187-4

FAO. (2021). *Quinoa production worldwide*.

FAO Seed and Plant Genetic Resources Service. (n.d.). *Seed and Seed Quality : Technical Information for FAO Emergency Staff*.

Ferreira-Villadiego, J., García-Echeverri, J., Vidal, M. V., Pasqualino, J., Meza-Castellar, P., & Lambis-Miranda, H. A. (2018). Chemical modification and characterization of starch derived from plantain (Musa paradisiaca) peel waste, as a source of biodegradable material. *Chemical Engineering Transactions*, *65*, 763–768. https://doi.org/10.3303/CET1865128

Finch-Savage, W. E., & Leubner-Metzger, G. (2006). Seed dormancy and the control of germination - Finch-Savage - 2006 - New Phytologist - Wiley Online Library. *The New Phytologist*, *171*(3), 501–523. Retrieved from http://www.ncbi.nlm.nih.gov/pubmed/16866955

Fister, H., Merkel, C., & Tauscher, B. (2002). *Changes in functional properties of vegetables induced by HP treatment_Butz 2002*. *35*, 295–300.

Gill, P., Moghadam, T. T., & Ranjbar, B. (2010). *Differential Scanning Calorimetry Techniques: Applications in Biology and Nanoscience*.

Guo, Z., Zeng, S., Lu, X., Zhou, M., Zheng, M., & Zheng, B. (2015). Structural and physicochemical properties of lotus seed starch treated with ultra-high pressure. *Food Chemistry*, *186*, 223–230. https://doi.org/10.1016/j.foodchem.2015.03.069

Guo, Z., Zeng, S., Zhang, Y., Lu, X., Tian, Y., & Zheng, B. (2015). The effects of ultra-high pressure on the structural, rheological and retrogradation properties of lotus seed starch. *Food Hydrocolloids*, *44*, 285–291. https://doi.org/10.1016/j.foodhyd.2014.09.014

Hashemi, R.H., Bradley, W.G., & Lisanti, C. J. (2010). *MRI: The basics*. Lippincott Williams & Wilkins.

Hemdane, S., Jacobs, P. J., Bosmans, G. M., Verspreet, J., Delcour, J. A., & Courtin, C. M. (2017). Study of biopolymer mobility and water dynamics in wheat bran using time-domain 1H NMR relaxometry. *Food Chemistry*, *236*, 68–75. https://doi.org/10.1016/j.foodchem.2017.01.020

Hernández-Sánchez, N., Hills, B. P., Barreiro, P., & Marigheto, N. (2007). An NMR study on internal browning in pears. *Postharvest Biology and Technology*, *44*(3), 260–270. https://doi.org/10.1016/j.postharvbio.2007.01.002

Hilhorst, H. W. M., Groot, S. P. C., & Bino, R. J. (1998). The tomato seed as a model system to study seed development and germination. *Acta Botanica Neerlandica*, *47*(2), 169–183.

Hills, B., Costa, A., Marigheto, N., & Wright, K. (2005). Applled Magnetic Resonance T~-T 2 NMR Correlation Studies of High-Pressure-Processed Starch and Potato Tissue. In *Appl. Magn. Reson* (Vol. 28).

Hills, B. P. (1998). Magnetic resonance imaging in food science. *Wiley*.

Hills, B. P., & Clark, C. J. (2003). Quality Assessment of Horticultural Products by NMR. *Annual Reports on NMR Spectroscopy*, Vol. 50, pp. 75–120. https://doi.org/10.1016/S0066-4103(03)50002-3

Hills, B. P., & Remigereau, B. (1997). NMR studies of changes in subcellular water compartmentation in parenchyma apple tissue during drying and freezing. *International Journal of Food Science and Technology*, *32*(1), 51–61. https://doi.org/10.1046/j.1365-2621.1997.00381.x

Horovitz, O., Cioica, N., Jumate, N., Pojar-Feneşan, M., Balea, A., Liteanu, V., … Tomoaia-Cotişel, M. (2011). SEM characterization of starch granules. *Studia Universitatis Babes-Bolyai Chemia*, (1), 211–219.

Jambrak, A. R., Herceg, Z., Šubarić, D., Babić, J., Brnčić, M., Brnčić, S. R., … Gelo, J. (2010). Ultrasound effect on physical properties of corn starch. *Carbohydrate Polymers*, *79*(1), 91–100. https://doi.org/10.1016/J.CARBPOL.2009.07.051

Jan, K. N., Panesar, P. S., & Singh, S. (2017). Process standardization for isolation of quinoa starch and its characterization in comparison with other starches. *Journal of Food Measurement and Characterization*, *11*(4), 1919–1927. https://doi.org/10.1007/s11694-017-9574-6

Joshi, M., Aldred, P., McKnight, S., Panozzo, J. F., Kasapis, S., Adhikari, R., & Adhikari, B. (2013). Physicochemical and functional characteristics of lentil starch. *Carbohydrate Polymers*, *92*(2), 1484–1496. https://doi.org/10.1016/j.carbpol.2012.10.035

Karoui, R. (2012). Food Authenticity and Fraud. *Chemical Analysis of Food: Techniques and Applications*, 499–517. https://doi.org/10.1016/B978-0-12-384862-8.00015-7

Katopo, H., Song, Y., & Jane, J. L. (2002). Effect and mechanism of ultrahigh hydrostatic pressure on the structure and properties of starches. *Carbohydrate Polymers*, *47*(3), 233–244. https://doi.org/10.1016/S0144-8617(01)00168-0

Kaur, B., Ariffin, F., Bhat, R., & Karim, A. A. (2012). Progress in starch modification in the last decade. *Food Hydrocolloids*, *26*(2), 398–404. https://doi.org/10.1016/J.FOODHYD.2011.02.016

Kawai, K., Fukami, K., & Yamamoto, K. (2007). Effects of treatment pressure, holding time, and starch content on gelatinization and retrogradation properties of potato starch-water mixtures treated with high hydrostatic pressure. *Carbohydrate Polymers*, *69*(3), 590–596. https://doi.org/10.1016/j.carbpol.2007.01.015

Kim, H. S., Kim, B. Y., & Baik, M. Y. (2012). Application of ultra high pressure (UHP) in starch chemistry. *Critical Reviews in Food Science and Nutrition*, *52*(2), 123–141. https://doi.org/10.1080/10408398.2010.498065

Kirtil, E., & Oztop, M. H. (2016, March 1). 1H Nuclear Magnetic Resonance Relaxometry and Magnetic Resonance Imaging and Applications in Food Science and Processing. *Food Engineering Reviews*, Vol. 8, pp. 1–22. https://doi.org/10.1007/s12393-015-9118-y

Kizil, R., Irudayaraj, J., And, †, & Seetharaman, K. (2002). *Characterization of Irradiated Starches by Using FT-Raman and FTIR Spectroscopy*. https://doi.org/10.1021/jf011652p

Knorr, D., Heinz, V., & Buckow, R. (2006). High pressure application for food biopolymers. *Biochimica et Biophysica Acta - Proteins and Proteomics*, *1764*(3), 619–631. https://doi.org/10.1016/j.bbapap.2006.01.017

Kohli, R. (2012). Methods for Monitoring and Measuring Cleanliness of Surfaces. In *Developments in Surface Contamination and Cleaning: Detection, Characterization, and Analysis of Contaminants* (Vol. 4). https://doi.org/10.1016/B978-1-4377-7883-0.00003-1

Konez, O. (2011). *Manyetik Rezonans Görüntüleme: Temel Bilgiler*.

Kramer, P. J. (1983). *Water relations of plants*. Academic Press.

Kugimiya, M., Donovan, J. W., & Wong, R. Y. (1980). Phase Transitions of

Amylose-Lipid Complexes in Starches: A Calorimetric Study. *Starch - Stärke*, *32*(8), 0–5.

Kumar, A., Satya, Y. &, & Singh, V. (n.d.). *Osmotic dehydration of fruits and vegetables: a review*. https://doi.org/10.1007/s13197-012-0659-2

Leite, T. S., de Jesus, A. L. T., Schmiele, M., Tribst, A. A. L., & Cristianini, M. (2017). High pressure processing (HPP) of pea starch: Effect on the gelatinization properties. *LWT - Food Science and Technology*, *76*, 361–369. https://doi.org/10.1016/j.lwt.2016.07.036

Li, G., Wang, S., & Zhu, F. (2016). Physicochemical properties of quinoa starch. *Carbohydrate Polymers*, *137*, 328–338. https://doi.org/10.1016/j.carbpol.2015.10.064

Li, G., & Zhu, F. (2018). Effect of high pressure on rheological and thermal properties of quinoa and maize starches. *Food Chemistry*, *241*(May 2017), 380–386. https://doi.org/10.1016/j.foodchem.2017.08.088

LibreTexts. (2020). *X-ray diffraction (XRD) basics and application*. Retrieved from https://chem.libretexts.org/@go/page/148442

Lindeboom, N., Chang, P. R., Falk, K. C., & Tyler, R. T. (2005). Characteristics of starch from eight quinoa lines. *Cereal Chemistry*, *82*(2), 216–222. https://doi.org/10.1094/CC-82-0216

Maheswari, M., Joshi, D. K., Saha, R., Nagarajan, S., & Gambhir, P. N. (1999). Transverse relaxation time of leaf water protons and membrane injury in wheat (Triticum aestivum L.) in response to high temperature. *Annals of Botany*, *84*(6), 741–745. https://doi.org/10.1006/anbo.1999.0974

Maity, A. (Texas A. U. (2021). Why are seeds of different sizes and shapes? Retrieved from Sustainable, Secure Food Blog website: https://sustainable-secure-food-blog.com/2021/03/22/why-are-seeds-of-different-sizes-and-shapes/

Malik, A., Erginkaya, Z., & Erten, H. (2019). Health and safety aspects of food processing technologies. In *Health and Safety Aspects of Food Processing Technologies*. https://doi.org/10.1007/978-3-030-24903-8

Manchun, S., Nunthanid, J., Limmatvapirat, S., & Sriamornsak, P. (2012). Effect of ultrasonic treatment on physical properties of tapioca starch. *Advanced Materials Research*, *506*, 294–297. https://doi.org/10.4028/www.scientific.net/AMR.506.294

Marigheto, N., Vial, A., Wright, K., & Hills, B. (2004). A combined NMR and microstructural study of the effect of high-pressure processing on strawberries. *Applied Magnetic Resonance*, *26*(4), 521–531. https://doi.org/10.1007/BF03166580

Mason, T. J., Paniwnyk, L., & Lorimer, J. P. (1996). The uses of ultrasound in food technology. *Ultrasonics Sonochemistry*, *3*(3). https://doi.org/10.1016/S1350-4177(96)00034-X

Musse, M., Quellec, S., Devaux, M.-F., Cambert, M., Lahaye, M., & Mariette, F. (2009). An investigation of the structural aspects of the tomato fruit by means of quantitative nuclear magnetic resonance imaging. *Magnetic Resonance Imaging*, *27*(5), 709–719. https://doi.org/10.1016/j.mri.2008.11.005

Nowak, V., Du, J., & Charrondière, U. R. (2016). Assessment of the nutritional composition of quinoa (Chenopodium quinoa Willd.). *Food Chemistry*, *193*, 47–54. https://doi.org/10.1016/j.foodchem.2015.02.111

Okur, I., Ozel, B., Oztop, M. H., & Alpas, H. (2019). Effect of high hydrostatic pressure in physicochemical properties and in vitro digestibility of cornstarch by nuclear magnetic resonance relaxometry. *Journal of Food Process Engineering*, *42*(6), 1–10. https://doi.org/10.1111/jfpe.13168

Patindol, J. A., Siebenmorgen, T. J., & Wang, Y. J. (2015). Impact of environmental factors on rice starch structure: A review. *Starch/Staerke*, *67*(1–2), 42–54. https://doi.org/10.1002/star.201400174

Pei-Ling, L., Xiao-Song, H., & Qun, S. (2010). Effect of high hydrostatic pressure on starches: A review. *Starch/Staerke*, *62*(12), 615–628. https://doi.org/10.1002/star.201000001

Raffo, A., Gianferri, R., Barbieri, R., & Brosio, E. (2005). Ripening of banana fruit monitored by water relaxation and diffusion 1H-NMR measurements. *Food Chemistry*, *89*(1), 149–158. https://doi.org/10.1016/j.foodchem.2004.02.024

Rahman, M. S. (2007). Handbook of Food Preservation. In *Food Science and Technology* (Vol. 2).

Seeds Market by Type, Trait, Crop Type And Region - Global Forecast to 2026. (2021). https://www.marketsandmarkets.com/Market-Reports/seed-market-126130457.html

Sibgatullin. (2005). *Combined Analysis of Diffusion and Relaxation Behavior of Water in Apple Parenchyma Cells*. https://doi.org/ffusion. For the fast-relaxing components, the diffusion coefficient an-omalously increases with time. DOI :

Sindhu, R., Binod, P., & Pandey, A. (2015). Microbial Poly-3-Hydroxybutyrate and Related Copolymers. In *Industrial Biorefineries and White Biotechnology*. https://doi.org/10.1016/B978-0-444-63453-5.00019-7

Snaar, J. E. M., & Van As, H. (1992). Probing water compartments and membrane permeability in plant cells by 1H NMR relaxation measurements. *Biophysical Journal*, *63*(6), 1654–1658. https://doi.org/10.1016/S0006-3495(92)81741-1

Spink, C. H. (2008). Differential Scanning Calorimetry. In *Methods in Cell Biology* (pp. 115–141). https://doi.org/10.1016/s0091-679x(07)84005-2

Stute, R., Klingler, R. W., Boguslawski, S., Eshtiaghi, M. N., & Knorr, D. (1996). Effects of high pressures treatment on starches. *Starch/Staerke*, *48*(11–12), 399–408. https://doi.org/10.1002/star.19960481104

Taiz, L., & Zeiger, E. (2006). *Plant Physiology, 3rd ed*.

Tananuwong, K., & Reid, D. S. (2004). DSC and NMR relaxation studies of starch-water interactions during gelatinization. *Carbohydrate Polymers*, *58*(3), 345–358. https://doi.org/10.1016/j.carbpol.2004.08.003

Tang, H. R., Godward, J., & Hills, B. (2000). Distribution of water in native starch granules - a multinuclear NMR study. *Carbohydrate Polymers*, *43*(4), 375–387. https://doi.org/10.1016/S0144-8617(00)00183-1

Thevelein, J. M., Van Assche, J. A., Heremans, K., & Gerlsma, S. Y. (1981). Gelatinisation temperature of starch, as influenced by high pressure. *Carbohydrate Research*, *93*(2), 304–307. https://doi.org/10.1016/S0008-6215(00)80862-9

Torrenegra, M., Solano, R., Herrera, A., León, G., & Pajaro, A. (2018). Fourier Transform Infrared Spectroscopy (FTIR) Analysis of Biodegradable Films Based On Modified Colombian Starches of Cassava and Yam. *International Journal of PharmTech Research*, *11*(4), 368–376. https://doi.org/10.20902/ijptr.2018.11408

Traffano-Schiffo, M. V., Laghi, L., Castro-Giraldez, M., Tylewicz, U., Romani, S., Ragni, L., … Fito, P. J. (2017). Osmotic dehydration of organic kiwifruit pre-treated by pulsed electric fields: Internal transport and transformations analyzed by NMR. *Innovative Food Science and Emerging Technologies*. https://doi.org/10.1016/j.ifset.2017.03.012

Unal, K., Alpas, H., Aktas, H., & Oztop, M. H. (2020). Time domain (TD)-NMR relaxometry as a tool to investigate the cell integrity of tomato seeds exposed to osmotic stress (OS), ultrasonication (US) and high hydrostatic pressure (HHP). *Journal of Food Science and Technology*, *57*(10), 3739–3747. https://doi.org/10.1007/s13197-020-04406-5

Vallons, K. J. R., & Arendt, E. K. (2009). Effects of high pressure and temperature on the structural and rheological properties of sorghum starch. *Innovative Food Science & Emerging Technologies*, *10*(4), 449–456. https://doi.org/10.1016/J.IFSET.2009.06.008

Van der Weerd, L., Claessens, M. M. A. E., Ruttink, T., Vergeldt, F. J., Schaafsma, T. J., & Van As, H. (2001). Quantitative NMR microscopy of osmotic stress responses in maize and pearl millet. *Journal of Experimental Botany*. https://doi.org/10.1093/jexbot/52.365.2333

Van, H., Van Der Weerd, L., Claessens, M. M. A. E., Efdé, C., & Van As, H. (2002). Nuclear magnetic resonance imaging of membrane permeability changes in plants during osmotic stress. *Plant, Cell and Environment*, *25*, 1539–1549.

van Soest, J. J. G., Tournois, H., de Wit, D., & Vliegenthart, J. F. G. (1995). Short-range structure in (partially) crystalline potato starch determined with attenuated total reflectance Fourier-transform IR spectroscopy. *Carbohydrate Research*, *279*(C), 201–214. https://doi.org/10.1016/0008-6215(95)00270-7

Vandusschoten, D., Dejager, P. A., & Vanas, H. (1995). Extracting Diffusion Constants from Echo-Time-Dependent PFG NMR Data Using Relaxation-Time Information. *Journal of Magnetic Resonance, Series A*, Vol. 116, pp. 22–28. https://doi.org/10.1006/jmra.1995.1185

Vasquez-tello, A., Zuily-fodil, Y., Thi, A. T. P., & Da Silva, J. B. V. (1990). Electrolyte and Pi leakages and soluble sugar content as physiological tests for screening resistance to water stress in Phaseolus and Vigna species. *Journal of Experimental Botany*, *41*(7), 827–832. https://doi.org/10.1093/jxb/41.7.827

Vilcacundo, R., & Hernández-Ledesma, B. (2017, April 1). Nutritional and biological value of quinoa (Chenopodium quinoa Willd.). *Current Opinion in Food Science*, Vol. 14, pp. 1–6. https://doi.org/10.1016/j.cofs.2016.11.007

Vilche, C., Gely, M., & Santalla, E. (2003). Physical properties of quinoa seeds. *Biosystems Engineering*, *86*(1), 59–65. https://doi.org/10.1016/S1537-5110(03)00114-4

Wang, J., Zhu, H., Li, S., Wang, S., Wang, S., & Copeland, L. (2017). Insights into structure and function of high pressure-modified starches with different crystalline polymorphs. *International Journal of Biological Macromolecules*, *102*, 414–424. https://doi.org/10.1016/J.IJBIOMAC.2017.04.042

Wang, S., & Zhu, F. (2016). Formulation and Quality Attributes of Quinoa Food Products. *Food and Bioprocess Technology*, *9*(1), 49–68. https://doi.org/10.1007/s11947-015-1584-y

Warren, F. J., Gidley, M. J., & Flanagan, B. M. (2016). Infrared spectroscopy as a tool to characterise starch ordered structure - A joint FTIR-ATR, NMR, XRD and DSC study. *Carbohydrate Polymers*, *139*, 35–42. https://doi.org/10.1016/j.carbpol.2015.11.066

Westbrook, C. (1993). *MRI in practice*. Great Britain, Oxford, Blackwell Scientific: John Wiley & Sons.

Xu, F., Zhang, L., Liu, W., Liu, Q., Wang, F., Zhang, H., … Blecker, C. (2021). Physicochemical and structural characterization of potato starch with different degrees of gelatinization. *Foods*, *10*(5), 1–15. https://doi.org/10.3390/foods10051104

Yamamoto, K. (2017). Food processing by high hydrostatic pressure. *Bioscience, Biotechnology and Biochemistry*, *81*(4), 672–679. https://doi.org/10.1080/09168451.2017.1281723

Yang, Z., Chaib, S., Gu, Q., & Hemar, Y. (2017a). Impact of pressure on physicochemical properties of starch dispersions. *Food Hydrocolloids*, *68*, 164–177. https://doi.org/10.1016/j.foodhyd.2016.08.032

Yang, Z., Chaib, S., Gu, Q., & Hemar, Y. (2017b). Impact of pressure on physicochemical properties of starch dispersions. *Food Hydrocolloids*, *68*, 164–177. https://doi.org/10.1016/j.foodhyd.2016.08.032

Yang, Z., Gu, Q., & Hemar, Y. (2013). In situ study of maize starch gelatinization under ultra-high hydrostatic pressure using X-ray diffraction. *Carbohydrate Polymers*, *97*(1), 235–238. https://doi.org/10.1016/j.carbpol.2013.04.075

Yang, Z., Swedlund, P., Hemar, Y., Mo, G., Wei, Y., Li, Z., & Wu, Z. (2016). Effect of high hydrostatic pressure on the supramolecular structure of corn starch with different amylose contents. *International Journal of Biological Macromolecules*, *85*, 604–614. https://doi.org/10.1016/j.ijbiomac.2016.01.018

Yrjö H., R. (2010). Glass Transition Temperature and Its Relevance in Food Processing. *Annu. Rev. Food Sci. Technol*, *1*, 469–496. https://doi.org/10.1146/annurev.food.102308.124139

Zhang, H., Li, M., Li, K., & Zhu, C. (2018). Effect of ultrasound pretreatment on physicochemical properties of corn starch. *International Journal of Biological Macromolecules*, *111*(Icmse), 848–856. https://doi.org/10.1016/j.ijbiomac.2017.12.156

Zhang, L., & McCarthy, M. J. (2012). Black heart characterization and detection in pomegranate using NMR relaxometry and MR imaging. *Postharvest Biology and Technology*, *67*, 96–101. https://doi.org/10.1016/j.postharvbio.2011.12.018

Zhu, F., & Li, H. (2019). Effect of high hydrostatic pressure on physicochemical properties of quinoa flour. *Lwt*, Vol. 114. https://doi.org/10.1016/j.lwt.2019.108367

APPENDICES

A. Statistical Analysis

Table A.4.1. One way Analysis of Variance (ANOVA) and Tukey's comparison test for T_2 relaxation time values of tomato seed samples exposed to different treatments

One-way ANOVA: T2 versus Sample

Method

Null hypothesis	All means are equal
Alternative hypothesis	Not all means are equal
Significance level	α = 0,05

Equal variances were assumed for the analysis.

Factor Information

Factor	Levels	Values
Sample	10	HHP 300MPa; HHP 400MPa; HHP 500MPa; OS 10%; OS 20%; OS 30%; Untreated; US 10min; US 20min; US 5min

Analysis of Variance

Source	DF	Adj SS	Adj MS	F-Value	P-Value
Sample	9	333653	37073	17,16	0,000
Error	20	43206	2160		
Total	29	376859			

Model Summary

S	R-sq	R-sq(adj)	R-sq(pred)
46,4790	88,54%	83,38%	74,20%

Means

Sample	N	Mean	StDev	95% CI
HHP 300MPa	3	650,4	12,50	(594,69; 706,64)
HHP 400MPa	3	590,6	53,0	(506,0; 618,0)
HHP 500MPa	3	585,3	8,74	(528,36; 640,31)
OS 10%	3	619,2	65,0	(563,0; 675,0)
OS 20%	3	741,3	84,8	(685,4; 797,3)
OS 30%	3	764,7	76,9	(708,7; 820,6)
Untreated	3	952,3	32,6	(896,4; 1008,3)
US 10min	3	698,7	9,64	(638,02; 749,98)
US 20min	3	712,46	9,17	(654,02; 765,98)
US 5min	3	710,42	2,08	(654,69; 766,64)

Tukey Pairwise Comparisons

Grouping Information Using the Tukey Method and 95% Confidence

Sample	N	Mean	Grouping	
Untreated	3	952,3	A	
OS 30%	3	764,7	B	
OS 20%	3	741,3	B	
US 20min	3	712,46	B	
US 5min	3	710,42	B	
US 10min	3	698,77	B	
HHP 300MPa	3	650,4	B	
OS 10%	3	619,2	B	
HHP 400MPa	3	590,6	B	C
HHP 500MPa	3	585,3		C

Means that do not share a letter are significantly different.

Table A.4.2. One way Analysis of Variance (ANOVA) and Tukey's comparison test for water solubility index (WSI, %) values of quinoa starches

One-way ANOVA: WSI (%) versus Sample

Method

Null hypothesis	All means are equal
Alternative hypothesis	Not all means are equal
Significance level	α = 0,05

Equal variances were assumed for the analysis.

Factor Information

Factor	Levels	Values
Sample	9	250/20; 250/40; 350/20; 350/40; 500/20; 500/40; Control; Control gelatinized (90 C); Ultrasonicated

Analysis of Variance

Source	DF	Adj SS	Adj MS	F-Value	P-Value
Sample	8	5434,77	679,347	8227,12	0,000
Error	18	1,49	0,083		
Total	26	5436,26			

Model Summary

S	R-sq	R-sq(adj)	R-sq(pred)
0,287357	99,97%	99,96%	99,94%

Means

Sample	N	Mean	StDev	95% CI
250/20	3	44,003	0,246	(43,655; 44,352)
250/40	3	43,3033	0,0404	(42,9548; 43,6519)
350/20	3	41,0033	0,0737	(40,6548; 41,3519)
350/40	3	37,7533	0,0833	(37,4048; 38,1019)
500/20	3	12,5467	0,1137	(12,1981; 12,8952)
500/40	3	11,8533	0,1222	(11,5048; 12,2019)
Control	3	43,1033	0,0404	(42,7548; 43,4519)
Control gelatinized (90 C)	3	58,000	0,721	(57,651; 58,349)
Ultrasonicated	3	36,103	0,345	(35,755; 36,452)

Pooled StDev = 0,287357

Tukey Pairwise Comparisons

Grouping Information Using the Tukey Method and 95% Confidence

Sample	N	Mean	Grouping
Control gelatinized (90 C)	3	58,000	A
250/20	3	44,003	B
250/40	3	43,3033	B C
Control	3	43,1033	C
350/20	3	41,0033	D
350/40	3	37,7533	E
Ultrasonicated	3	36,103	F
500/20	3	12,5467	G
500/40	3	11,8533	G

Means that do not share a letter are significantly different.

Table A.4.3. One way Analysis of Variance (ANOVA) and Tukey's comparison test for swelling power (SP, %) values of quinoa starches

One-way ANOVA: SP (g/g) versus Sample

Method

Null hypothesis	All means are equal
Alternative hypothesis	Not all means are equal
Significance level	α = 0,05

Equal variances were assumed for the analysis.

Factor Information

Factor	Levels	Values
Sample	9	250/20; 250/40; 350/20; 350/40; 500/20; 500/40; Control; Control gelatinized (90 C); Ultrasonicated

Analysis of Variance

Source	DF	Adj SS	Adj MS	F-Value	P-Value
Sample	8	1561,66	195,208	134,30	0,000
Error	18	26,16	1,454		
Total	26	1587,83			

Model Summary

S	R-sq	R-sq(adj)	R-sq(pred)
1,20563	98,35%	97,62%	96,29%

Means

Sample	N	Mean	StDev	95% CI
250/20	3	23,047	0,913	(21,584; 24,509)
250/40	3	23,2367	0,1069	(21,7743; 24,6991)
350/20	3	21,700	0,180	(20,238; 23,162)
350/40	3	17,567	0,494	(16,104; 19,029)
500/20	3	11,17	2,31	(9,71; 12,64)
500/40	3	11,133	1,706	(9,671; 12,596)
Control	3	22,4033	0,0569	(20,9409; 23,8657)
Control gelatinized (90 C)	3	38,317	1,542	(36,854; 39,779)
Ultrasonicated	3	19,123	1,150	(17,661; 20,586)

Pooled StDev = 1,20563

Tukey Pairwise Comparisons

Grouping Information Using the Tukey Method and 95% Confidence

Sample	N	Mean	Grouping			
Control gelatinized (90 C)	3	38,317	A			
250/40	3	23,2367		B		
250/20	3	23,047		B		
Control	3	22,4033		B	C	
350/20	3	21,700		B	C	
Ultrasonicated	3	19,123			C	D
350/40	3	17,567				D
500/20	3	11,17				E
500/40	3	11,133				E

Means that do not share a letter are significantly different.

Table A.4.4. One way Analysis of Variance (ANOVA) and Tukey's comparison test for particle size (D [4,3] (μm)) values of quinoa starches

One-way ANOVA: D [4,3] (μm) versus Sample

Method

Null hypothesis	All means are equal
Alternative hypothesis	Not all means are equal
Significance level	α = 0,05

Equal variances were assumed for the analysis.

Factor Information

Factor	Levels	Values
Sample	9	250/20; 250/40; 350/20; 350/40; 500/20; 500/40; Control; Control gelatinized (90 C); Ultrasonicated

Analysis of Variance

Source	DF	Adj SS	Adj MS	F-Value	P-Value
Sample	8	6541,6	817,70	45,29	0,000
Error	18	325,0	18,05		
Total	26	6866,6			

Model Summary

S	R-sq	R-sq(adj)	R-sq(pred)
4,24892	95,27%	93,16%	89,35%

Means

Sample	N	Mean	StDev	95% CI
250/20	3	18,40	2,12	(13,25; 23,55)
250/40	3	19,33	3,02	(14,18; 24,49)
350/20	3	27,37	5,21	(22,21; 32,52)
350/40	3	36,367	1,484	(31,213; 41,520)
500/20	3	48,40	8,53	(43,25; 53,55)
500/40	3	53,53	5,49	(48,38; 58,69)
Control	3	13,967	1,012	(8,813; 19,120)
Control gelatinized (90 C)	3	56,933	1,222	(51,780; 62,087)
Ultrasonicated	3	21,00	3,76	(15,85; 26,15)

Pooled StDev = 4,24892

Tukey Pairwise Comparisons

Grouping Information Using the Tukey Method and 95% Confidence

Sample	N	Mean	Grouping		
Control gelatinized (90 C)	3	56,933	A		
500/40	3	53,53	A		
500/20	3	48,40	A	B	
350/40	3	36,367		B	C

350/20	3	27,37	C	D	
Ultrasonicated	3	21,00		D	E
250/40	3	19,33		D	E
250/20	3	18,40		D	E
Control	3	13,967			E

Means that do not share a letter are significantly different.

Table A.4.5. One way Analysis of Variance (ANOVA) and Tukey's comparison test for consistency index (K) values of quinoa starches

One-way ANOVA: K versus Sample

Method

Null hypothesis	All means are equal
Alternative hypothesis	Not all means are equal
Significance level	α = 0,05

Equal variances were assumed for the analysis.

Factor Information

Factor	Levels	Values
Sample	9	250/20; 250/40; 350/20; 350/40; 500/20; 500/40; Control; Control gelatinized (90 C); Ultrasonicated

Analysis of Variance

Source	DF	Adj SS	Adj MS	F-Value	P-Value
Sample	8	1,87491	0,234363	5718,63	0,000
Error	18	0,00074	0,000041		
Total	26	1,87564			

Model Summary

S	R-sq	R-sq(adj)	R-sq(pred)
0,0064017	99,96%	99,94%	99,91%

Means

Sample	N	Mean	StDev	95% CI
250/20	3	0,85250	0,00433	(0,84474; 0,86027)
250/40	3	0,80111	0,01170	(0,79334; 0,80887)
350/20	3	1,06825	0,00714	(1,06048; 1,07601)
350/40	3	1,00369	0,00323	(0,99593; 1,01146)
500/20	3	0,61167	0,00289	(0,60390; 0,61943)
500/40	3	0,44167	0,01041	(0,43390; 0,44943)
Control	3	1,15423	0,00367	(1,14647; 1,16200)
Control gelatinized (90 C)	3	0,42420	0,00365	(0,41643; 0,43196)
Ultrasonicated	3	1,09167	0,00289	(1,08390; 1,09943)

Pooled StDev = 0,00640175

Tukey Pairwise Comparisons

Grouping Information Using the Tukey Method and 95% Confidence

Sample	N	Mean	Grouping
Control	3	1,15423	A
Ultrasonicated	3	1,09167	B
350/20	3	1,06825	C
350/40	3	1,00369	D
250/20	3	0,85250	E
250/40	3	0,80111	F
500/20	3	0,61167	G
500/40	3	0,44167	H
Control gelatinized (90 C)	3	0,42420	H

Means that do not share a letter are significantly different.

Table A.4.6. One way Analysis of Variance (ANOVA) and Tukey's comparison test for flow behavior index (n) values of quinoa starches

One-way ANOVA: n versus Sample

Method

Null hypothesis	All means are equal
Alternative hypothesis	Not all means are equal
Significance level	α = 0,05

Equal variances were assumed for the analysis.

Factor Information

Factor	Levels	Values
Sample	9	250/20; 250/40; 350/20; 350/40; 500/20; 500/40; Control; Control gelatinized (90 C); Ultrasonicated

Analysis of Variance

Source	DF	Adj SS	Adj MS	F-Value	P-Value
Sample	8	0,236969	0,029621	297,37	0,000
Error	18	0,001793	0,000100		
Total	26	0,238762			

Model Summary

S	R-sq	R-sq(adj)	R-sq(pred)
0,0099805	99,25%	98,92%	98,31%

Means

Sample	N	Mean	StDev	95% CI
250/20	3	0,7733	0,0252	(0,7612; 0,7854)
250/40	3	0,77500	0,01500	(0,76289; 0,78711)
350/20	3	0,7554	0,0000	(0,7433; 0,7675)
350/40	3	0,7850	0,0000	(0,7729; 0,7971)
500/20	3	0,9330	0,0000	(0,9209; 0,9451)
500/40	3	0,9828	0,0000	(0,9707; 0,9949)
Control	3	0,76287	0,00618	(0,75076; 0,77497)
Control gelatinized (90 C)	3	0,9870	0,0000	(0,9749; 0,9991)
Ultrasonicated	3	0,7799	0,0000	(0,7678; 0,7920)

Pooled StDev = 0,00998052

Tukey Pairwise Comparisons

Grouping Information Using the Tukey Method and 95% Confidence

Sample	N	Mean	Grouping		
Control gelatinized (90 C)	3	0,9870	A		
500/40	3	0,9828	A		
500/20	3	0,9330		B	
350/40	3	0,7850			C
Ultrasonicated	3	0,7799			C D
250/40	3	0,77500			C D
250/20	3	0,7733			C D
Control	3	0,76287			C D
350/20	3	0,7554			D

Means that do not share a letter are significantly different.

Table A.4.7. One way Analysis of Variance (ANOVA) and Tukey's comparison test for average T_2 relaxation times of quinoa starches

One-way ANOVA: T2 versus Sample

Method

Null hypothesis	All means are equal
Alternative hypothesis	Not all means are equal
Significance level	α = 0,05
Rows unused	1

Equal variances were assumed for the analysis.

Factor Information

Factor	Levels	Values
Sample	9	250/20; 250/40; 350/20; 350/40; 500/20; 500/40; Control; Control gelatinized (90 C); Ultrasonicated

Analysis of Variance

Source	DF	Adj SS	Adj MS	F-Value	P-Value
Sample	8	1043500	130438	371,24	0,000
Error	17	5973	351		
Total	25	1049473			

Model Summary

S	R-sq	R-sq(adj)	R-sq(pred)
18,7446	99,43%	99,16%	98,72%

Means

Sample	N	Mean	StDev	95% CI
250/20	3	70,11	2,15	(47,28; 92,95)
250/40	3	74,12	2,02	(51,28; 96,95)
350/20	3	90,87	2,98	(68,04; 113,71)
350/40	3	100,86	5,46	(78,03; 123,69)
500/20	3	547,4	43,1	(524,6; 570,2)
500/40	3	546,4	32,5	(523,5; 569,2)
Control	2	65,96	2,29	(38,00; 93,92)
Control gelatinized (90 C)	3	22,710	0,877	(-0,123; 45,543)
Ultrasonicated	3	91,49	4,43	(68,65; 114,32)

Pooled StDev = 18,7446

Tukey Pairwise Comparisons

Grouping Information Using the Tukey Method and 95% Confidence

Sample	N	Mean	Grouping		
500/20	3	547,4	A		
500/40	3	546,4	A		
350/40	3	100,86		B	
Ultrasonicated	3	91,49		B	
350/20	3	90,87		B	
250/40	3	74,12		B	C
250/20	3	70,11		B	C
Control	2	65,96		B	C
Control gelatinized (90 C)	3	22,710			C

Means that do not share a letter are significantly different.

CURRICULUM VITAE

PERSONAL INFORMATION

Surname, Name: Ünal, Kübra

EDUCATION

Degree	Institution	Year of Graduation
BS	METU Food Engineering	2012
High School	Aydınlıkevler Foreign Language High School, Ankara	2007

WORK EXPERIENCE

Year	Place	Enrollment
2016-Present	Türkish Patent and Trademark Office (TÜRKPATENT)	Patent Examiner
2013-2016	METU Department of Food Eng.	Research Assistant
2010 July	PINAR Milk Factory, Eskişehir	Intern Eng. Student
2011 July	NESTLE Karacabey Factory, Bursa	Intern Eng. Student

FOREIGN LANGUAGES

Advanced English, Basic German

PUBLICATIONS

1. Unal, K., Alpas, H., Aktas, H., & Oztop, M. H. (2020). Time domain (TD)-NMR relaxometry as a tool to investigate the cell integrity of tomato seeds exposed to osmotic stress (OS), ultrasonication (US) and high hydrostatic pressure (HHP). Journal of Food Science and Technology, 57(10), 3739–3747. https://doi.org/10.1007/s13197-020-04406-5
2. Kirtil, E., Dag, Damla, Guner, S., Unal, K. & Oztop, M. H. (2017), Dynamics of unloaded and green tea extract loaded lecithin based liposomal dispersions investigated by nuclear magnetic resonance T2 relaxation. Food Research International. https://doi.org/10.1016/j.foodres.2017.06.064

SELECTED ORAL and POSTER PRESENTATIONS

1. Unal,K., Alpas, H., Aktas, H., Oztop,M.H. (2017). Hydration Behaviour of Quinoa Seed by Nuclear Magnetic Resonans (NMR) Relaxometry. 8th International Conference on Biotechnology and Food Science, ICBFS2017, Seoul, South Korea. (Oral Presentation)

2. Unal,K., Alpas, H., Aktas, H., Oztop,M.H. (2017). Use of Nuclear Magnetic Resonance (NMR) relaxometry as a tool to assess seed characteristics induced by Osmotic Stress (OS), Ultrasound (US) and High Hydrostatic Pressure (HHP). 3rd International Conference on Food and Agricultural Engineering, ICFAE 2017, NARIC Food Science Research Institute, Budapest, Hungary (Oral Presentation)

3. Unal,K., Alpas, H., Oztop,M.H. (2017). Kinoa Tohumunun Su Çekme Davranışının NMR Relaksasyon Spektrum Analizi ile İncelenmesi. 10. Gıda Mühendisliği Kongresi. Antalya, Turkey (Abstract-Poster Presentation)

4. Unal,K., Alpas, H., Cevik, B., Aktas, H., Oztop,M.H. (2015). Early stage detection of tobacco mosaic virus in tomato seeds by NMR Relaxometry. 4th International Conference and Exhibition on Food Processing & Technology, London, UK (Abstract-Poster Presentation)

5. Unal, K., Aktaş, T., Oztop M.H. (2015) Domates Tohumundaki Tütün Mozaik Virüsünün NMR Relaxometry ile Erken Evre Tespiti, 5th Gıda Güvenliği Kongresi, İstanbul, Turkey (Abstract-Poster Presentation)

6. Unal, K., Aktas, H. Oztop, M.H. (2013). Domates ve Biber Tohumlarının Su Çekme Kapasitesinin T2 NMR Relaksometre Spektrası ile İncelenmesi. İç Anadolu Bölgesi, 1. Tarım ve Gıda Kongresi, Niğde, Turkey (Abstract-Poster Presentation)

HOBBIES

Travelling, photography, walking, painting